

TECTONIC RELATIONS BETWEEN IZMIR-ANKARA ZONE AND KARABURUN BELT

Burhan ERDOĞAN*

ABSTRACT.- In the Western Anatolia around Izmir region, three tectonic belts are located. These are from east to west, the Menderes massif, the Izmir-Ankara zone and the Karaburun belt. The Menderes massif is composed of metamorphic rocks, the uppermost section of which is Early Eocene in age. The Izmir-Ankara zone, which thrusts over the Menderes massif, is represented by a melange of Campanian-Danian age in a large region between Manisa and Seferihisar. This chaotic unit which is named here as Bornova melange, is made up of matrix of sedimentary rocks of flysch facies and mafic volcanic intercalations and blocks of limestones more than 20 km in length in some areas. The limestone blocks and megablocks were incorporated during the sedimentation of the matrix and, as a result, various soft sediment deformations and chaotic contact relations were formed around them. The generalized stratigraphy of the megablocks, constructed from measured incomplete sections, is similar to the stratigraphy of the Karaburun carbonate succession. Besides that, lithological and paleontological correlations show that the blocks are broken parts of the Karaburun succession. In the Karaburun peninsula, the Upper Cretaceous lies with an angular unconformity, on the Triassic-Lower Cretaceous comprehensive carbonate succession, around Balıkhöva village. Besides this, at two more locations, one near the villages of Karaburun and the other near Urla where the peninsula joins Anatolia, chaotic rocks similar to the Bornova melange are observed. At these last two locations, the contact relations between the Karaburun carbonate succession and those of the chaotic rocks are similar to those seen around the megablocks of the Bornova melange, and can not be explained easily with normal stratigraphic concepts. It shows all the evidences indicative of the Karaburun succession had moved into the flysch depositing still soft sedimentary environment. Various data collected are all in agreement with the idea that the Karaburun carbonate succession was evolved as a platform of the Izmir-Ankara zone and it was tectonically transported during the flysch deposition as nappes. As the nappes moved into the Izmir-Ankara zone, broken large silices formed the megablocks, whereas, the Karaburun carbonate belt an allochthonous pack of nappes or the toe of the nappes itself.

INTRODUCTION

Three tectonic belts, trending in the NE–SW direction, are separated in the paleotectonic structure of the Western Anatolia (Fig.1). The easternmost belt is the Menderes massif which is composed of metamorphic rock assemblages. The second belt is the Izmir-Ankara zone and, the third one, which lies to the farther west with a platform-type carbonate succession, is called the Karaburun belt, Şengör and Yılmaz (1981) have included this last belt into the continuation of the Sakarya continent in their classification of the cratonic realms of the Western Anatolia.

The east-west trending neotectonic structures, that started forming from Middle-Late Miocene and constructed the graben structures of the Western Anatolia, cut and dislocate these paleotectonic belts (Şengör, 1980). Although the graben forming tectonics has not separated the paleotectonic belts from each other to an unrecognizable extent, the sediment fillings in most places have covered and concealed their boundaries. Especially, the contact between the Karaburun belt and the Izmir-Ankara zone, except in a few places, is overlain by the Neogene sedimentary pile.

In the interpretation of the tectonic evolution of the Western Anatolia, the boundary relations of these paleotectonic belts will provide invaluable information. Various earlier workers have stated that the Izmir-Ankara zone thrusts over the Menderes massif along low-angle faults in the southward direction (Dürr, 1975; Dürr et al., 1978; Channel et al., 1979; Şengör and Yılmaz, 1981; Akdeniz et al., 1982; Akkök, 1983). It has also been put

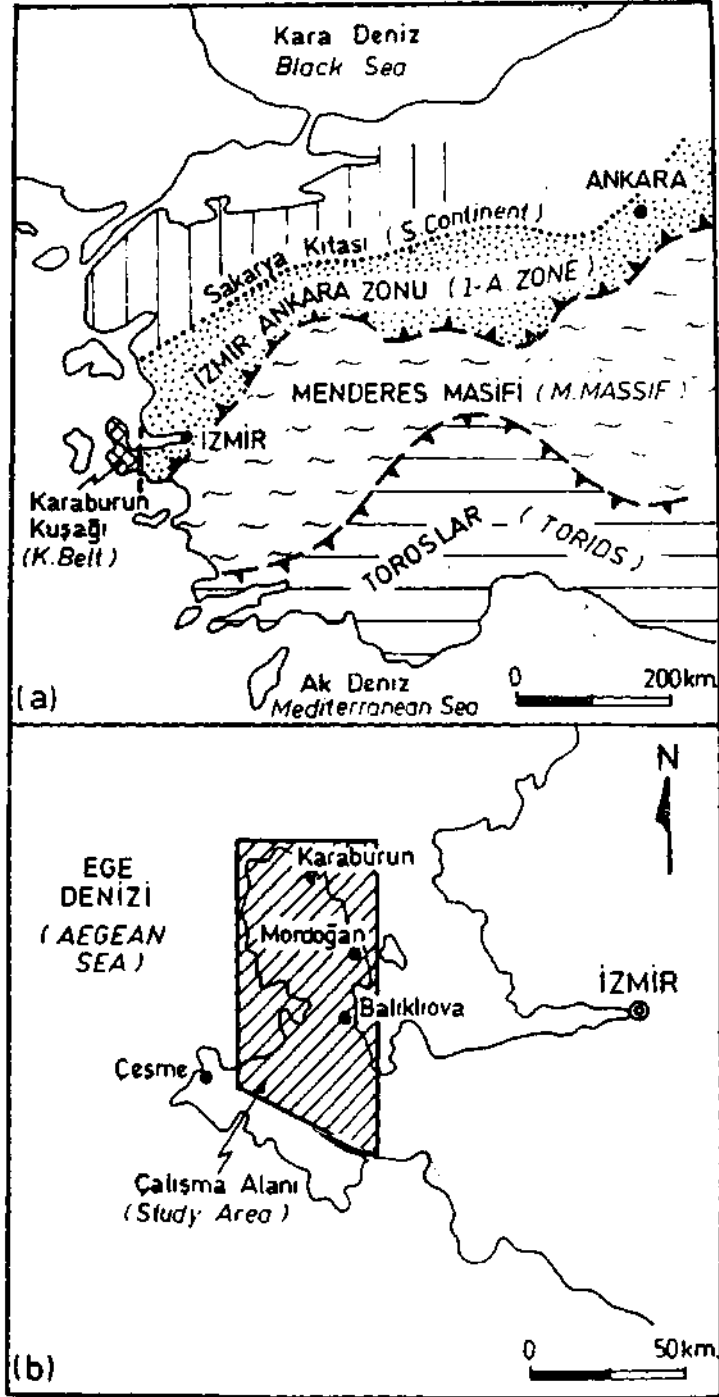


Fig.1— Paleotectonic belts of Western Anatolia; general trends of the Menderes massif, İzmir-Ankara zone and the Karaburun belt.

forward that, the displacement along these thrust faults reaches a continental scale and the roots of the Lycian nappes were located somewhere in the İzmir-Ankara zone and that they rode over the Menderes massif southward to take their present position (Dürr, 1975; Şengör and Yılmaz, 1981; Akkök et al., 1985).

Although various authors have discussed the boundary relations between the Izmir-Ankara zone and the Menderes massif, there is no detailed discussion on the contact relations between the Karaburun belt and the İzmir-Ankara zone. In this study this boundary will be examined.

The Izmir-Ankara zone which was first defined by Brinkmann (1966, 1972 and 1976), is represented by flysch-type sedimentary rocks, various limestones, mafic volcanic and ultramafic rocks. There are differences in opinion among workers who have constructed the generalized stratigraphic column of this zone around İzmir. Verdier (1963), Oğuz (1966), Marengwa (1968), Konuk (1977) and Akdeniz et al. (1982) have put forward that in the lower part there is a thick and continuous shallow-marine carbonate succession with age range from Early Triassic to Early Cretaceous. In the upper part of the stratigraphic column, they have separated a flysch unit of the Late Cretaceous age. According to these authors, the present chaotic internal structures and stratigraphy of the İzmir-Ankara zone were formed by the later tectonic deformations.

Yağmurlu (1980), however, has mapped three different flysch associations in the same area and considered several angular unconformities in the stratigraphic column of the Izmir-Ankara zone. One of its flysch associations lies below the shallow-marine carbonate succession and the other two are above this platform-type carbonate section.

The author of this paper has studied the stratigraphy of the Izmir-Ankara zone between Izmir and Manisa (Erdoğan, 1985) and, reached a different conclusion about the stratigraphic relations between the flysch and the carbonate section. It is found that the stratigraphic base of the flysch does not crop out in any place around Izmir and the carbonate sections are merely block up to 20 km in length and they float into the flysch matrix with an age of Campanian-Danian. The shallow-marine carbonate blocks of the Triassic-Upper Cretaceous age were incorporated into the flysch basin during the deposition in Maestrichtian and Danian (B. Erdoğan; D. Altın and S. Özer, in preparation). As a result, below the limestone blocks structures of soft sediment deformation are common and the flysch matrix smears all sides of the blocks along very irregular surfaces. This blocky unit, which was formed in the Izmir-Ankara zone, is called the Bornova melange (Erdoğan, 1985, 1988).

The stratigraphic data provide, presently, the only information to evaluate the tectonic evolution of the İzmir-Ankara zone (Özer and İrtəm, 1982; Erdoğan, 1985, 1988). However, because its chaotic internal structures and the rootless nature of the carbonate masses, the stratigraphic tracks of this zone were considerably erased. Another area in which the tracks of the initiation of the opening of the Izmir-Ankara zone may be searched is the Menderes massif. However the massif is metamorphic up to the Eocene section (Boray et al., 1973; Dürr, 1975; Dürr et al., 1978; Gutnic et al., 1979) and so it does not appear to be a suitable area to look at the answer of this question. However, the stratigraphy of the uppermost part of the Karaburun peninsula, may provide a valuable information about the evolution of the Izmir-Ankara zone, because it has a continuous and fossil-rich carbonate section from lower Triassic to Upper Cretaceous.

In this study, the stratigraphic characteristics of the Upper Cretaceous that form the uppermost part of the Karaburun belt will be presented and their lower boundary with the underlying platform-type carbonate succession (Karaburun series) will be discussed. At the end of the paper the tectonic relation between the Karaburun belt and the İzmir-Ankara zone will be evaluated.

KARABURUN UPPER CRETACEOUS OUTCROPS

In the Karaburun peninsula, two different Upper Cretaceous with different internal stratigraphy are present and they crop out in three separate areas (Fig.2). These areas, from the north to the south, are the Kalecik, Balık-

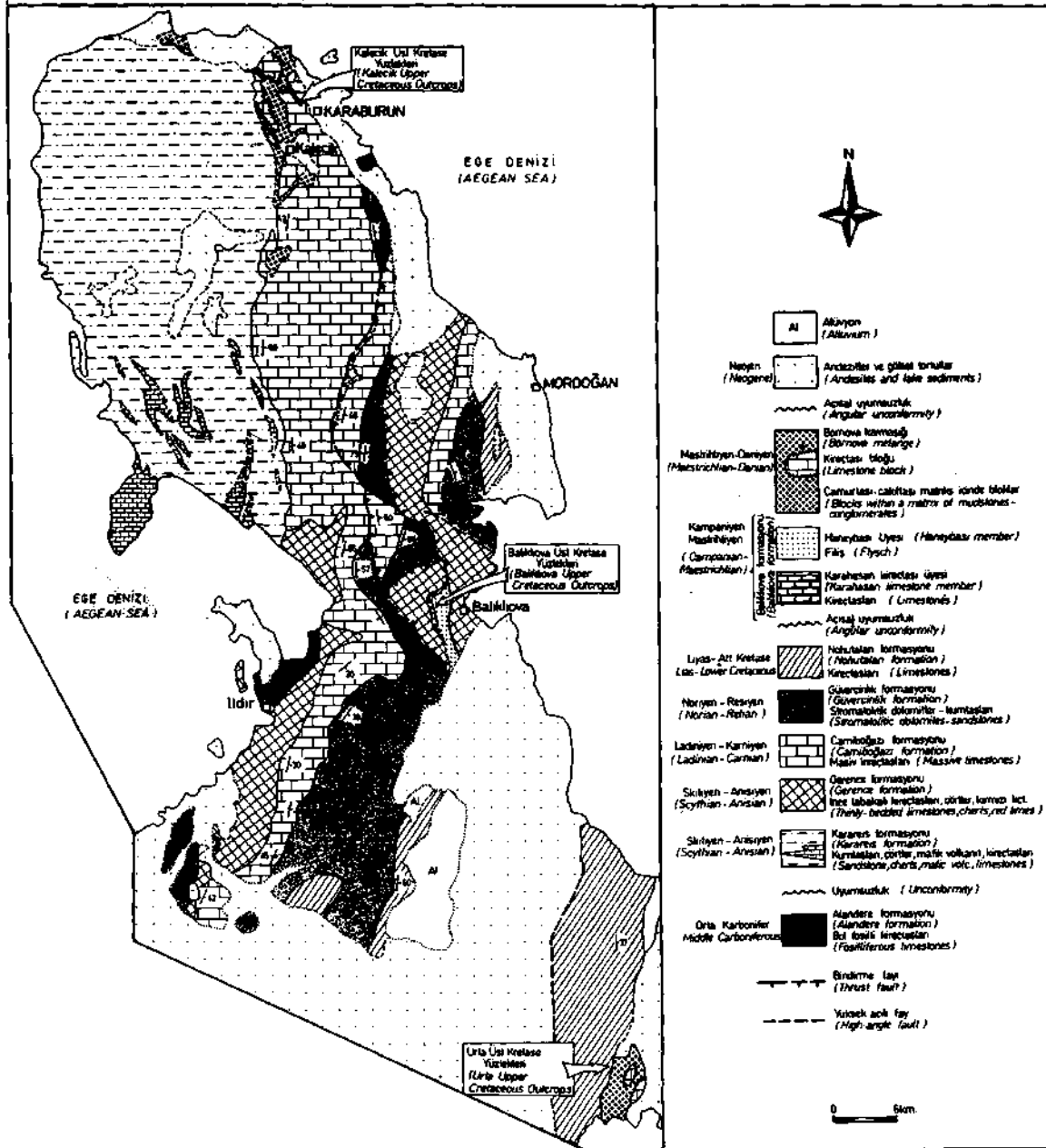


Fig.2-- Simplified geological map of the Karaburun peninsula showing the locations of the Upper Cretaceous outcrops discussed in the text.

liova and the Urla outcrops. The Upper Cretaceous in the Kalecik and Urla outcrops resembles to each other on the basis of internal stratigraphy and contact relations with the underlying platform succession (Karaburun series). In the following section these two areas will be presented together. The Upper Cretaceous in the Balıkklova area, however, is different and will be discussed under a separate heading.

The Balıkklova Upper Cretaceous lies above the Karaburun series with a continuous stratigraphic boundary. At the lower part, it starts with a shallow-marine carbonates above an unconformity surface and passes upward into detrital sedimentary rocks of flysch-facies. So the Balıkklova Cretaceous is unique among others cropping out

in a large region covering İzmir, Manisa and Seferihisar. It is the only area in which the flysch unit is stratigraphically connected to the underlying continuous carbonate succession. In other areas around İzmir, however, the Upper Cretaceous flysch forms the matrix and the carbonate masses are blocks into it, which are all together called the Bornova melange (Erdoğan, 1985, 1988).

The Kalecik and Urla outcrops are different from the Balıklıova ones and the Upper Cretaceous in these last two areas resembles to the Bornova melange. The lower contacts of the Upper Cretaceous with the Karaburun series in the Kalecik and Urla areas, are also like the flysch matrix and the limestone blocks in the İzmir-Ankara zone, and this unit with a similar way spreads over a very irregular paleotopography.

Balıklıova Upper Cretaceous outcrops

Around the Balıklıova village, the Upper Cretaceous forms the uppermost part of the Karaburun series (Fig.3). Open outcrops are also seen near the Çatalkaya village and Mersincik tepe location. In these areas the Upper Cretaceous starts at the base with a shallow-marine carbonates and passes upward first into pelagic limestones and finally into a flysch. In this study, the carbonates and the flysch are together called the Balıklıova formation; the lower carbonate section is called the Karahasan limestone member and the upper flysch is the Haneşbaşı member.

The Karahasan limestone member is 90 m in thickness as measured at the type locality near Balıklıova village. The lower 29 m-thick section of the member is composed of massive limestones which contain abundant rudist particles, echinoderm plates and algae. Above the massive limestones there is a 29 m-thick bioclastic limestones and sandy limestones which are gray in the lower part but become pink in color in the upper half. The detrital limestones pass upward into layers of cherts-or nodule-bearing limestones that are about 36 m in thickness. At the uppermost part of the Karahasan limestone member there are red micritic limestones which are thinly bedded and measure up to 4 m in total thickness at the type locality.

The lower half of the Karahasan limestone member is poorly fossiliferous; the middle and upper parts contain *Globotruncana stuarti*, *G. lapparenti*, *G. bulloides*, *G. arca*, *G. fornicata*, *G. coronata*, *G. cf. mazyoni*, *G. linneiana*, *Praeglobotruncana* sp., *Globorotalites* sp., *Bolivina* sp., *Ovalveolina* sp. and *Rotalia* sp. which indicate a Campanian age. Supporting the above age assignment, Brinkmann et al. (1977) have stated the middle and upper parts of the same limestones as Campanian and Early Campanian.

The uppermost red pelagic limestones of the Karaburun limestone member yield foraminifera *Globotruncana stuarti*, *G. tricarinata*, *G. stuartiforriis*, *G. falsostuarti*, *G. linneiana*, *G. cf. mazyoni*, *G. cf. sentricosa*, *G. cf. gansseri*, *G. elevata*, *G. area*, *G. calcarata*, *G. cf. gagnebini*, *Praeglobotruncana* sp. and *Ruglobigerina* sp. indicating a Maestrichtian age'. Accordingly, Brinkmann et al. (1977) have assigned a Maestrichtian age for the same levels of the Upper Cretaceous limestones.

The lower parts of the Karahasan limestone member, which are light gray in color, show thick and massive bedding, and contain abundant benthic fossil fragments, indicating a high-energy shallow marine or a slope environment of deposition. As the presence of chert lenses and nodules in the upper part of the member implies the depositional site gradually become deeper and probably an open sea environment, and finally during the deposition of the uppermost red micritic limestones a pelagic condition prevailed.

The Karahasan limestone member which up to 90 in thickness near Balıklıova village, thins along the strike in short distance and around the Mersincik tepe location becomes 20 m and near Çatalkaya measures only 2-4 m.

The uppermost red micritic limestones of the Karahasan limestone member grade upward into mudstones

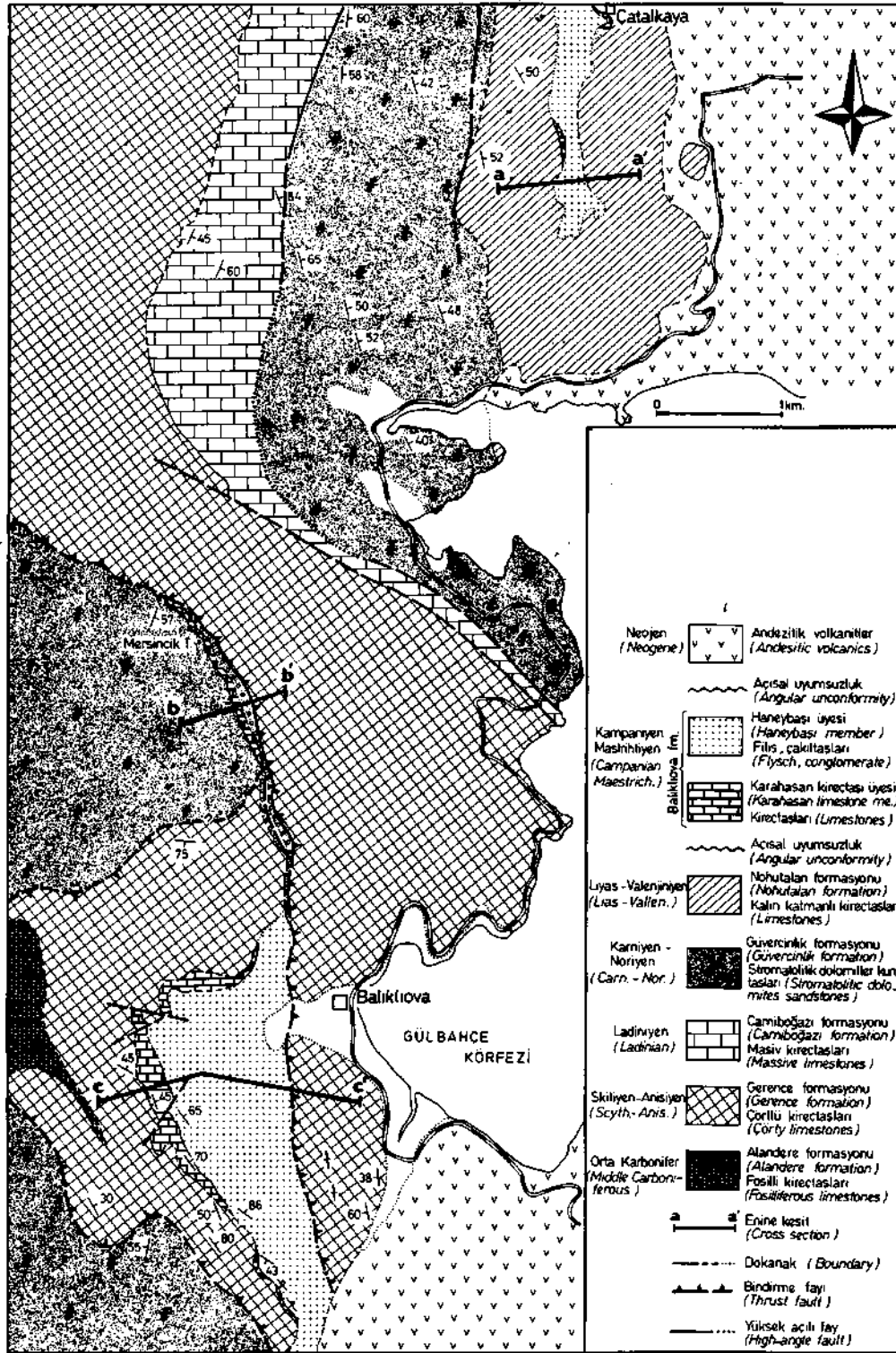


Fig.3— Geological map of the Balıklıova area.

and intercalations of mudstones and sandstones. This detrital sedimentary rocks of the Balıklıova formation is called the Haneysbaşı member (Fig.3). In the lower part of the Haneysbaşı member, mudstones dominate and in upper parts sandstone and mudstone intercalations give the member a flysch-type appearance. Around the Mersincik tepe there are conglomerate intervals the particles of which are entirely derived from various limestones of the Karaburun series. These conglomerates with matrix-supported angular blocks show all kinds of gradation laterally and vertically to the flysch-type detrital sedimentary rocks.

The maximum thickness of the Haneysbaşı member reaches 200 m at the type locality of the Balıklıova formation, but the upper contact is a low-angle thrust fault (Fig. 3,4), so that the true thickness must be more than this.

The Balıklıova formation lies above various formations of the Karaburun series along an unconformity surface. Around the Balıklıova village the unit overlies the Gerence formation of Early-Middle Triassic, around Mersincik tepe it directly lays above the Güvercinlik formation of Late Triassic, and farther north near Çatalkaya village it is above the Nohutalan formation of Liassic-Early Cretaceous (Fig. 3,4). In this last location, the carbonate member of the Balıklıova formation is very thin and the unit overlies the irregular topography of the Nohut-

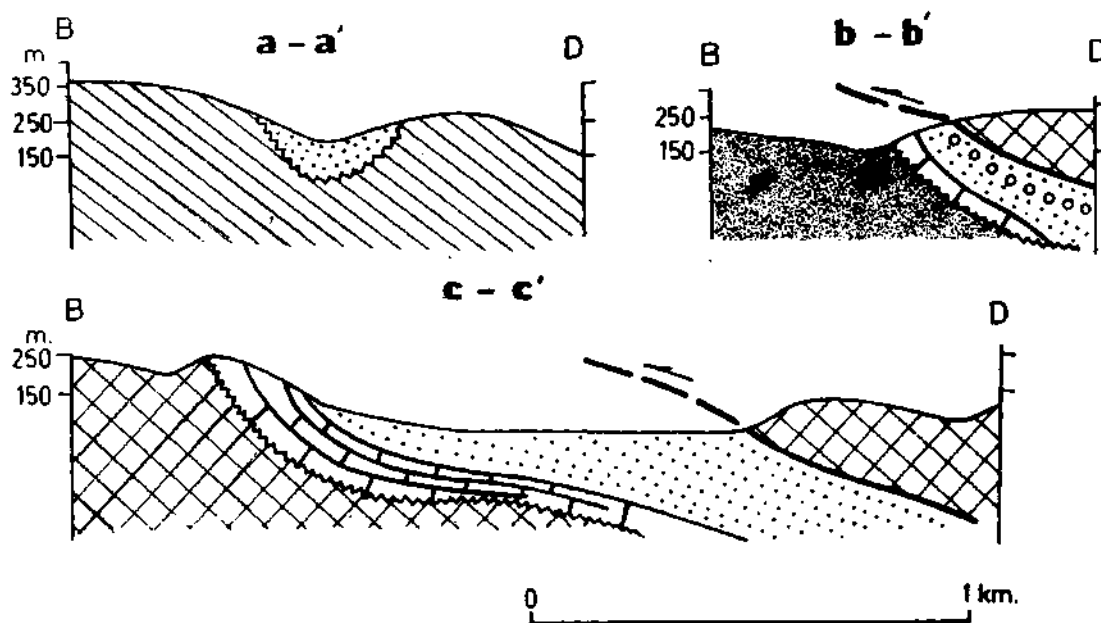


Fig.4— Geological cross-sections of the Balıklıova area; locations of the sections are shown on Figure 3.

alan formation directly with sandstone and mudstone intercalations (Fig.4, section a-a')

The upper contact of the Balıklıova formation is a structural surface and the Gerence formation of Early-Middle Triassic thrust over this unit along a low-angle fault (Fig. 3,4, section c-c'). Near the Mersincik tepe without any cataclastic or mylonitic zone the Lower Triassic Unit overlays the conglomeratic intervals of the Haneysbaşı member. Along the southward continuation of the same fault near Balıklıova village mudstones of the Haneysbaşı member intrude, upward along the hanging-wall of the thrust fault and soft sediment deformational structures like load-casts are common.

The Karaburun platform uplifted before the deposition of the Balıklıova formation. During Campanian a shallow sea invaded the area and the Karahasan limestone member was deposited. During Maestrichtian the platform subsided rapidly to form a deep marine environment in which at the beginning the pelagic limestones and later the flysch-type detrital sedimentary rocks were formed. A compressif deformation effected the platform during Maestrichtian and, the N–S trending and eastwardly dipping thrust faults were formed, at the bases of which the flvsch was deformed in a viscous condition. The conglomeratic intervals within the Maestrichtian flysch

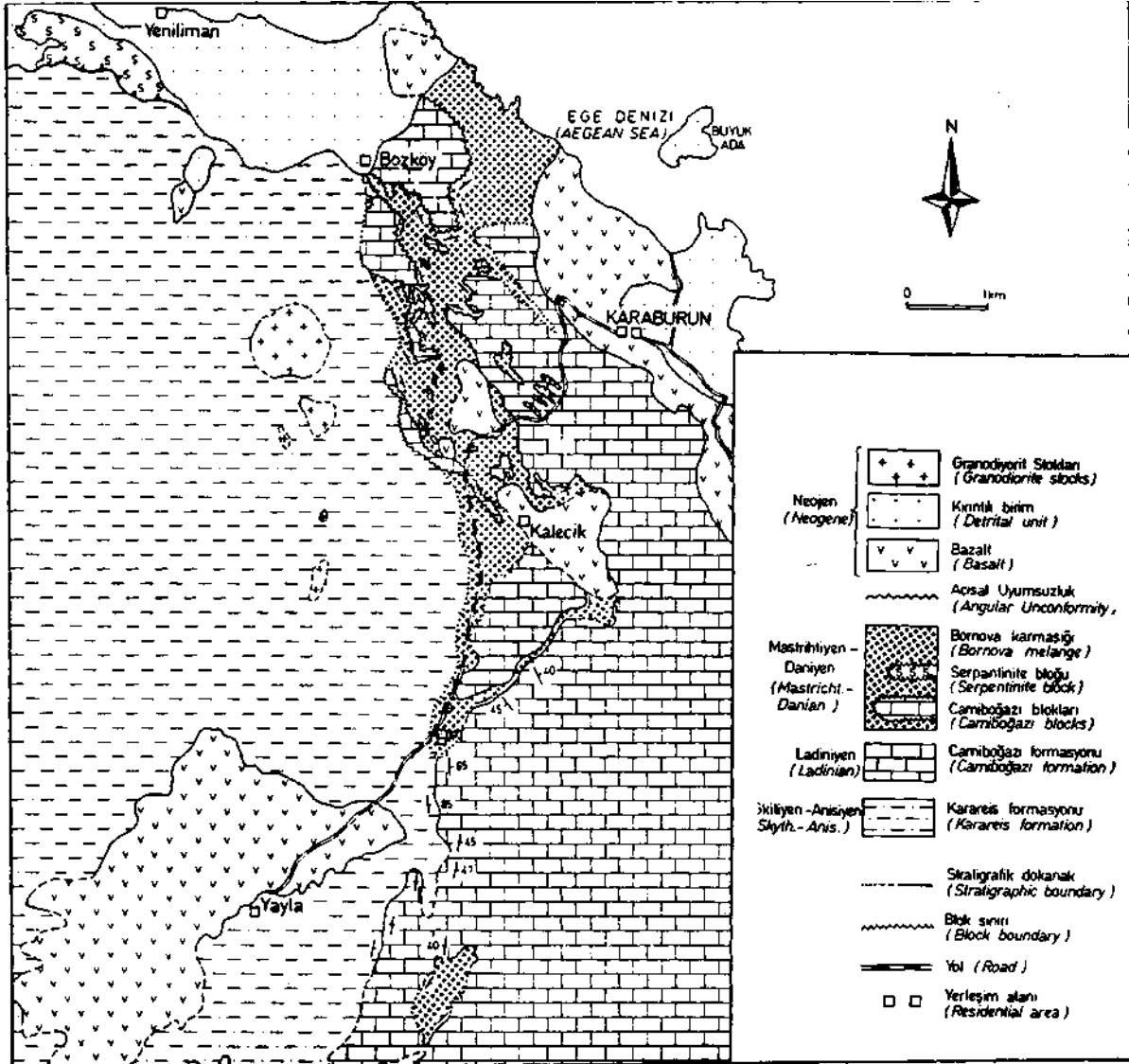


Fig.5- Geological map of the Kalecik area.

and soft sediment deformations along the base of the thrusts indicate that the deformation was active during the deposition.

Kalecik and Urla Upper Cretaceous outcrops

In the north of the Karaburun peninsula near Kalecik village and in the south near Urla, a melange with chaotic internal structure crops out (Fig. 2,5). The melange at these two locations, include blocks of various limestones, serpentinites and mafic volcanic rocks set in a matrix of sandstones and mudstones.

İZMİR-ANKARA ZONE AND KARABURUN BELT

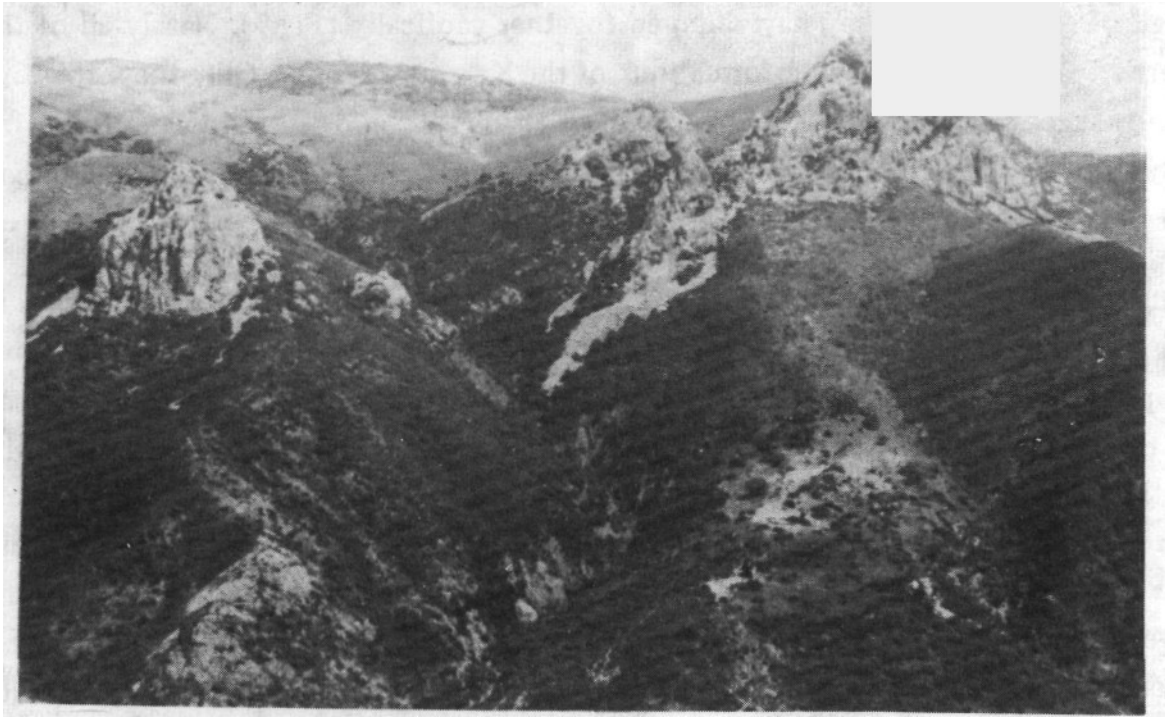


Fig.6— General view of the Upper Cretaceous melange in the Kalecik area. Areas with a gentle topography are underlain by the matrix with sandstone and mudstone intercalation. Blocks of the Camiboğazı limestone are floating within a matrix of the melange.

Near Kalecik village the blocks of the melange are generally massive limestones up to 2 km in length with a shallow-marine facies (Fig.6). These massive limestone blocks, which are Ladinian in age, belong to the Camiboğazı formation of the Karaburun series and so they are shown by the same hatching on the geological maps but with a *zigzag* boundary.

Beside the large blocks, around Kalecik, there are small masses of red pelagic limestones with thin-shelled lamellibranch-fossils that give an Early Triassic age, black cherts of the same age and blocks of mafic volcanics and



Fig.7— Olistostromal materials exposed at the base of the melange unit and also inside the massive limestones of the Camiboğazı formation. Angular limestone fragments are cemented by mudstones with matrix-supported texture.

serpentinites of unknown ages. These small angular blocks range from centimeter to hundreds of meter across without any sign of erosion and they have lumped together caotically (Fig.7). Nearly all of the large and small blocks were derived from the underlying formations of the Karaburun series. Only the serpentines do not belong to the Karaburun succession and the probable origin of them will be discussed in the following section on the conclusions. The matrix of the blocky unit is composed of mudstones and sandstones and it comprises 10 to 15 volume-percent of the melange.

The youngest age that give the closest age of the blocky unit has been obtained from a red micritic limestone outcropping approximately 2 km to the southeast of Bozköy (Fig.5). At this location the micritic limestones form an outcrop 20 m in length but it is not defmately determined whether it is a small block set into the matrix of the melange or it is the matrix itself. The samples collected from the micrites have been examined by Ercüment Sirel and with the following list of the microfossils Campanian age has been determined. These are *Globotruncana area*, *G. linneiana*, *G. cf. rozetta*, and *G. elevata*. Therefore, the melange in the Kalecik area must be Campanian and/or younger in age. The melange of the Kalecik area closely resembles to the Bornova melange of the Campanian-Danian age that crops out in a extensive region between Manisa and Seferihisar in the İzmir-Ankara zone. The only noticeable difference between the two units is the percentage of their matrixes; while it comprises 40-50 percent of the Bornova melange, the matrix is about 10-15 percent in the Kalecik area.

The lower contact of the melange in the Kalecik area with the Karaburun series is so complicated that can not be explained easily with normal stratigraphic concepts. On the geological map (Fig.5) the melange outcrops form caps above the units of the Karuburun series and patches of them overlay the older unit with widely different angular relations. The formational boundaries of the Karaburun series trend in the N—S direction and dip with high angles. The contacts of the melange, on the other hand, overly stratigraphically various levels of the underlying series. As it is seen on the geological map, this unit in places starts directly with mudstones at the base, or in other areas with olistostromes that are composed of angular, particles derived from nearby areas (Fig.8). These olistostromal materials with mudstone matrix cover an irregular paleotopography or crop out within the Camiboğazı formation in narrow zones nearly 300 m topographically lower than their drown contact on the geo-

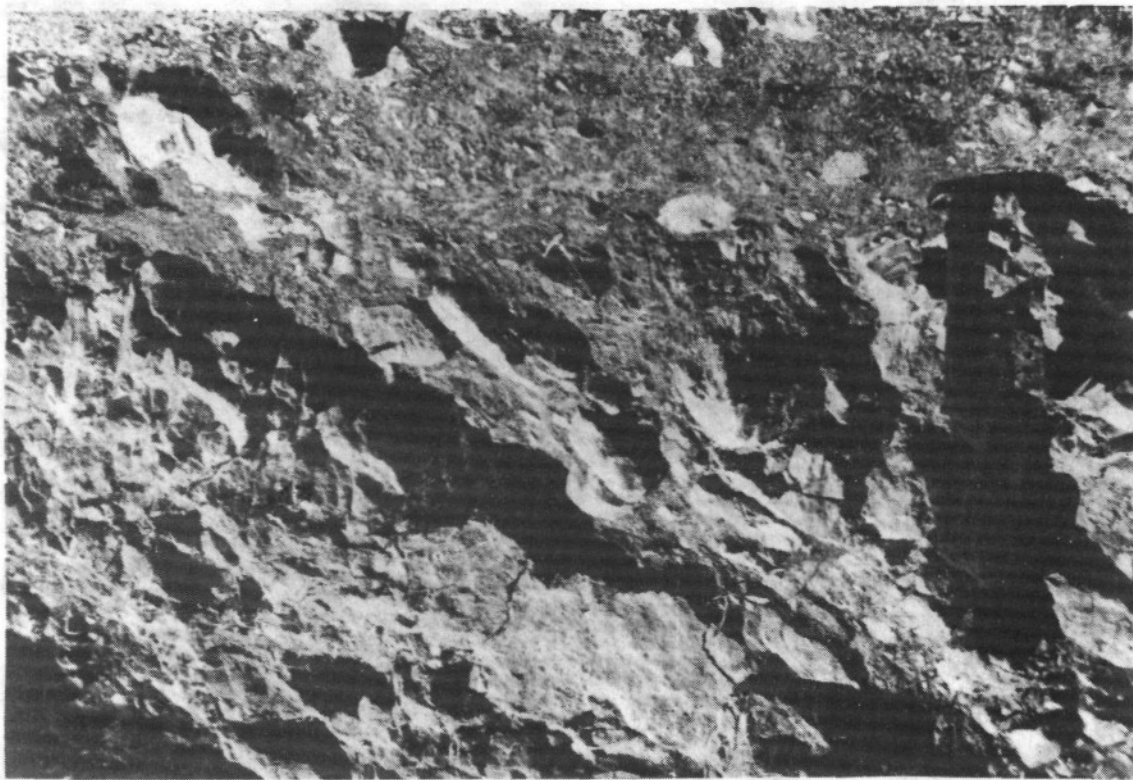


Fig.8— Along road-cuts between Karaburun and Kalecik, inside the limestones of the Camiboğazı formation flysch outcrops of the melange unit are seen along irregular zones.

logical map. The road connecting the Karaburun district to the Kalecik village (Fig.9) cuts the massive limestones of the Camiboğazı formation along a level topographically 300 m below the lower contact of the melange. Along the road cut, however, inside the Camiboğazı limestones the mudstones of the melange unit are seen along irregular zones (Fig.7). In these zones angular particles of the Camiboğazı limestones are found cemented by the mudstones (Fig.8). These chaotic materials with flysch matrix are found along 4 large zones as shown on the geological map (Fig.5).

The same kind of structures are common around the limestone blocks of the Bornova melange. Near İzmir in the Bornova district, there are numerous quarries opened in the limestone megablocks of the Bornova melange, along the high excavation scarps of which the flysch matrix crops out in irregular zones. The flysch matrix, that is composed of sandstones and mudstones, cements broken irregular particles of the limestones.

In the Karaburun peninsula, around Kalecik village the size of the limestone blocks in the melange unit reaches up to 2 km in length, and at the bases of them in places olistostromes are found. The mudstone matrix of these olistostromes is seen injected 4-5 meter upward into the base of the blocks (Fig.9), showing clearly that



Fig.9— Soft sediment deformations are common below large limestone blocks of the melange unit in the Kalecik area. In the photograph, upward injection of mud is seen below a broken base of a limestone block.

it was in a soft state when the blocks were carried above the melange unit.

The various data described above are all in accord with the interpretation that the Karaburun belt is an allochthonous mass that had been displaced as a nappe or a toe of a nappe into the melange unit during its deposition. The structural relation between the chaotic unit of the Kalecik area, which is considered to be the continuation of the Bornova melange, and that of the Karaburun belt is shown schematically in Figure 10.

The melange unit of the Kalecik area also crops out, with the same lower contact relations, near Urla (Fig. 2), where it overlies the various levels of the Nohutalan formation of the Liassic-Early Cretaceous age. The blocks of the melange in this last location are cherty limestones of Early Triassic, massive limestones of Ladinian that are together belong to the Karaburun series, and serpentinites. They range in size from a small particle to a block up to 1 km in length 500 m in thickness. The base and the internal structure of the unit are observed along cliffs of

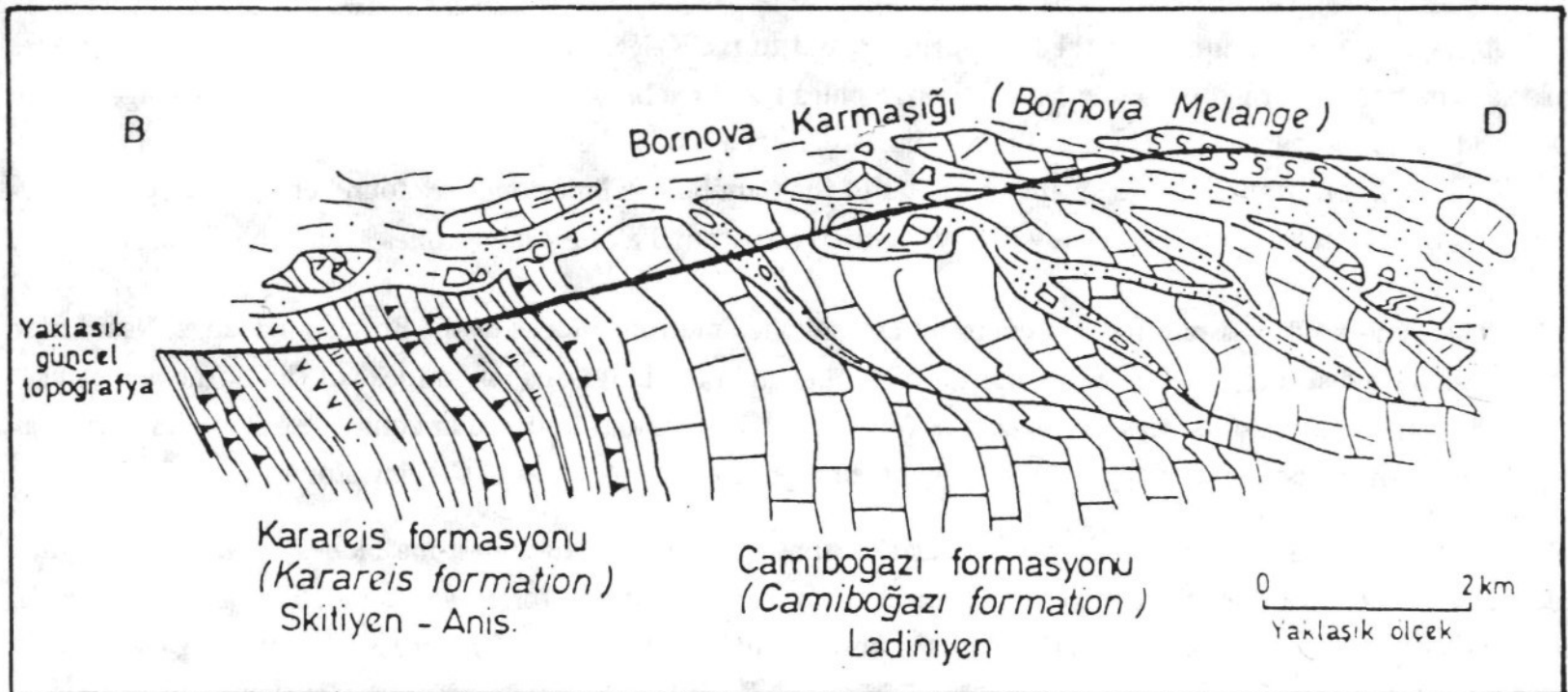


Fig.10— A schematic cross section showing the relations between the Karaburun series and the melange unit, in the Kalecik area.

the seashore, in the Urla area (Fig.2). At the base, there is a blockstone interval that is 50-60 m in thickness with a caotic internal structure (Fig.10). The blockstones probably formed as a submarine fan deposit, are not continuous laterally and pinch out within 100 m. The melange with blocks and olistostromal intercalations, that can be traced 4 to 5 km along the shore, forms a thickness more than 1-2 km and lays below Neogene deposits along an unconformity (Fig.2).

If lateral extents of the Kalecik and Urla outcrops are considered together, the blocky unit does not appear to be a local in origin rather surrounds the entire Karaburun peninsula. It is apparently the continuation of the Bornova melange that characterizes the İzmir-Ankara zone in Western Anatolia and hence on the geological maps and cross sections it is shown with the same name.



Fig.11 – Blockstones in the melange unit of the Urla area. Very angular blocks set in a flysch matrix. Probably submarine fan deposits.

DISCUSSIONS AND CONCLUSIONS

A platform-type shallow marine carbonate successions with an age range from Early Triassic to Aptian-Albian crops out in the Karaburun peninsula (Brinkmann et al., 1972; Erdoğan et al., 1988). Above this succession around Balıklıova the Campanian limestones were deposited. During Maestrichtian the Karaburun platform subsided rapidly and a basin was formed in which first pelagic limestones and later sedimentary rocks with flysch facies were deposited. These Upper Cretaceous rocks with a continuous section from the platform and with a relatively orderly internal stratigraphy are collectively named here the Balıklıova formation. As a result of the Maestrichtian subsidence, the flysch section encroached upon the different levels of the platform and overlaid the older units along an unconformity.

The Izmir-Ankara zone, that was evolved nearby to the Karaburun platform, was a basin in which flysch-type sedimentary rocks and spilitic volcanics were formed. Limestone blocks of the Karaburun succession measured up to 20 km in length, were carried into the Izmir-Ankara basin and a blocky unit with chaotic internal structure, that is named here the Bornova melange, was formed from Campanian to Danian.

Mapping of a large area in the Karaburun peninsula shown that the platform is imbricated by N-S trending and eastward dipping thrust faults (Fig. 2,3,5). The thrusting took place during the deposition of the flysch section of the Balıklıova formation and later the whole platform was carried as a nappe into the Izmir-Ankara basin. As a result of this deformation, the Upper Cretaceous melange outcropping near the Kalecik and Urla areas was formed, which is considered here to be the continuation of the Bornova melange. Hence, the boundary between the Karaburun belt and the Izmir-Ankara zone shows all kinds of gradation although it is concealed in most places by an overlying Neogene sedimentary pile.

In the Kalecik and Urla outcrops, the melange contains serpentinite blocks that are entirely foreign to the Karaburun series (Brinkmann et al., 1972; Erdoğan et al., 1988). They may belong to broken parts of the oceanic crust of the Izmir-Ankara zone, as the study carried out by us in an extensive area in the Western Anatolia suggests. The presence of slices of oceanic crust of the Izmir-Ankara zone in the melange above the Karaburun belt, may imply a complicated mechanism incorporating overthrusting of the oceanic crust in the tectonic transportation of the nappes of the Karaburun platform.

The initial age of the opening of the Izmir-Ankara zone has a critical importance in the tectonic evolution of the Western Anatolia. The stratigraphic record of the Karaburun series indicate an uninterrupted platform condition from Middle Triassic to Aptian-Albian, which is the youngest age obtained from the uppermost part of the platform succession (Erdoğan et al., 1988). A subaerial condition had intervened between Albian and Campanian as the unconformity below the Balıklıova formation implies. During Campanian a shallow marine carbonate deposition took place which gave way, by a rapid subsidence in Maestrichtian, to a deep basin in which a flysch was formed. The stratigraphic record of the Karaburun platform indicate, therefore that the first opening of the Izmir-Ankara zone took place after Albian and most probably during Campanian and Maestrichtian. Stratigraphic and paleontologic data derived from the limestone blocks within the Izmir-Ankara zone also suggest a platform condition dominating from Late Triassic to Santonian, and a basin was formed during the Campanian-Danian interval (B. Erdoğan; D. Altın and S. Özer, in preparation).

The various data presented above are all in accord with the interpretation that the Izmir-Ankara zone had opened in a relatively short time interval and that its closing initiated in Maestrichtian was completed in Middle Eocene by thrusting entirely above the Menderes massif. Therefore, it is implied that, in the Western Anatolia there had never been an extensive ocean named, as the Izmir-Ankara zone and a large oceanic crust had never been produced. This interpretation necessitates a critical reconsideration of the roots of the large ophiolite slices of the Lycian nappes that have been suggested to come from the north of the Menderes massif somewhere around the Izmir-Ankara zone.

ACKNOWLEDGEMENT

This research has been supported by TOBITAK project TBAG/644 and TPAO.

Foraminiferas from the Balıklıova area were determined by Dr. İzver Tansel (İstanbul) and those from the Kalecik area by Dr. Ercüment Sirel (Ankara); I am grateful to them for their help. I thank Prof.Dr. Erol Akyol for comments on an earlier version of this manuscript and Kerime Nacaklı for drawing the illustrations.

Manuscript received February 2, 1989

REFERENCES

- Akdeniz, N.; Öztürk, Z.; Konak, N.; Çakır, H.M.; Serdaroğlu, M.; Armağan, F. and Çatal, E., 1982, İzmir Manisa dolaylarının stratigrafi ve yapısal özellikleri : Türkiye Jeoloji Kongresi Bildiri Özetleri, 49-50.
- Akkök, R., 1983, Structural and metamorphic evolution of the northern part of the Menderes Massif: New data from the Derbent area, and their implication for the tectonics of the massif: Jour. Geology, 91, 342-350.
- ; Satır, M. and Şengör, A.M.C., 1985, Menderes masifinde tektonik olayların zamanlaması ve sonuçları: Ketin Simpozyumu, Türkiye Jeol. Kur. 93-94.
- Boray, A.; Akat, U.; Akdeniz, N.; Akçören, Z.; Çağlayan, A.; Günay, E.; Korkmazer, B.; Öztürk, E.M. and Sav, H., 1973, Menderes Masifi'nin güney kenarı boyunca bazı önemli sorunlar ve bunların muhtemel çözümleri: Cumhuriyetin 50. Yılı Yerbilimleri Kongresi Tebliğleri, MTA Publ., 11-20, Ankara.
- Brinkmann, R., 1966, Geotektonische Gliederung von Westanatolien: Neus Jahrb. Geol. Palaontol., Monatsh, 10, 603-618.
- , 1972, Mesozoic troughs and crustal structure in Anatolia: Geol.Soc. America Bull., 83,819-826.
- , 1976, Geology of Turkey: enke, Stuttgart, 158.
- ; Flügel, E.; Jacobshagen, V.; Lechner, H.; Rendel, B. and Trick, P., 1972, Trias, Jura und Unterkreide der Halbinsel Karaburun (West-Anatolien): Geologica et Palaentologica, 6, 139-150.
- ; Gümüş, H.; Plumhoff, F. and Salah, A.A., 1977, Höhere Oberkreide in Nordwest-Anatolien und Thrakien: NJb.GeoL Palaont. Abh., 154, 1-20.
- Channel, J.E.T.; d'Argenio, B. and Horvath, F., 1979, Adria, The African promotory in Mesozoic Mediterranean paleogeography: Earth Sci.Rev., 15, 213-292.
- Dürr, S., 1975, Über Alter und geotektonische Stellung des Menderes-Kristallins/SW-Anatolien und seine Aequivalente in der mittleren Aegaeis: Marbury/Lahn, Habilitations-Schrift, 107.
- ; Altherr, R.; Keller, J.; Okrusch, M. and Seidel, E., 1978, The median Aegean crystalline belt: Stratigraphy, metamorphism: in Closs, H.; Roeder, D. and Schmidt, K., eds., Alps, Apenines and Helenids: Stuttgart, Schweizerbart, 455-476.
- Erdoğan, B., 1985, Bornova karmaşığının bazı stratigrafik ve yapısal özellikleri: Türkiye Jeoloji Kurultayı, Bildiri Özetleri, 14.
- 1988, İzmir-Ankara Zonu ile Karaburun Karbonat istifinin tektonik ilişkisi: Hacettepe Üniversitesi Yerbilimlerinin 20. Yılı, Simpozyumu, Bildiri Özleri, 16.
- ; Altın, D.; Özer, S. and Güngör, T., 1988, Karaburun Yarımadası (İzmir) karbonat istifinin stratigrafisi: Hacettepe Üniversitesi Yerbilimlerinin 20.Yılı Simpozyumu, Bildiri Özleri, 22.
- Gutnic, M.; Monod, O.; Poisson, A. and Dumont, J.F., 1979, Geologique des Taurides occidentals (Turquie): Mem.Soc.GeoL.F., 58(N.S.), 112.

İZMİR-ANKARA ZONE AND KARABURUN BELT

- Konuk, T., 1977, Bornova filişinin yaşı hakkında: Ege Üniv. Fen Fak. Bull., Sen B, 1/1, 65-74.
- Marengwa, B.S., 1968, Geologie des Gebietes zwischen Işıklar and Buca östlich İzmir (Türkei): Diplomarbeit, Univ. Hamburg 70.
- Oğuz, M., 1966, Manisa Dağı'nın kuzey ve kuzeybatısının jeolojisi: Ege Üniv. Fen Fak. İlmî Rap.Ser., S3, 3-19.
- Özer, S. and İrtem, O., 1982, Işıklar-Altındağ (Bornova-İzmir) alanı Üst Kretase kireçtaşlarının jeolojik konumu, stratigrafisi ve fasiyes özellikler: Türkiye Jeol. Kur. Bull., 25, 41-47.
- Şengör, A.M.C., 1980, Türkiye'nin neotektoniğinin esasları: Türkiye Jeol.Kur. Konf.Ser., 2, 40.
- and Yılmaz, Y., 1981, Tethyan evolution of Turkey: a plate tectonic approach: Tectonophysics, 75, 181-241.
- Verdier, J., 1963, Kemalpaşa Dağı etüdü: MTA Bull., 61, 37-40.
- Yağmurlu, F., 1980, Bornova (İzmir) güney filiş topluluklarının jeolojisi: Türkiye Jeol.Kur.Bull., 23,141-152.

GEOCHEMICAL IMPLICATIONS FOR TECTONIC SETTING OF THE OPHIOLITIC ROCKS FROM THE OPHIOLITE MELANGE BELT OF THE ANKARA MELANGE

Ayla TANKUT*

ABSTRACT.— Ophiolite melange of Cretaceous age is the youngest belt of the Ankara melange and consists mainly of ophiolitic rock fragments such as serpentinite, gabbro, dolerite and basalt of varying sizes, together with pelagic radiolarites and limestones. The ophiolitic melange includes also large isolated masses which are considered to be preserved slices of oceanic lithosphere. The mafic clasts in the melange and the basic dyke rocks of an oceanic lithosphere fragment, Edige body, have comparable compositions. The petrographic and geochemical characteristics of the ultrabasic rocks of the ophiolite melange are correlated with those of depleted mantle peridotite whereas trace element contents, particularly REE, of the basic rocks are within the range of abyssal tholeiites. These ophiolites are believed to be representative of suboceanic environment. However the basic rocks, with their higher LIL and lower HFS element contents relative to MORB, demonstrate island arc characteristics. Such features imply a marginal basin tectonic setting rather than a major ocean basin for the ophiolitic rocks of the melange. The magmas of the basic rocks have most probably been generated by back arc spreading and have been modified by subduction related fluids later.

INTRODUCTION

Ophiolitic melange of Cretaceous age (Norman, 1973) is the youngest belt of Ankara melange (Fig.1) and characterized by the existence of ophiolitic rocks. The Ankara melange has been the subject of a number of publications since its first description (Bailey and McCallien, 1950). Although much attention has been paid to geological and structural features the field distribution and geochemistry of ultramafic and mafic rocks, which record important information about the original geotectonic environment, have not yet been well documented. Tankut (1985) reported limited geochemical data on the mafic volcanic clasts from the ophiolitic and metamorphic melange belts. Tankut and Sayın (1989) studied petrography and major element geochemistry of an isolated peridotite-gabbro body within the ophiolitic melange near Edige. Incompatible trace element chemistry of rocks of the same body has been discussed by Tankut and Gorton (in press) to demonstrate its similarity to oceanic lithosphere. On the other hand, the ophiolitic rocks are reported (Pearce, 1980; Saunders et al., 1980; Hawkins, 1980; Millward et al., 1984) to be generated at the major oceans or at the back arc regions (marginal basins). In this respect, no attempt has so far been made to identify the most probable tectonic setting of that body.

The purpose of the, present paper is to define the geochemical features of the ultramafic and basic rocks of the ophiolitic melange; to demonstrate the relationship between these rocks and the ultramafic and basic dyke rocks of the Edige peridotite-gabbro body; and to discuss the tectonic setting of the ophiolitic rocks of the melange, in terms of incompatible element discriminants, by comparing basic rocks of the melange with those from different geologic settings.

GENERAL FEATURES

The ophiolitic melange belt includes almost all the magmatic rock members of an ophiolite suite, such as serpentinite, occasionally unserpentinized peridotite, gabbro, mafic volcanic and dyke rocks together with pelagic radiolarites and limestones. They occur as clasts of rudite size, but, individual serpentinite lenses and detached

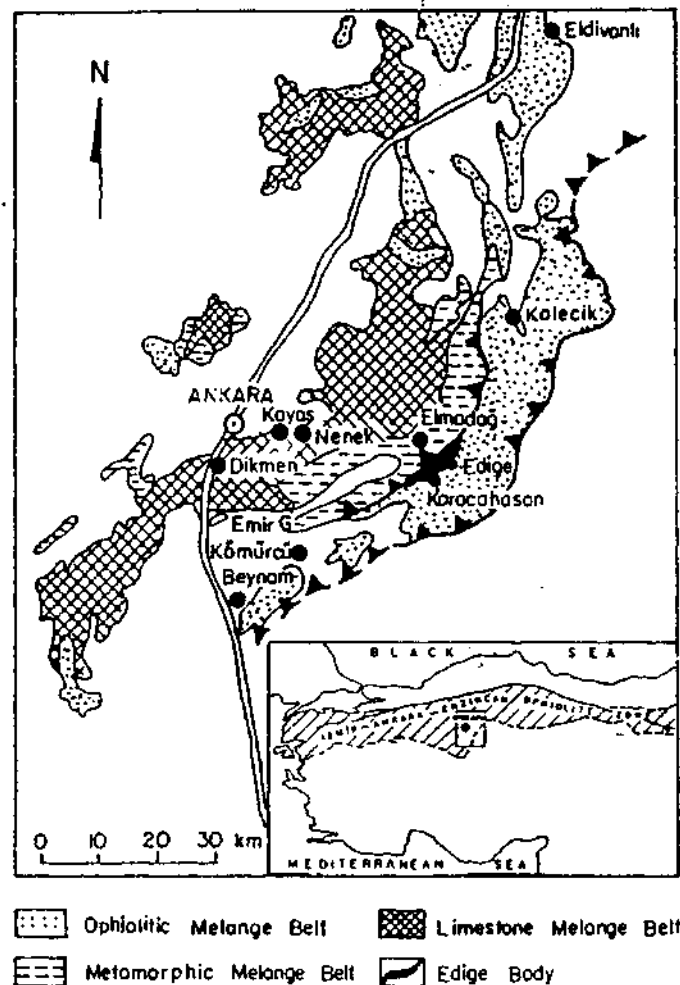


Fig.1- Distribution of Belts in the Ankara Melange (Bailey and McCallien, 1950; Çapan et al., 1983). Inset shows the location of the Ankara melange.

cumulate gabbro blocks from a meter up to hundred meters in size, are not uncommon. The melange is also reported to contain a few isolated peridotite gabbro bodies, comprising ophiolite sequences, which are considered to be preserved slices of oceanic lithosphere (Akyürek, 1981; Norman, 1985; Tankut and Sayın, 1989; Tankut and Gorton, in press). One of these bodies is located near Edige village, called Edige ultramafic body. Tankut and Sayın (1989) described it to be a north east trending lens shaped mass, 10 km in length and 0.2-4 km in width. It is constituted by an ultramafic-tectonic unit composed of ultramafic rocks only, and a mafic-cumulate unit, composed mainly of cumulate gabbros and some ultramafic rocks. Subparallel doleritic dyke rocks cut both of the units. Since the pillow lava and sedimentary sequences are missing in the body it is an incomplete sequence. Detailed geochemical study by Tankut and Gorton (in press) revealed that, it is a remnant of an oceanic lithosphere fragment in the melange.

The ultramafic rocks of the melange, the clasts within the melange and those from the Edige body, display tectonic fabrics and comprise serpentinite, serpentized harzburgite, dunite and websterite. The gabbros (clasts and those of the Edige body) show primary cumulate textures, and are commonly layered. The basic rock clasts

are basalts and dolerites. They are holocrystalline, the basalts are mostly porphyritic with low proportion of phenocrysts. Basic dyke rocks of the Edige body are dolerites. There are also vesicular and occasionally amygdaloidal mafic volcanics which are reported from Kalecik area (Tankut, 1985).

GEOCHEMISTRY

Major elements were determined on glass pellets, Sr, Rb, Zr, Nb, Y, Ni, Cr, V on powder pellets, by X-Ray fluorescence at the Geology Department of the University of Toronto, and other trace elements by the instrumental neutron activation analysis technique after irradiating the rocks in the Slowpoke Reactor of the University of Toronto according to the technique of Barnes and Gorton (1984).

Ultramafic rocks and gabbros

The trace element data of a serpentinized dunite (92 A) from the clasts in Beynam area and ultramafic rocks from the Edige body are given in Table 1. The rocks have high compatible (Cr and Ni) and very low incompatible

Table 1 Trace element contents of ultramafic rocks from the ophiolite melange

	P1	P5	92A
Nb	2.35	1.85	1.27
Zr	0.59	2.13	1.75
Sr		8.47	-
Rb	4.49	4.39	4.90
Sc		2.65	-
Cr	4450	3687	4388
Ni	2511	498	2237
V	74	100	40
La	0.4	0.1	0.16
Sm	0.02	0.02	0.51
Eu	0.9	-	0.14
Yb		0.13	0.2
Lu	0.02	0.03	0.51

P1- serpentinized harzburgite, tectonite unit, Edige body; P5- websterite, cumulate zone, Edige body; 92A- serpentinized dunite, Beynam.

element contents such that, some of the rare earth elements (REE) could not even be detected. However, the incomplete REE patterns, obtained by the elements detected, generate the "U" shape (Fig.2), typical of ophiolitic ultramafic rocks (Coleman, 1977). The profile (Fig.2) of an average of three cumulate gabbros from the Edige body (Tankut and Gorton, in press) is comparable with that of "average mafic cumulate gabbros" of an ophiolite sequence (Coleman, 1977).

Basic rocks

The geochemical data (Table 2) presents major and trace elements of the basic rocks (SiO_2 , < 52 %). The clast samples BM1 and BM5 are basalts, BM3 is a doleritic rock from Beynam area, U44 is a very fine grained do-

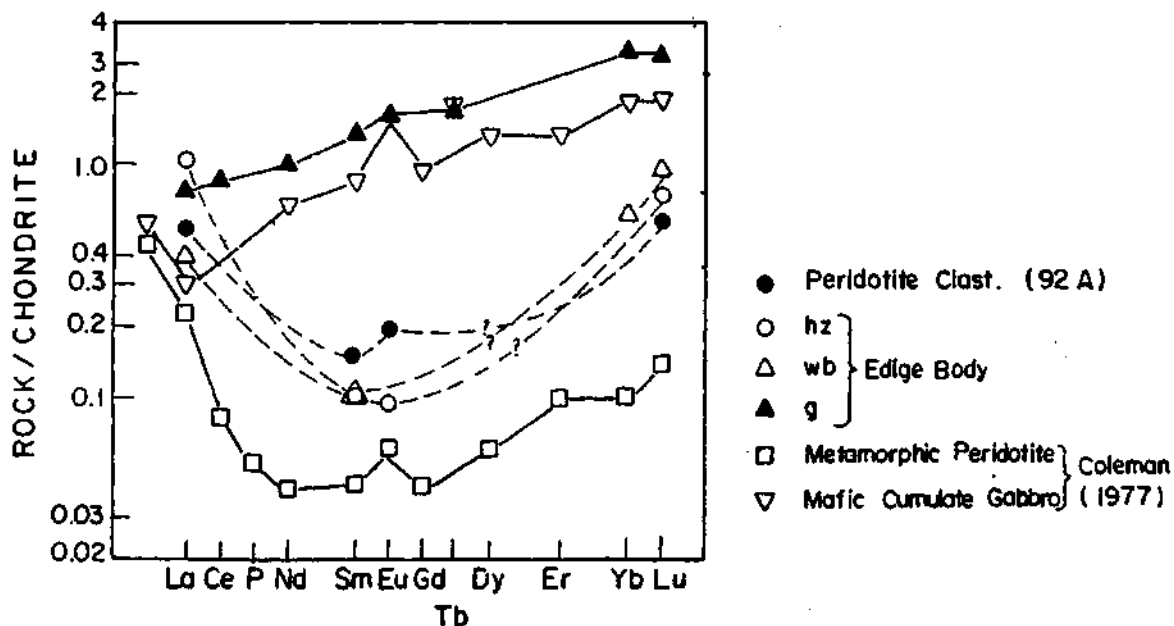


Fig.2- REE patterns of the ultramafic rocks and gabbros, from the ophiolitic melange, hz- harzburgite tectonite unit (Edge body); wb- websterite, cumulate unit (Edge body); g- averages of three cumulate gabbros.

leritic rock from Karacahasan village and EK3 is a basalt from Kalecik area. The basic rocks of the Edge body are represented by the averages of dyke rocks from the tectonite and cumulate units.

The basic rock clasts of the melange and basic dyke rocks of the Edge body have comparable compositions. Jensen (1976) plots (Fig.3) and $P2O_5$ -Zr variation (Fig.4) demonstrate the tholeiitic character of all the rocks. In the Ti/100—Zr—3Y diagram (Fig.5) the majority of the rocks fall in the ocean floor basalt (OFB) field. The

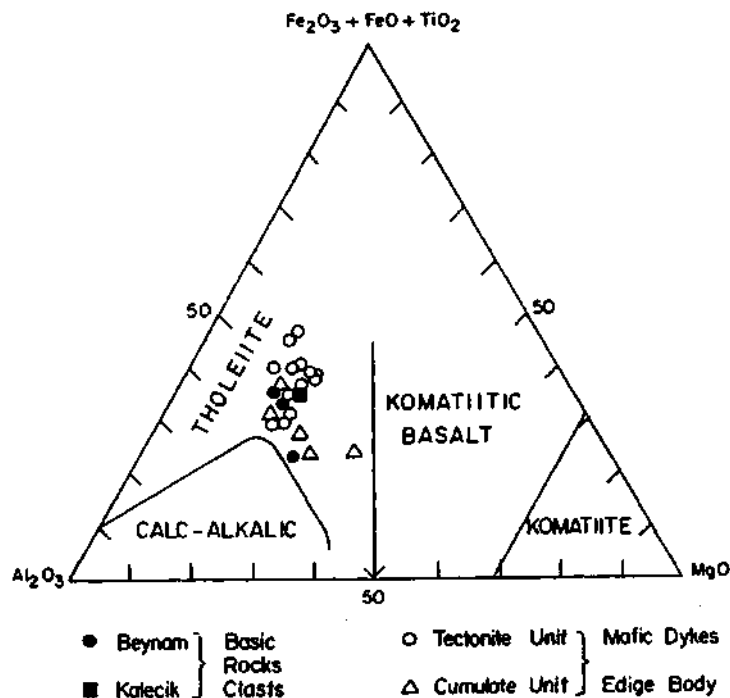


Fig.3- Jensen plots of the basic rocks from the ophiolitic melange.

Table 2— Major (%) and trace element (ppm) contents of basic rocks from the ophiolite melange

	<i>Basic Rock Clasts</i>				<i>U44</i>	<i>Edge Body</i>	<i>Dyke Ave.</i>
	<i>BM1</i>	<i>BM3</i>	<i>BM5</i>	<i>EK3</i>		<i>Tect. *</i> <i>unit</i>	<i>Cumul. *</i> <i>unit.</i>
SiO ₂	50.53	51.34	50.47	44.72	—	49.90	52.02
TiO ₂	1.12	0.26	1.13	0.75	—	1.63	0.72
Al ₂ O ₃	15.96	17.16	15.93	13.29	—	14.70	15.51
Fe ₂ O ₃ ^T	11.14	7.57	11.11	10.42	—	12.07	8.84
MnO	0.14	0.12	0.14	—	—	0.17	0.14
MgO	6.32	8.17	5.89	6.25	—	6.08	7.52
CaO	4.88	11.07	5.33	12.33	—	7.65	8.58
Na ₂ O	3.31	2.30	3.34	0.38	—	4.82	3.61
K ₂ O	0.28	0.28	0.29	5.76	—	0.35	0.26
P ₂ O ₅	0.13	0.07	0.12	—	—	0.19	0.12
LOI ^{**}	6.81	2.05	6.94	5.54	—	—	—
Total	100.62	100.39	100.69	99.44	—	—	—
Nb	3	2.6	4	4	—	4	1.5
Zr	96	21	98	112	—	104	31
Y	25	7	25	96	—	30	18
Sr	441	100	420	752	—	187	123
Rb	11	9	12	136	—	8	8
Hf	1.7	0.3	2.2	—	1.2	2	1.4
Ta	—	—	—	—	—	0.26	0.1
Cr	53	166	36	—	—	122	151
Ni	10	101	8	—	—	94	126
La	3.9	2.9	4.3	—	2.1	6	3
Ce	10.7	3.7	8.2	—	5.2	16	5
Nd	5.7	2.2	6.9	—	4.1	10	2
Sm	2.9	0.5	3	—	2.5	3.5	2
Eu	0.9	0.18	1	—	0.75	1	0.5
Tb	0.6	0.15	0.7	—	0.7	0.7	0.5
Yb	3.1	0.96	2.9	—	3.0	3.1	2.16
Lu	0.49	0.16	0.5	—	0.5	0.48	0.34

B- Beynam, EK- Kalecik, U- Karacahasan.

* Tectonite, cumulate

** Loss on ignition

Fe₂O₃^T=Total Fe₂O₃

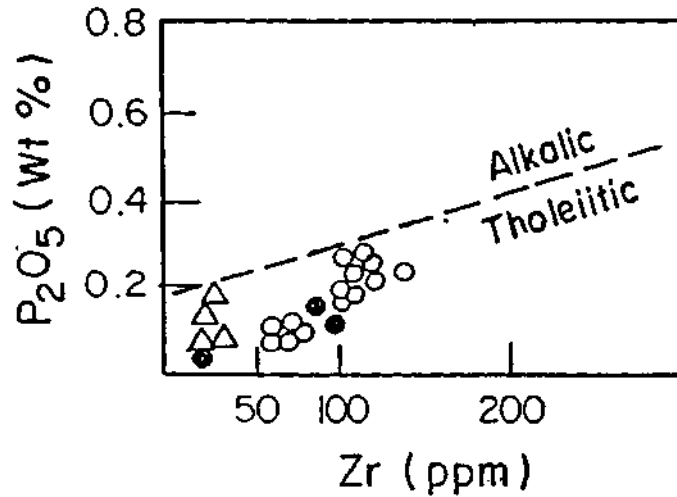


Fig.4— P_2O_5 -Zr variation of the mafic rock from the Ankara melange. The symbols are as in Figure 3 (discrimination line after Floyd and Winchester, 1975).

REE contents of the Beynam (BM1, BM3, BM5) and the Karachasan (U44) samples are within the range of the dykes of the Edge body and are comparable with the rocks of the depleted MORB (Fig.6). Only one of the Beynam samples, BM3, displays a profile with much lower values than the other rocks.

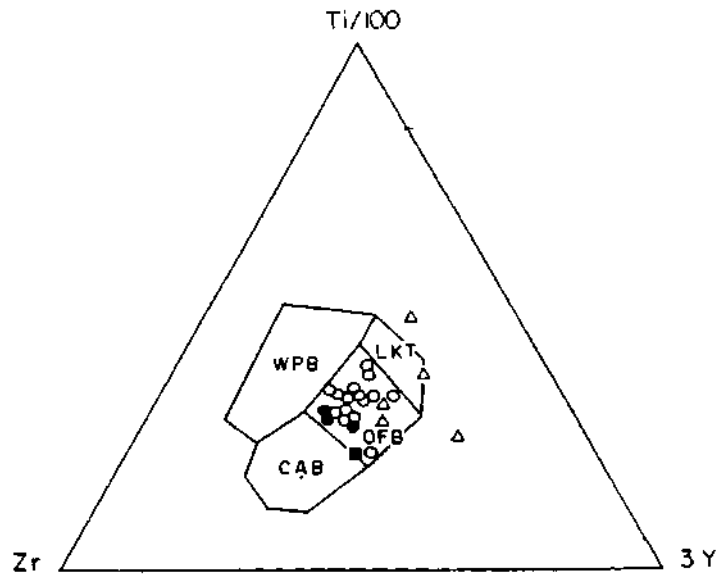


Fig.5— Ti/100-Zr-3Y variation for the mafic rocks from the ophiolitic melange. The symbols are as in Figure 3 (Pearce and Cann, 1973).

The multielement patterns (Fig.7), normalized to an average MORB composition (Pearce, 1980), of the mafic rock clasts of the melange and of the dykes from the Edge body show similarities. Most of the rocks are comparable in HFS (high field, strength) element content with MORB, except the rocks from the cumulate unit, which give similar HFS values to that of island arc tholeiite. In all the samples the content of LIL (large ion lithophile)

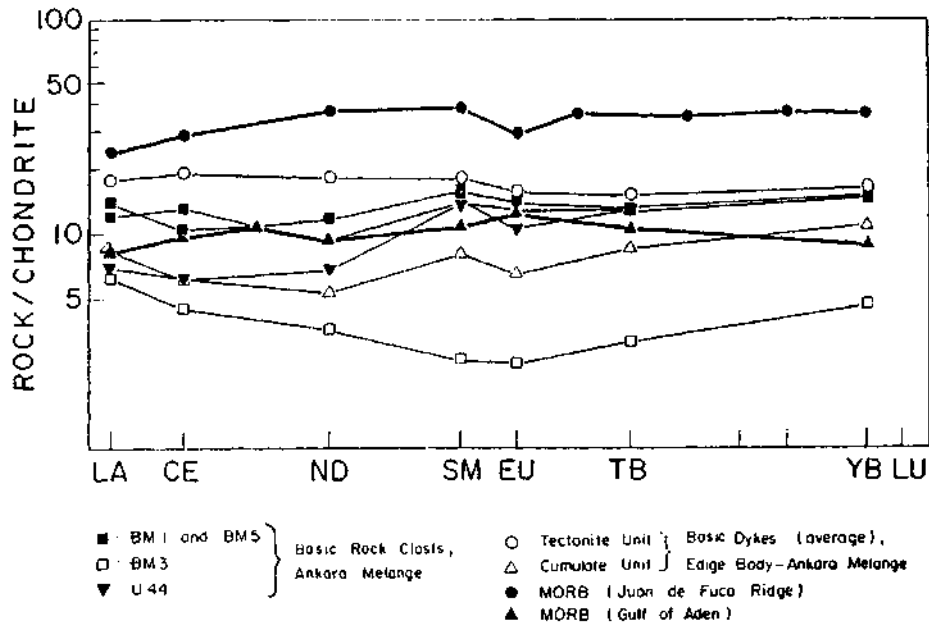


Fig.6— REE patterns of the mafic rocks from the ophiolitic melange. Values for the dykes in Edge body from Tankut and Gorton (in press), for Juan de Fuca Ridge from Pearce (1980), for Gulf of Aden from Schilling (1970).

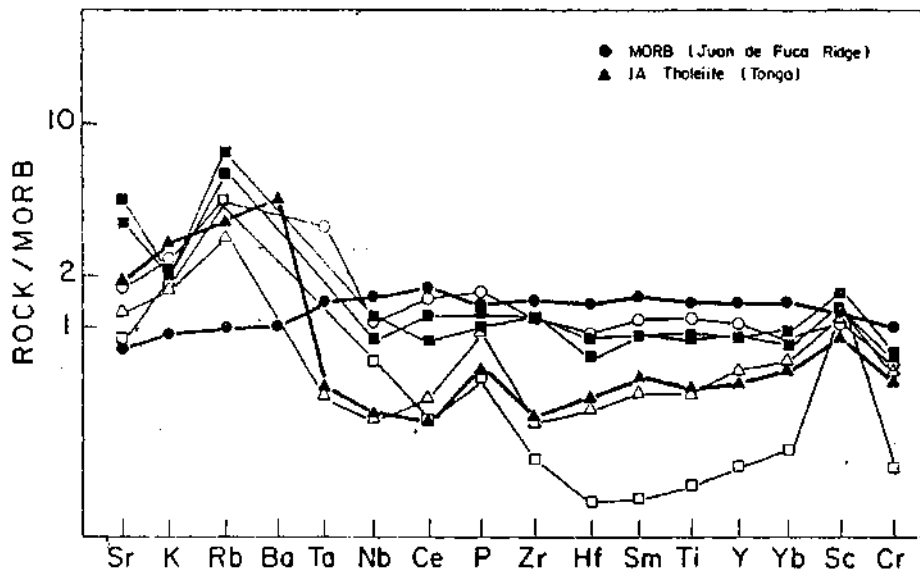


Fig.7— Multielement variation of the mafic rocks from the ophiolitic melange (values for the dykes in Edge body from Tankut and Gorton (in press); for MORB and IA from Pearce (1980)). Symbols are as in Figure 6.

elements is high compared to MORB. The plots of Ti and Y against the fractionation index Cr fall in LKT (low potassium tholeiite) and IA (island arc) fields (8a, 8b). Hf-Ta-Th variation (Fig.9) also show the intermediate features of these rocks between MORB and IAT.

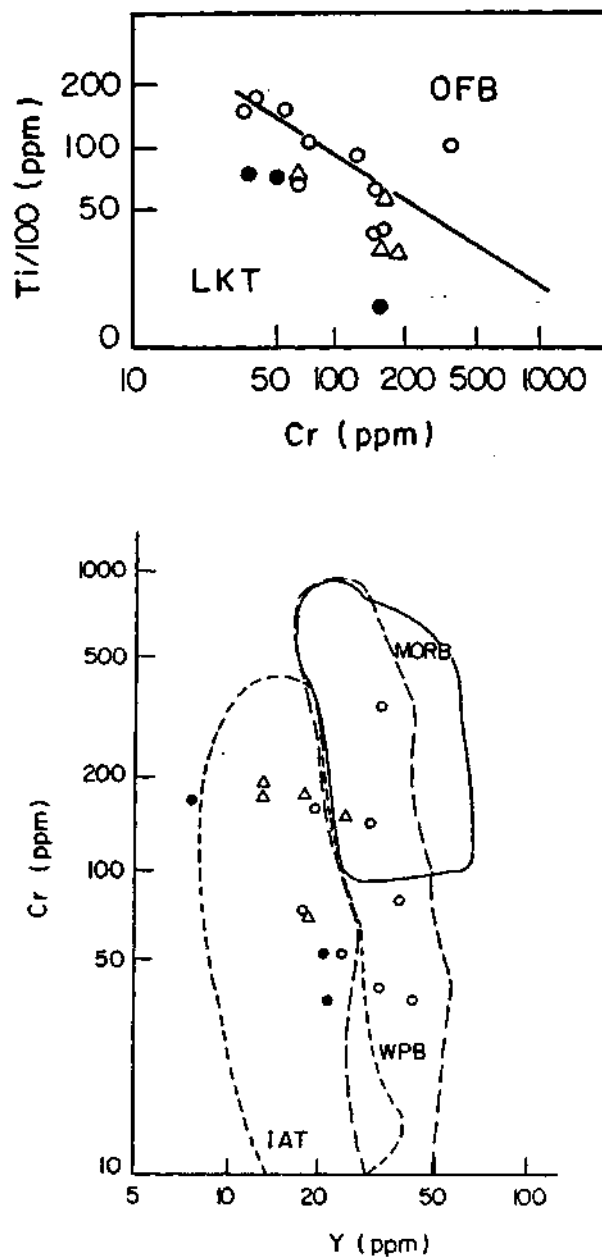


Fig.8— Ti-Cr variation of mafic rocks from the ophiolitic melange.

a- Symbols are as in Figure 3 (discrimination fields after Pearce, 1975).

b— Cr-Y variation of mafic rocks from the ophiolitic melange. Symbols are as in Figure 3 (the discrimination fields after Pearce, 1980).

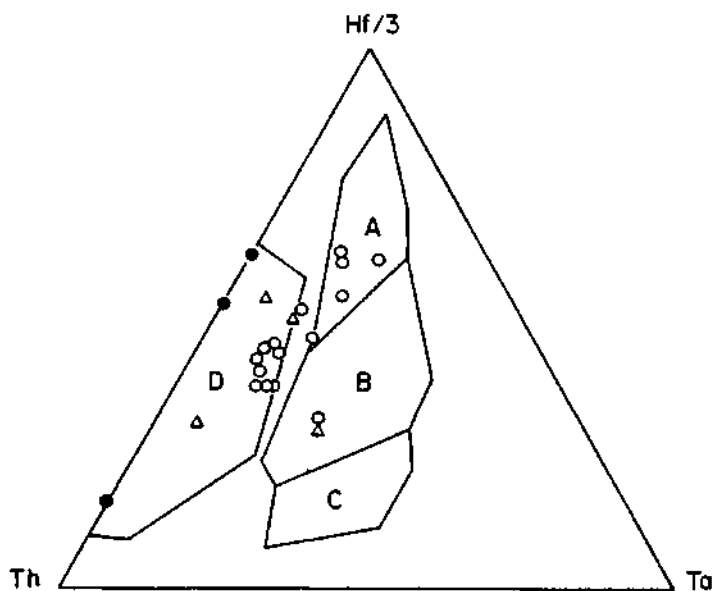


Fig.9- Hf-Th-Ta variation of basic rocks from the ophiolitic melange. Symbols are as in Figure 3. The fields:
 A- N-type MORB; B- E-type MORB; C- WP basalt; D- IA volcanics (after Wood, 1980).

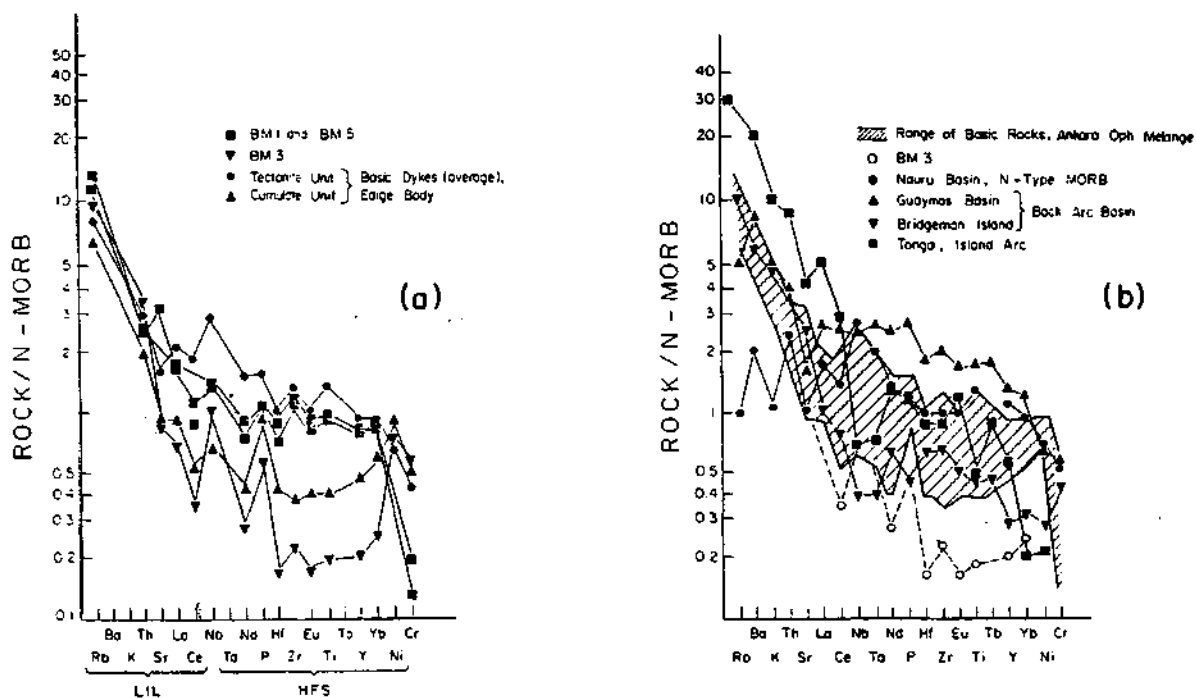


Fig.10- Multi-element variation of rocks
 a- Basic rocks from the ophiolitic melange
 b- Rocks from different tectonic settings (Millward et al., 1984).

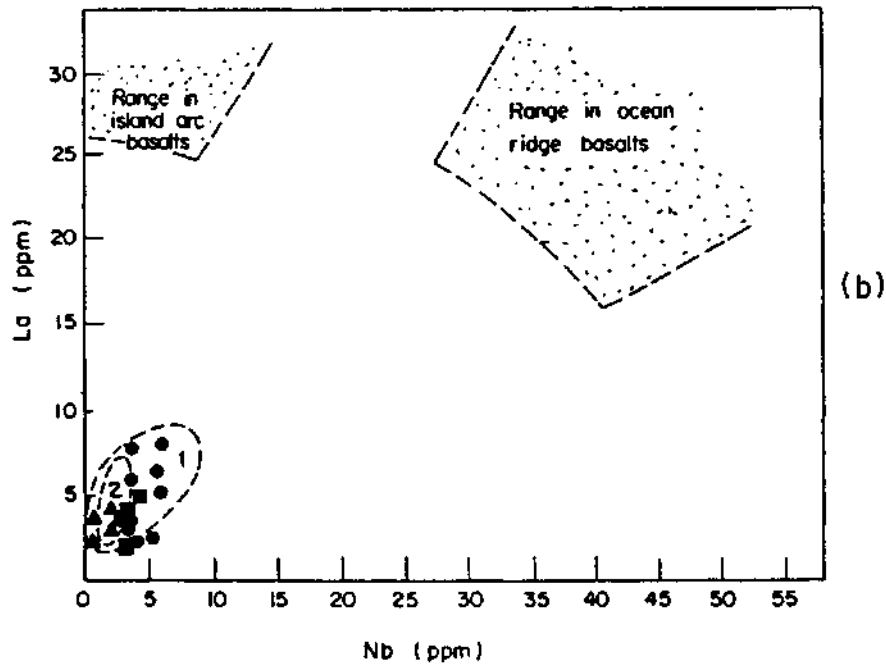
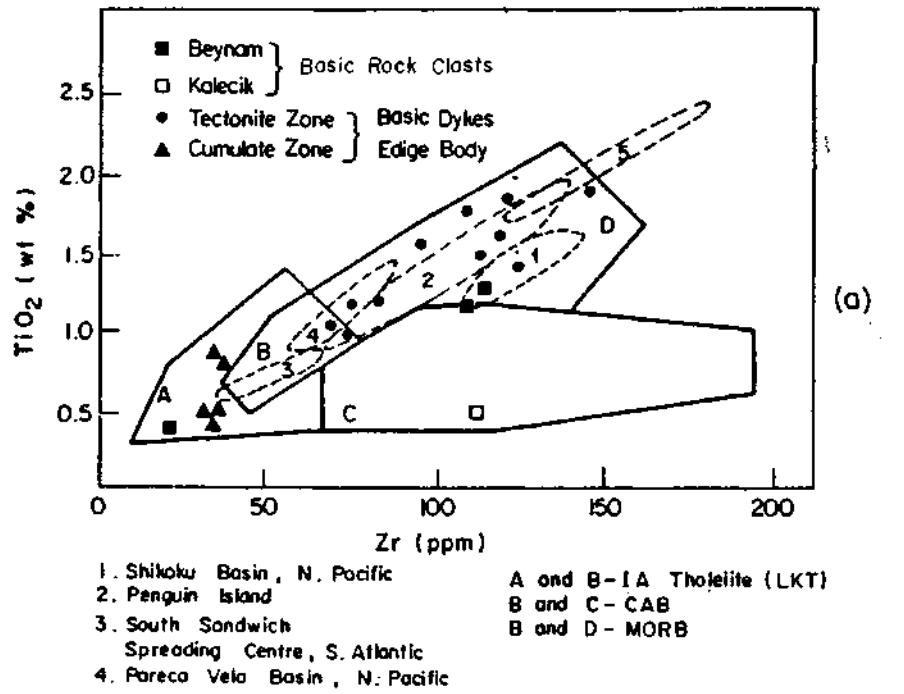


Fig.11 - Comparison of the basic rocks of the melange with basalts from various areas of known back arc tectonic settings. The symbols are as in Figure 3 (Saunders et al., 1980).

a - TiO_2 - Zr variation

b - La - Nb variation

DISCUSSION AND CONCLUSION

The large number of trace element data simply demonstrate the similarity of the ultramafic and basic rock clasts to the corresponding rocks of the lithosphere fragment called Edige body (Tankut and Gorton, in press) in the Ankara melange. According to the Ti, Y, Nb and Zr the rocks form two chemical groups. The basic rock clasts from Beynam and Kalecik, and basic dyke rocks from the tectonite zone of the Edige body have the higher concentrations of these elements particularly of Zr, whereas, the basic rock clasts BM3, except its very low HFS content, somewhat resembles the dyke rocks from the cumulate zone of the lithosphere fragment. Such compositional variation between the two groups may imply different MORB type of magma sources, which have possibly been produced by variable degrees of partial melting from the oceanic upper mantle. The rocks with low Zr, Ti, Nb, Y have higher Ni and Cr contents relative to those with high Zr, Ti, Nb, Y therefore, seem to be less fractionated and may represent the more primitive source. The possibility of formation of the two groups from a common magma by differentiation can not be tested in the light of the available data. However the relationship of the two groups will also be better understood with isotope studies and with precise radiometric age determinations of the rocks.

On the other hand, the island arc signature, revealed by LIL, HFS distribution (Fig.7), implies a magma type, transitional between abyssal tholeiite and arc tholeiite for the above discribed two groups of mafic rocks. Millward et al. (1984) compared the chemical composition of basaltic rocks from various modern tectonic environments, using the multielement plots normalized to N-type MORB (Fig.10 a, b). The patterns of high-Zr group display similarity to Bridgeman island whereas the low-Zr group to Guaymas Basin basalts, both areas are reported to be of back arc type of basins (Millward et al., 1984). Saunders et al.(1980) plotted the basalts from various back arc tectonic environments and defined discrimination fields on the Zr-Ti₂ diagram of Pearce and Cann (1973). The plots of the high-Zr group rocks fall in the fields of characteristic back arc basin basalts (Fig. 11 a). Similarly, the La-Nb, discriminants (Saunders et al.,1980) also indicate the back arc setting (Fig. 11 b) for all the rocks. In the Eastern Mediterranean part of the Tethyan domain, Hatay, Baer-Bassit (Delaloye and Wagner, 1985) and Oman (Pearce, 1980) are defined to show features in common with the back arc basins.

Finally, all the evidences discussed above may lead to the conclusion that the studied ophiolitic rocks of the melange have possibly been formed by back arc spreading in a basin close to the subduction zone where the source magmas of the basic rocks were modified by subduction related contamination.

ACKNOWLEDGEMENT

The author wishes to thank Drs. M.P. Gorton, C. Cermignani, R. Hancock for their help during the analytical part of the work. Prof. T. Norman is thanked for valuable discussions. Drs. A. Türkmenoğlu, Mr. N. Sayın, acknowledged with thanks for their help in various stages of the work.

The gratitudes are extended deeply to Prof. T. Tankut and Prof. M. Üzümeri for their kind concern.

Manuscript received January 18, 1989

REFERENCES

- Akyürek, B., 1981, Ankara melanjının kuzey bölümünün temel jeoloji özellikleri : İç Anadolu'nun jeolojisi. Simpozyum Tebliğler Kitabı, TJK 35.Bilimsel ve Teknik Kurultayı, Ankara-Turkey.
- Bailey, E.B. and McCallien, W.J., 1950, The Ankara Melange and the Anatolian Thrust: Nature, 166, 938-940.

- Barnes, S.J. and Gorton M.P., 1984, Trace element analysis by neutron activation with a low flux Reactor (Slowpoke—II). Results for International Reference Rocks: *Geostandards Newsletter*, 8, 1, 17-23.
- Coleman, R.G., 1977, *Ophiolites*. New York, Springer Verlag, 229 p., New York.
- Capan, U.; Lauer, J.P. and Whitechurch, H., 1983, Ankara melanjı (Orta Anadolu): Tetis kapanışını belirlemede önemli bir eleman: *Yerbilimleri*, 10, 35-43.
- Delaloye M. and Wagner, J.J., 1985, *Ophiolites and volcanic activity near the western edge of the Arabian plate*: Dixon J.E. and Robertson A.H.F., ed., *The Geological Evolution of the Eastern Mediterranean* : Special Publication of the Geological Society, 17, Blackwell Scientific Publications, 848 p., 225-233.
- Floyd, P.A. and Winchester, J.A., 1975, Magma type and tectonic setting discrimination using immobile elements: *Earth Planet. Sci. Lett.*, 27, 211-18.
- Hawkins, J.W., 1980, Petrology of back-arc basins and island arcs: Their possible role in the origin of Ophiolites. In: Panayiotou, A. ed., *Ophiolites*, *Proc.Int.Oph.Symp. Cyprus 1979*, 244-272.
- Jensen, L.S., 1976, A new cation plot for classifying subalkalic volcanic rocks: Ontario Division of Mines, Geological Report 66, 1-20.
- Millward, D.; Marriner, G.F. and Saunders, A.D., 1984, Cretaceous tholeiitic volcanic rocks from the Western Cordillera of Colombia: *J.GeoLSoc.London*, 141, 847-860.
- Norman, T., 1973, Ankara Yahşihan Bölgesinde Üst Kretase-Alt Tersiyer Sedimentasyonu: *TJK Bull.*, XVI, 1, 41-66.
- , 1985, The role of the Ankara Melange in the development of Anatolia (Turkey); Dixon J.E. and Robertson A.H.F., ed., *The Geological evolution of the Eastern Mediterranean* : Special Publication of the Geological Society, 17, Blackwell Scientific Publications, 884 p., 441-447.
- Pearce, J.A., 1975, Basalt geochemistry used to investigate past tectonic environments on Cyprus : *Tectonophysics*, 25, 41-67.
- , 1980, Geochemical evidence for the genesis and eruptive setting of lavas from Tethyan Ophiolites: Panayiotou, A.Ed., *Ophiolites: Proc.Int.Oph.Symp., Cyprus 1979*, 702-713.
- and Cann, J.R., 1973, Tectonic setting of basic volcanic rocks determined using trace element analyses: *Earth Planet. Sci.Lett.*, 19, 290-300.
- Saunders, A.O.; Tarner, J.; Marsh, N.G. and Wood, O.A., 1980, Ophiolites as ocean crust or marginal basin crust: A geochemical approach: Panayiotou, A., ed., *E.Ophiolites Proc.Int.Sph.Symp., Cyprus 1979*, 702-7 13.
- Schilling, J.G., 1970, Sea-floor evolution: rare earth evidence: *Proc.Symposium Petrology of Igneous and Metamorphic Rocks from the Ocean Floor*. London, 1969.
- Tankut, A., 1985, Basic and ultrabasic rocks from the Ankara Melange, Turkey: Dixon, J.E. and Robertson, A.H.F., ed., *The Geological Evolution of the Mediterranean: Special Publication of the Geological Society*, 17, Blackwell Scientific Publications, 884 p., 449-454.
- and Sayın, M.N., 1989, Edige ultramafik kütlesi: *Turkish Journal of Engineering and Environmental Sciences*, 13/2, 229-244.
- and Gorton, M.P. (in press), Fragment of Tethyan oceanic lithosphere in Ankara Melange Turkey : ed., Moores, *Proc. Symposium Troodos 87, Ophiolites and Oceanic Lithosphere*. Nicosia, Cyprus October 5-10, 1987.
- Wood, D.A., 1980, The application of a Th-Hf-Ta diagram to problems of tectonomagnetic classification and to establishing nature of basaltic lavas of the British Tertiary Volcanic Province *Earth Planet. Sci.Lett.*, 50, 11-30.

IMPLICATIONS ON GEOLOGY, GENESIS AND ORIGIN OF ÇAYIRLI MANGANESE DEPOSIT, ANKARA, CENTRAL ANATOLIA

Vedat OYGÜR*

ABSTRACT.— Çayırli manganese deposit occurs in radiolarite related to Ankara ophiolitic melange of Lower Cretaceous-Upper Cenonian age. The ore body consistent with the host rock is located in the minor folds within this unit. The ore minerals are pyrolusite and psilomelane. Regarding the chemical composition of the ore, it appears that the ore is Mn-rich ($Fe/Mn < 0.1$) and resembles to the deposits precipitated rapidly from the hot aqueous solutions near the submarine hydrothermal sources. The barium content of the deposit is higher than that of the normal seawater. In addition, the concentrations of the elements such as Ni, Co and Cu are lower than that of the present-day hydrogenous manganese deposits. According to these data, it might be suggested that Çayırli manganese deposit is formed by the hydrothermal convection processes at the seafloor spreading centers.

FEATURES AND ORIGIN OF BİLLURİK DERE (ELAZIĞ) MINERALIZATIONS

Ahmet ŞAŞMAZ* and Ahmet SAĞIROĞLU*

ABSTRACT.— Mineralization of Billurik dere is located in and on the contact zone of granitic and dioritic magmatics of the Yüksekova complex. The mineralization which occur in the magmatic, emplaced along E—W striking tension fractures and of vein type in nature. The mineral assemblages of these veins are pyrite, chalcopyrite, sphalerite, galena, magnetite, specularite and some of these minerals are dominant ore minerals in some veins. The mineralizations which occur on the contact zones are contact type in nature and they bear additional minerals such as Cu-sulphosalts, Bi-sulphosalts and Ag-fahlore. The mineralizations are associated with serialization, kaolinization, silicification, tourmalinization and epidote formation. The mineralizations developed possibly during thrusting of the Keban metamorphics on the Yüksekova complex in a time span from Upper Cretaceous to Paleocene and related with the tectonic evolution of the area.

INTRODUCTION

The Billurik dere mineralizations which are the subject of this study, placed approximately 25 km. north of Elazığ township (Fig.1). The mineralizations occur in the Yüksekova complex and show various features. The

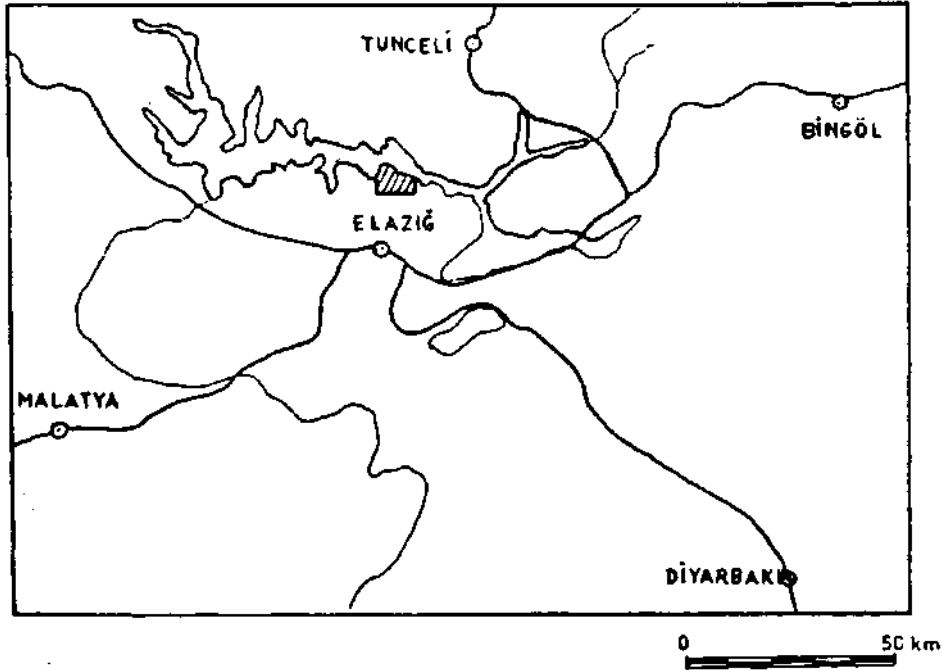


Fig.1— Location map.

mineralizations have not been studied before and because of their small size they have not attracted interests of the mining sector. However, Eastern Taurus belt where the mineralizations placed, is studied by many workers for various reasons: Perinçek (1979), Hempton and Savcı (1982), Yazgan (1981,1984), Bingöl (1982,1984), Asutay

(1985) and Akgül (1987) studied petrological and petrographic aspects of the Yüksekova complex. Published first studies of the mineralizations of the Yüksekova complex in Elazığ- vicinity were carried out by Sağiroğlu (1986, 1987) on the Kızıldağ (Elazığ) mineralizations.

Within the framework of this research following studies, were carried out; geological mapping of Billurik dere vicinity in 1: 25.000 scale, structural analysis of the area, and, mineralogy and petrography of country rocks, mineralized bodies and alteration zones. In the light of findings of these studies a mineralization model and origin of the mineralization are discussed.

LITHOLOGY

Coniasian-Campanian Yüksekova complex forms the basement rocks of the studied area. Middle to Upper Eocene Kırkgeçit formations overly the complex with angular disconformity'and are covered by Upper Miocene Karabakır basalts in places (Fig.2).

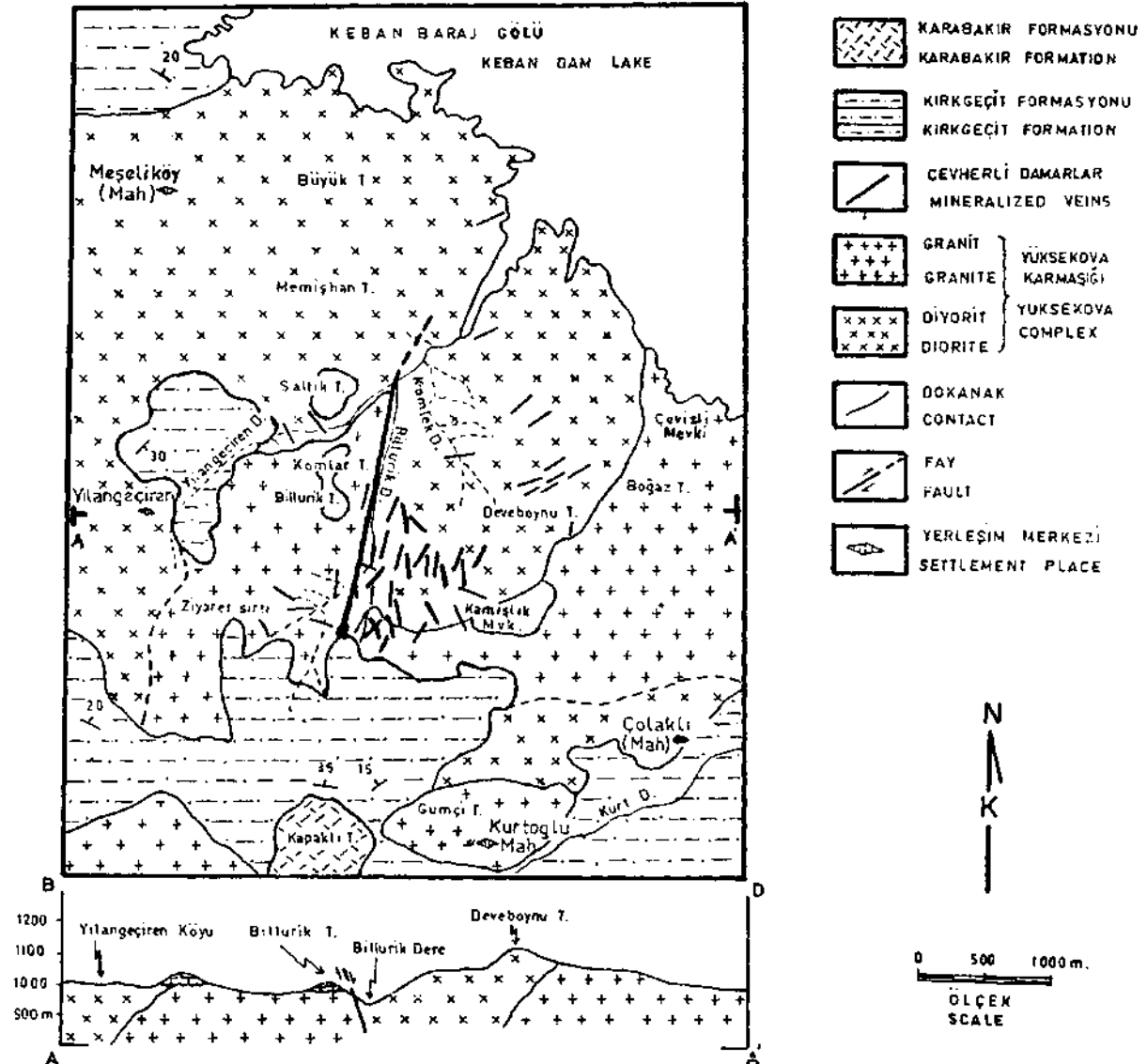


Fig.2 Geology and cross-section of the studied area.

The Yüksekova complex

This complex was first described by Perinçek (1979) and its typical locality is Yüksekova (Hakkari) area.

The complex is the dominant unit in the studied area and covers large areas around Yılangeçiren and Meşeliköy villages, Boğaz Tepe and Billurik Dere. The complex is made up from various units in Elazığ region. The rocks of the complex are studied in three groups in this study. These are; granitic rocks, dioritic rocks and subvolcanics (aplites and microdiorites) what cut the first two.

Granitic rocks.— These rocks occur in the middle and eastern parts of the studied area and are distinguished easily by their lighter colours. Equigranular texture is the dominant texture of these rocks. Mineral constituents of these rocks are quartz, K—feldspar, plagioclase, biotite and amphibole. Accessory minerals are zircon, apatite, sphene and magnetite.

Dioritic rocks.— Felsic minerals of these rocks are plagioclase and quartz and mafic minerals are amphibole. Although compositions of these rocks vary between monzonite-diorite it is not possible to determine these variations macroscopically. Dioritic rocks show different textures, granular texture being the most common. Another common feature of dioritic rocks is extensive alteration.

Subvolcanic rocks.— The plutonic rocks of the studied area are cut by aplites and microdiorites whose thicknesses are 1 to 200 cm. According to K/Ar radiometric dating of Yazgan (1984) the subvolcanic rocks of Baskil area, which are thought to be equivalent of the subvolcanic rocks of the studied area, are of Campanian age.

The Kırkgeçit formation

This formation first described by TPAO geologists and named after its typical locality in the south of Van (Tuna, 1979). Kırkgeçit formation overlies Yüksekova complex with an angular unconformity. Its lithologies are conglomerate, sandstone, sandy limestone, limestone and marble from the bottom to the top. According to paleontologic studies of Avşar (1983) the formation is of Middle to Upper Eocene.

The Karabakır formation

This unit first described by Naz (1979) in Karabakır village of Pertek. In the studied area the Karabakır formation is represented by basaltic lava flows. Sirel et al. (1979) gave Upper Miocene age to this unit on the basis of the fossils they found in this unit around Palu.

STRUCTURAL GEOLOGY

In the studied area magmatic rocks form the basement and therefore fractures are the major structural features instead of folding. The Yüksekova complex fractured densely because of tectonic movements. Analysis of the strikes of the fracture planes indicate that the main fracture strikes are in N20° to 40° E (Fig.3). Because of extensive alteration minor fracture and fault planes are not openly visible. The main fault in the studied area is the one which strikes parallel to Billurik dere. This fault can be traced from the surface along a length of 2 km and forms the contact line of granite and diorite. This fault is thought to be a gravity fault, however its displacement distance can not be determined (Fig.2). The Kırkgeçit formation is not affected from the faulting and for the equivalents of the granites and diorites in Baskil Yazgan (1984) gave Coniasian-Campanian age. Therefore it is reasonable to conclude that the faultings took place during a time span of end of Cretaceous-Paleocene. This age

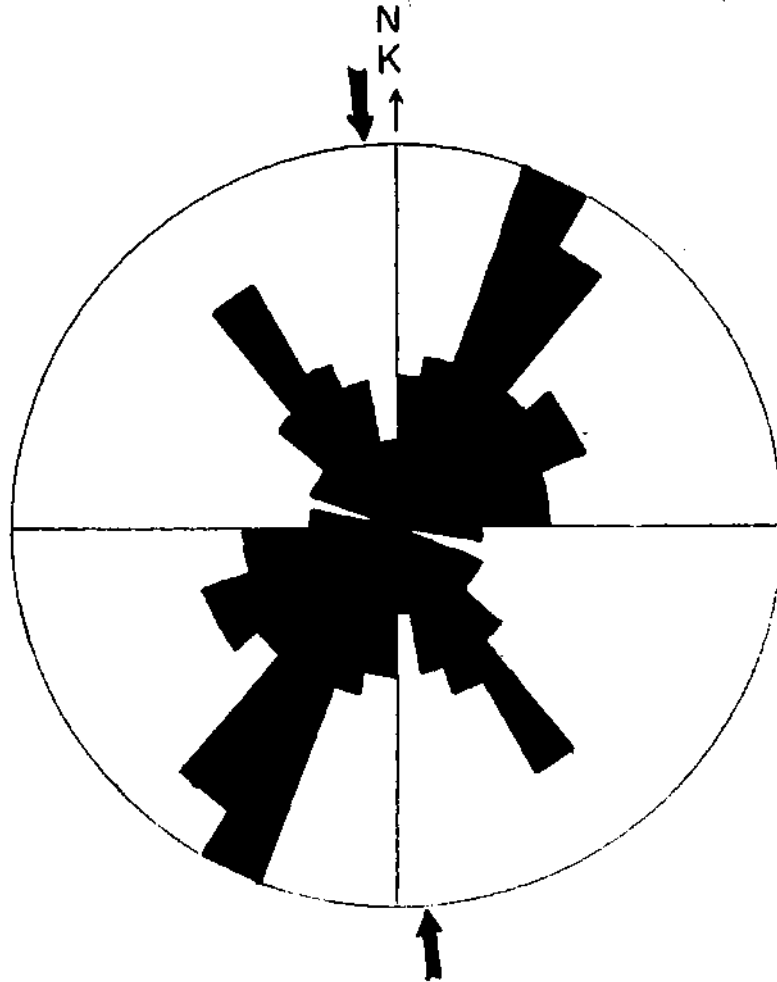


Fig.3– Joint diagram of Yüksekova complex (total measurements 100).

span is given by Yazgan (1984) as the period during which the Keban metamorphics thrust over the Yüksekova complex.

The Kırkgeçit formation show good layering which strikes E–W and dips to north with angles between 15–30°.

The analysis of the fractures strikes show that they concentrate in two maximums at 25° and 325° (Fig.3). Thus, the main compression direction was N–S and the area gained its structural pattern with this compression. This direction is in good agreement with the compression direction determined by Tatar (1986) for the Elazığ region, using the fracture analysis techniques on Lanstad remote sensing images. This compression should be the cause of the thrusting of the Keban metamorphics over to the Yüksekova complex.

MINERALIZATION

Although numerous mineralizations are known in the Yüksekova complex in Elazığ region, published studies on these mineralizations are scarce. The first studies of this kind carried out by Sağiroğlu (1986, 1987) on the Kızıldağ (Elazığ) mineralizations.

Billurik dere mineralizations are located in granitic and dioritic rocks and on the contact zone of granite

and diorite, of the Yüksekova complex. The first ones are vein type and the second ones are contact type mineralizations. The mineralizations are studied in 3 groups on the basis of their placements:

The mineralizations in granitic rocks

These are vein type and occur around Ziyaret Sırtı densely (Figs.2 and 6). The thicknesses of the mineralizations vary between 10-30 cm and their continuations on the surface are 4 to 5 m. The mineralizations are placed in the joints and fractures and the exposed parts are completely oxidized. Their textures are either stockwork or disseminated type. The ore minerals of this group are; galena, sphalerite, chalcocopyrite, pyrite and specularite.

Galena.— Galena is found in veins of 7-8 cm thicknesses and as large (0.5 cm) euhedral crystals. Galena replaces the chalcocopyrite exsolutions in sphalerite and as a result chalcocopyrite grains are placed on the borders of galena-sphalerite grains (Plate I, fig.1). The galena is altered to anglesite and cerussite along its grain boundaries and cleavage planes. This replacement causes the kidney-like textures to form in galenas.

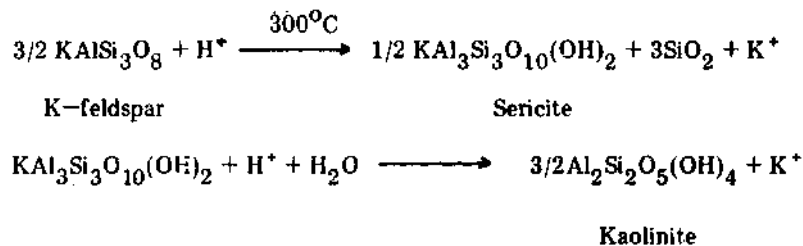
Sphalerite.— This is a rare mineral in the veins placed in granitic rocks. Their grain size vary between 0.3-0.5 mm and they are often altered to smithsonite along their grain boundaries. Some sphalerites bear chalcocopyrite exsolutions (Plate I, fig.1).

Chalcocopyrite.— Found along joints of granitic rocks. Their grain sizes are in 0.5 to 1 mm and they bear galena inclusions of 100 to 150 μ in size. Chalcocopyrite also accommodate "sphalerite stars" (Plate I, fig.2) what are interpreted as indicators of high temperature formation (Ramdohr, 1980,p.529). In the exposed portions chalcocopyrite is altered to chalcocite-covellite first then to limonite (Plate I, fig.3).

Pyrite.— This is the earliest forming ore minerals in the granitic rocks. Their grain sizes are between 1-2 mm and they are euhedral. The pyrites are replaced by chalcocopyrite and therefore they are older than chalcocopyrites (Plate I, fig.4).

Specularite.— Specularite is found as thin covers on fracture walls. Average grain size is about 0.5 mm and grains have tabular shapes.

In the granitic rocks sericitization and kaolinization accompany to the mineralizations. These two alteration take place according to the following chemical reactions under 300°C (Barnes, 1979, p.195);



K—feldspar is altered to the sericite first and then to the kaolinite. This alteration stages can be easily determined under the microscope.

The mineralizations in dioritic rocks

Most of the mineralized bodies of the studied area are found in the dioritic rocks. The mineralized zones are again covered by gossans. Almost always an altered zone is present between mineralized body and country rocks

(Plate I, fig.5). The thicknesses of the mineralized zones change a great deal; from a few cm to 10 m and their exposure lengths can reach up to 40-50 meters. The strikes of the mineralized bodies (veins) are NNE—SSW. The mineralized bodies of the dioritic rocks have disseminated or stockwork textures and poor mineral assemblages; pyrite, magnetite, hematite and chalcopyrite.

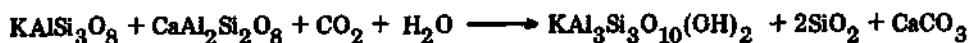
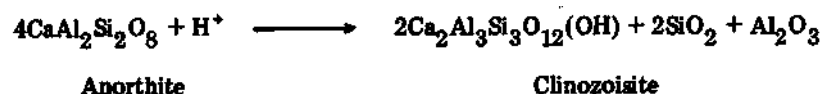
Pyrite.— Its average grain size is 2-3 mm and often accomodates magnetite inclusions. Most of the pyrites are altered to limonite in the upper parts of mineralized bodies.

Magnetite.— Magnetite is usually found together with pyrite along the mineralized fracture zones. The magnetites are usually found in radiating pyramatic shapes (musketovite). The marginal parts of the magnetite grains show martitization. The magnetites are strongly magnetic.

Hematite and chalcopyrite are scarce minerals in the dioritic rocks. Hematite occurs as granular masses and chalcopyrite as minute grains.

The alteration types observed along the mineralized zones of the dioritic rocks are epidotization, chloritization and carbonatization. The altered parts usually placed along the mineralization-country rocks border.

Epidote and carbonate are thought to be formed as consequences of the following reactions (Winkler, 1979, p.149).



The mineralizations along granite-diorite border

These mineralizations are of contact type. The ore texture is either disseminated or stockwork type; first type is found in the country rocks and second type along joints and fractures. The ore mineral assemblage of this type mineralization differs from the first two types and some additional minerals; Ag-fahlore (freibergite), Cu-sulphosalts and Bi-sulphosalts occur. The dominant minerals of the mineralizations along granite-diorite border are chalcopyrite, galena and sphalerite (Plate I, fig.6).

Galena.— This is the most dominant mineral along the contact and bears Ag-fahlore (freibergite) inclusions (Plate I, fig.7). The grain sizes of the inclusions are about 12-30 μm and inclusions are found as replacing chalcopyrite.

Sphalerite.— Sphalerite is present as large (1-1,5 cm) crystals and because of low Fe-content their internal reflections are white to light brown.

Cu-sulphosalt— It is found as replacing the chalcopyrite which occur along the cracks of pyrite grains (Plate I, fig.8). Its colour is beige and probably it is emplectite.

Bi-sulphosalt.— It is found as minute pyramatic grains along the fractures of pyrite and chalcopyrite (Plate I, fig.8). Because of their very small grain sizes it is difficult to determine their kinds. However, they are strongly anisotropic and their colour creamy white and therefore they resemble bismuthinite, aikinite and cosalite.

The alteration products occur with this type of mineralizations are; epidote, carbonate (calcite), sericite, kaolinite and silica.

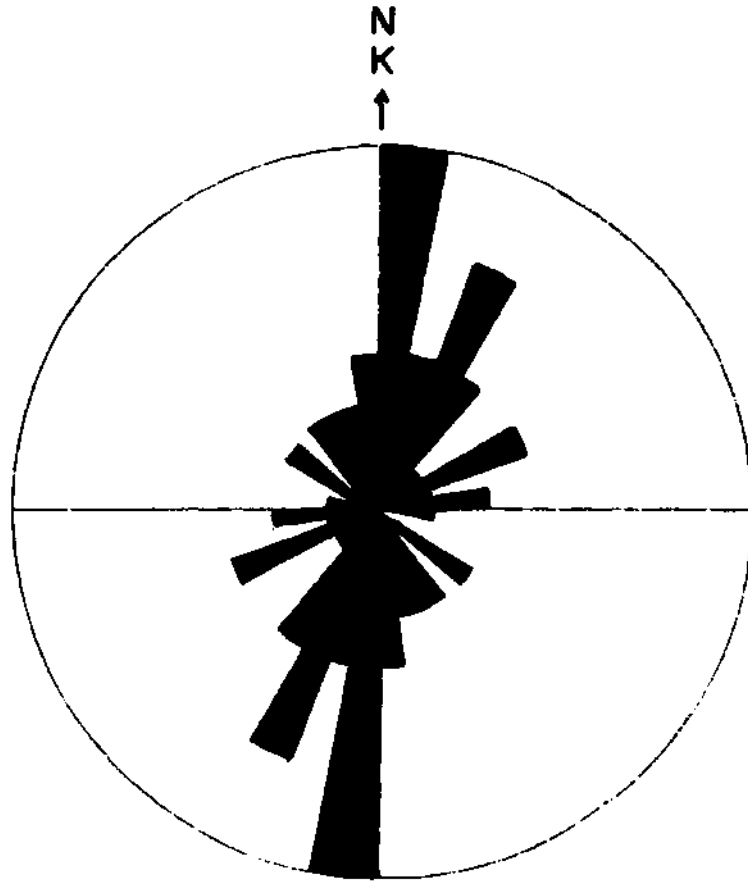


Fig.4— Analysis of the joint diagrams of mineralized zones.

THE STRUCTURAL GEOLOGY-MINERALIZATION RELATIONSHIP

As indicated before the mineralizations are placed in the fault and fracture zones. Because of close connection between structural geology and mineralization structural elements of the studied area are analyzed (Structural Geology part and Fig.3). In addition, strikes of the 38 exposed veins are analyzed (Fig.4) and correlated with structural analysis (Fig.5).

Most of mineralized veins strikes in N—S. As discussed before the main stress direction what caused fracturing in the area is N to S. Therefore, the fractures in Figure 5 represent shear fractures and the mineralized veins are tension fractures instead of shear fractures. This should be due to the suitability of tension fractures to the movement of the mineralized solutions.

DISCUSSIONS AND CONCLUSIONS

1— The analysis of fracture plane strikes (Fig.3) indicate that the area was subjected to a N—S (355°) compression. Evidences show that the compression took place during Coniasian-Middle/Late Eocene. These conclusions are in good agreement with the conclusion of the researchers who worked in the region (Yazgan, 1984; Sagirolu, 1986).

2— The geometry of the faults is in agreement with the areal structural geometry. The compression period coincides with the period, according to Yazgan (1984) and Bingöl (1984), during which the Keban metamorphics were thrust over the Yüksekova complex.

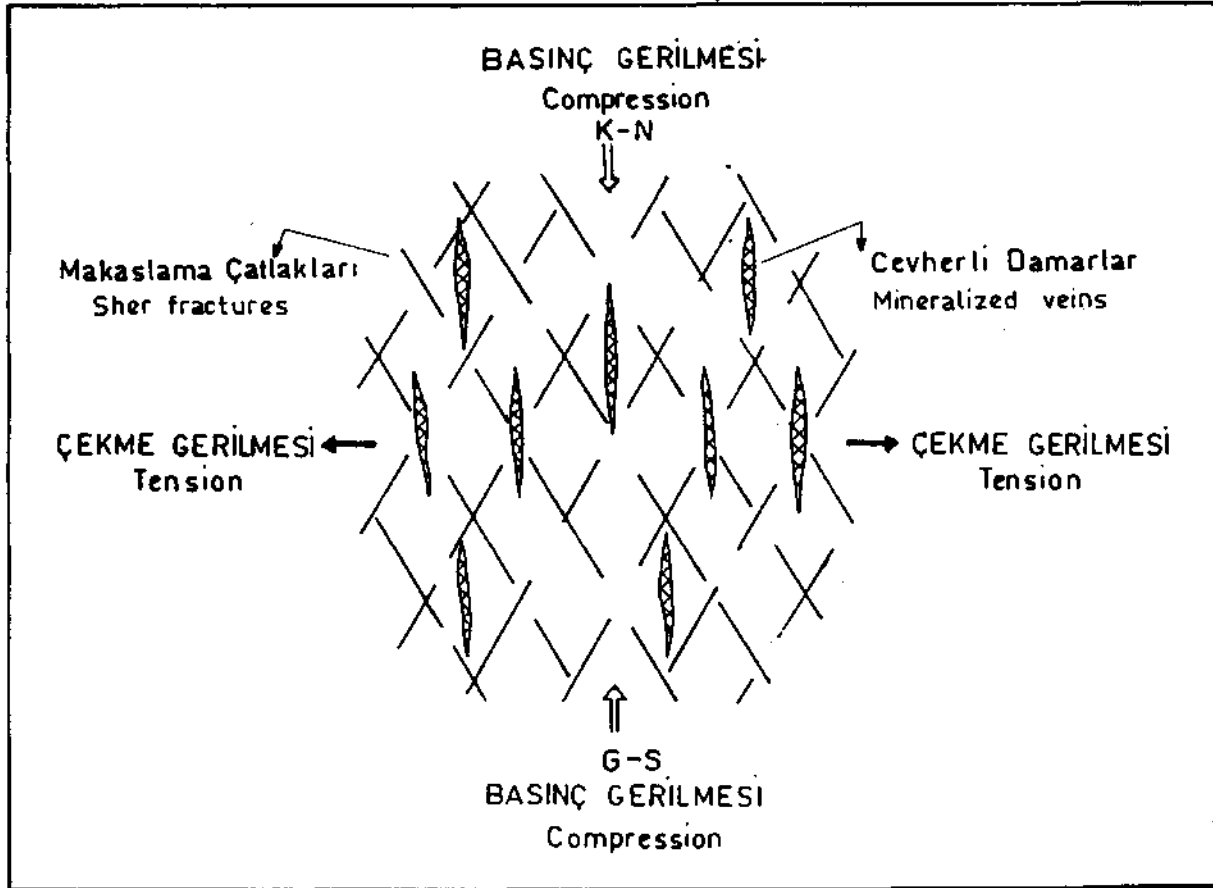


Fig.5— The relationship between main fractures and mineralized veins.

3— The mineralizations of Billurik Dere are related to the faults and the contact between the granite and the diorite. The analysis of the strikes of mineralized veins (Fig.4) indicates that the fractures are in N—S dominantly. The correlation between the mineralized veins analysis and general fracture analysis show that mineralized veins are placed in the tension fractures which formed by tension in E—W direction.

4— The mineralizations were formed with two different mechanisms and periods. The first period was emplacement period of the granites into the diorites and during this emplacement deep-seated hydrothermal solutions formed mineralizations along the contact zone. Therefore, in the contact zone high temperature minerals (Cu and Bi-sulphosalts, tourmaline, epidote and quartz veins), sphalerite with chalcopyrite inclusions and chalcopyrites with sphalerite stars were formed. All of these evidence indicate a formation temperature of 350° to 450°C.

In the second period the Keban metamorphics thrust over to the Yüksekova complex and as a consequence the granites and the diorites of the complex were densely faulted and fractured. During these events magmatism was in progress and the fault zones and fractures were mineralized and veins type mineralizations were formed. The ore mineral assemblage and the related alterations of this type indicate a formation temperature in a region 300°350°C.

5— The reserves of Billurik dere mineralizations are small with what is seen on the surface they do not have an economic importance. However, the mineral assemblage and reserves may change with depth (Evans, 1980,

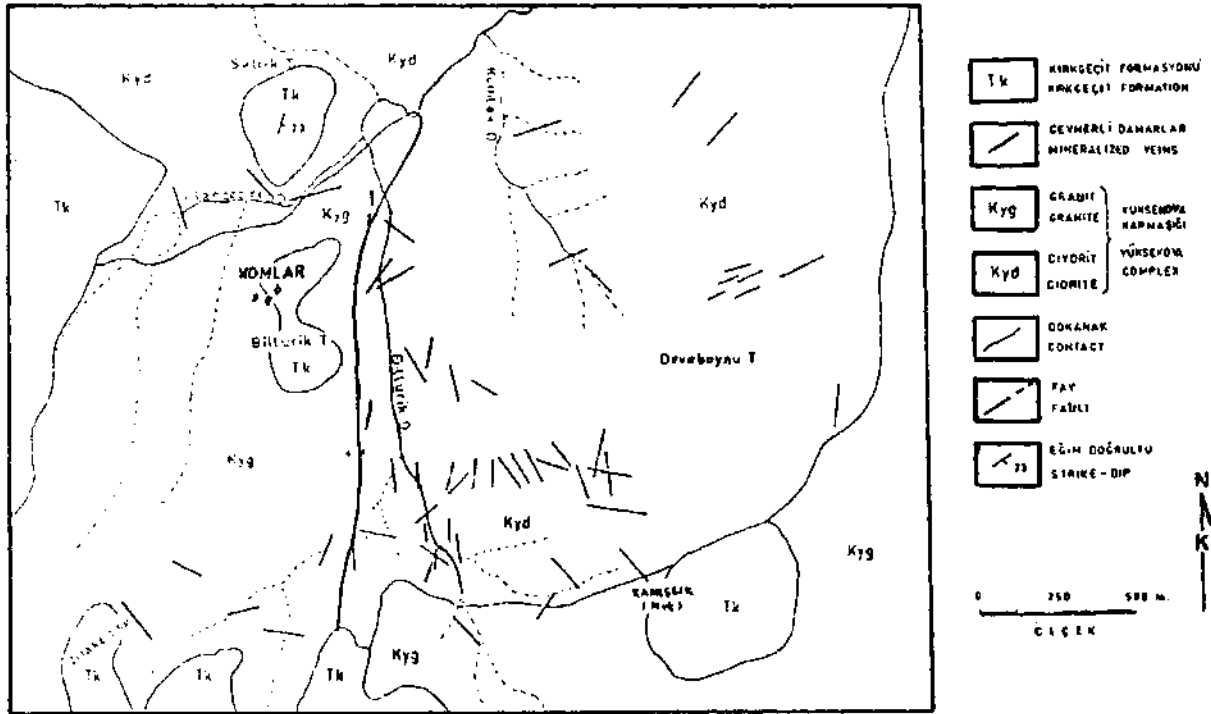


Fig.6— Locations of the ore bodies of Billurik dere.

p.60; Park and Diarmid, 1975, p.169).

ACKNOWLEDGEMENTS

This paper is prepared as a brief summary of M.Phil thesis. During preparation of the thesis we benefited invaluable participations from Prof.Dr. Yusuf Tatar, Doç., Dr. A.Fevzi Bingöl (Fırat University) and Dr.Ahmet Çağatay (MTA). We sincerely thank them.

Manuscript received February 21, 1989

REFERENCES

- Akgül, M., 1987, Baskil granotoyidinin petrografik ve petrolojik incelenmesi : Thesis (Master), K.Ü Fen Bilimleri Ens. (unpublished), Trabzon,
- Asutay, H.J., 1985, Baskil (Elazığ) çevresinin jeolojik ve petrografik incelenmesi : Ph.D.Thesis, AD Fen Bilimleri Ens. (unpublished), Ankara.
- Avşar, N., 1983, Elazığ yakın kuzeybatısında stratigrafik ve paleontolojik araştırmalar : Ph.D.Thesis, Ft) Fen Bilimleri Ens. (unpublished), Elazığ.
- Barnes, H.L., 1979, Geochemistry of hydrothermal ore deposits: John Wiley-Sons Inc., 798 p. New York-Chichester-Brisbane—Toronto.
- Bingöl, A.F., 1982, Elazığ-Pertek-Kovancılar arası volkanik kayaların petrolojisi: FÜ Fen Fakültesi Bull., 1, 9-21 p., Elazığ.

- Bingöl, A.F., 1984, Geology of the Elazığ area in the Eastern Taurus region: Proceedings Int.Symp. on the Geology of the Taurus Belt, 209-216 p., Ankara.
- Evans, A.M., 1980, Introduction to one geology: Blackwell Sc.Publication, 231 p., Oxford.
- Hempton, M.R. and Savcı, G., 1982, Elazığ volkanik kayaçlarının petrolojik ve yapısal özellikleri: TJK Bull., 25, 2, 143-151, Ankara.
- Naz, H., 1979, Elazığ-Palu dolayının jeolojisi : TPAO Rep., 1360 (unpublished), Ankara.
- Park, C.F. and Mac Diarmid, R.A., 1975, Ore Deposits, Freeman and Co., 530 p., San Francisco.
- Perinçek, D., 1979, The Geology of Hazro-Korudağ-Çüngü;-Maden-Ergani-Elazığ-Malatya area: Guide Book, TJK Bull., Ankara.
- Ramdohr, P., 1980, The Ore minerals and their intergrowths: Academia-Verlag, Berlin, 1202 p.
- Sağiroğlu, A., 1986, Kızıldağ-Elazığ cevherleşmelerinin özellikleri ve kökeni: Jeoloji Mühendisliği, v.29, 5-13, Ankara.
- and Preston, R~M.F., 1987, Ore mineralogy of Kızıldağ Pb-Zn veins-with a special emphasis on the composition of the tetrahedrites: FÜ Fen Bilimleri Ens., 2-2, 83-94 p., Elazığ.
- Sirel, E.; Metin, S. and Sözeri, B., 1975, Palu (KD Elazığ) denizel Oligosenin stratigrafisi ve mikropaleontolojisi: TJK Bull., 18, 2, 175-180, Ankara.
- Tatar, Y., 1986, Elazığ çevresinde Fırat Havzasının yapısal jeoloji özellikleri: Elazığ çevresinde Fırat Havzasının jeoloji ve yeraltı zenginlikleri sempozyumu bildiri özetleri, 4-5 p., Elazığ.
- Tuna, E., 1979, Elazığ-Palu-Pertek dolayının jeolojisi : TPAO Rep., 1363 (unpublished), Ankara.
- Winkler, H.G.F., 1979, Petrogenesis of metamorphic rocks : Springer-Verlag, 3485, Berlin-Heidelberg-New York.
- Yazgan, E., 1981, Doğu Toroslar'da etkin bir paleokita kenarı etüdü (Üst Kretase-Orta Eosen) Malatya-Elazığ Doğu Anadolu: Yerbilimleri, 7,83-104, Ankara.
- , 1984, Geodynamic evolution of the Eastern Taurus region: Proceedings Int.Symp. on the Geology of the Taurus Belt, 199-208 p., Ankara.

PLATES

PLATE-I

Fig.1— Chalcopyrite of sphalerite replaced by galena. Plain reflected light,
gl- galena; sf- sphalerite; kp- chalcopyrite.

Fig.2- Sphalerite stars in chalcopyrite. Plain reflected light.
Light parts are chalcopyrite and dark parts are sphalerite stars.

Fig.3— Chalcopyrite altered to covellite-chalcocite first and then to limonite.
Plain reflected light.
kp- chalcopyrite; kk- covellite-chalcocite; lm: limonite.

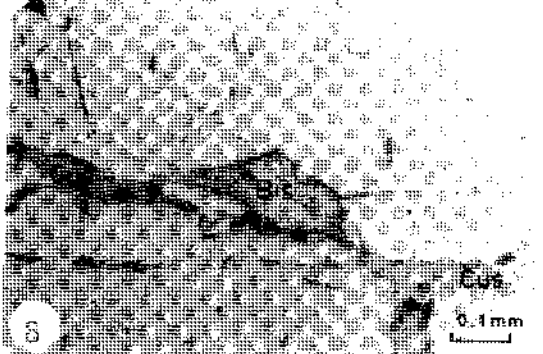
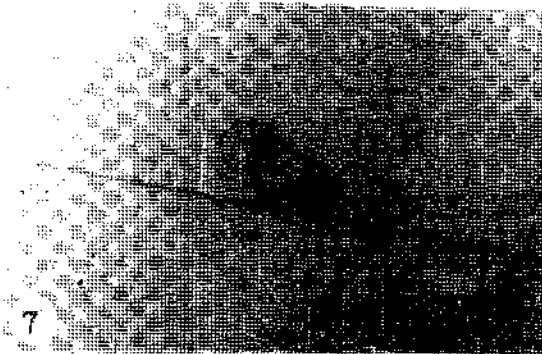
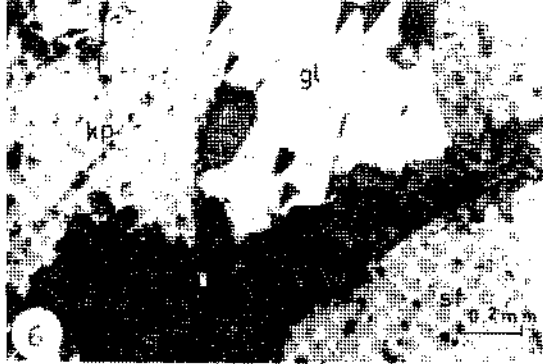
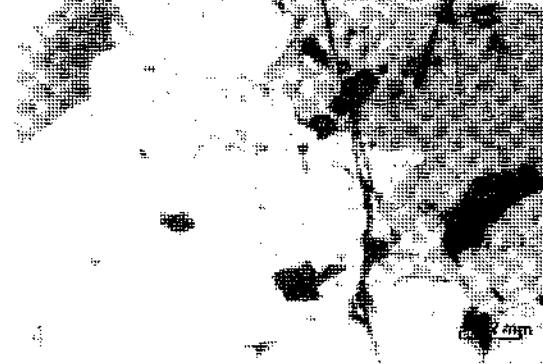
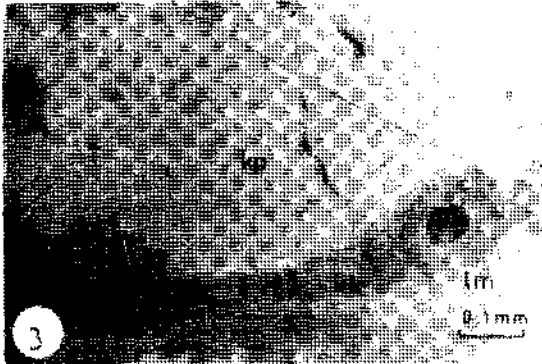
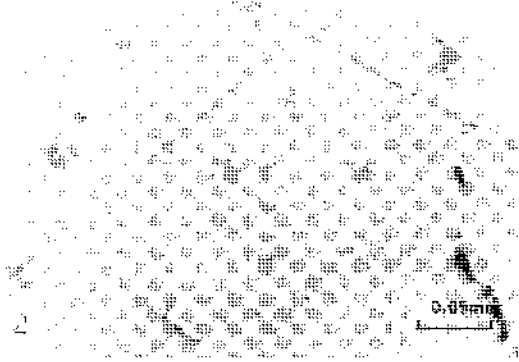
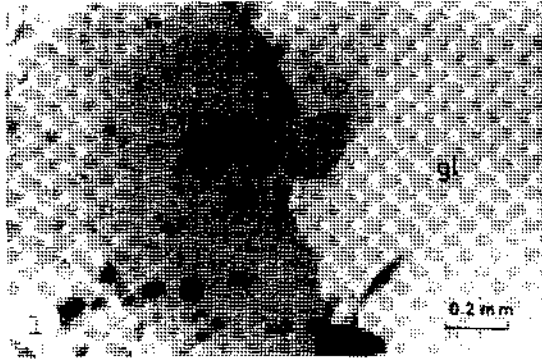
Fig.4— Age relationship between pyrite and chalcopyrite. Plain reflected light.
Light parts are pyrite and dark parts are chalcopyrite.

Fig.5— Field appearance of mineralized vein (1), altered zone (2) and country rock (3).

Fig.6— Massive ore of the contact zone. Plain reflected light,
gl- galena; sf- sphalerite; kp- chalcopyrite.

Fig.7— Ag-phases exsolved in galena. Plain reflected light.
Light parts are galena and dark parts are Ag-fahlore.

Fig.8- Cu and Bi-sulphosalts in the fractures of pyrite. Plain reflected light,
py- pyrite; Bis- Bi-sulphosalts; Cus- Cu-sulphosalts.



THE STRATIGRAPHY, SEDIMENTOLOGY AND ORIGIN OF THE COPPER (SILVER-URANIUM) DEPOSITS FOUND IN AN AREA BETWEEN DELİCE AND YERKÖY (MIDDLE ANATOLIA)

Halil ARAL*

ABSTRACT.— The stratigraphic position, sedimentologic characteristics and origin of the copper deposits of Oligocene (—Miocene?) age are investigated in an area between Delice and Yerköy, on the northern side of Delice river. Copper mineralization is observed mainly in three different stratigraphic positions in the region. The first type is the native copper ore, found in red and gray colored continental sandstones and conglomerate which overlie marine fossiliferous (Middle Eocene) limestones. The second type is the malachite ore, found in Oligocene (—Miocene?) units of the Toprakk tepé formation which consists of red sandstones, conglomerate and mudstones. This ore is restricted into the fine-grained, gray-colored sandstone and is rich in carbonized plant remains. The third type is the primary native copper and malachite ore found at the upper parts of the Toprakk tepé formation. While the native copper mineralization is strictly associated with fault zones and slickensided surfaces, the malachite mineralization occurs in the form of a cement, binding mostly the aetritic volcanic material. Malachite type mineralization represents point bar and flood plain environmental condition of sedimentation. The local occurrence of malachite ore together with plant remains in gray-colored sandstone of the red-bed series indicates that this type of ore was deposited primarily (probably as a sulfide or native copper or malachite) during the deposition of the host rock material under chemically reducing conditions. On the other hand, the native copper ore is supposedly an epigenetic type and related to the tectonic and compressional forces. Cuprite and malachite found with native copper was formed secondarily under surface conditions.

INTRODUCTION

Sedimentary rocks, the age of which are assumed generally as Oligo-Miocene, cover large areas in Central Anatolia. There are many scattered copper exposures (Fig.1) in these rocks. These exposures are mostly concen-

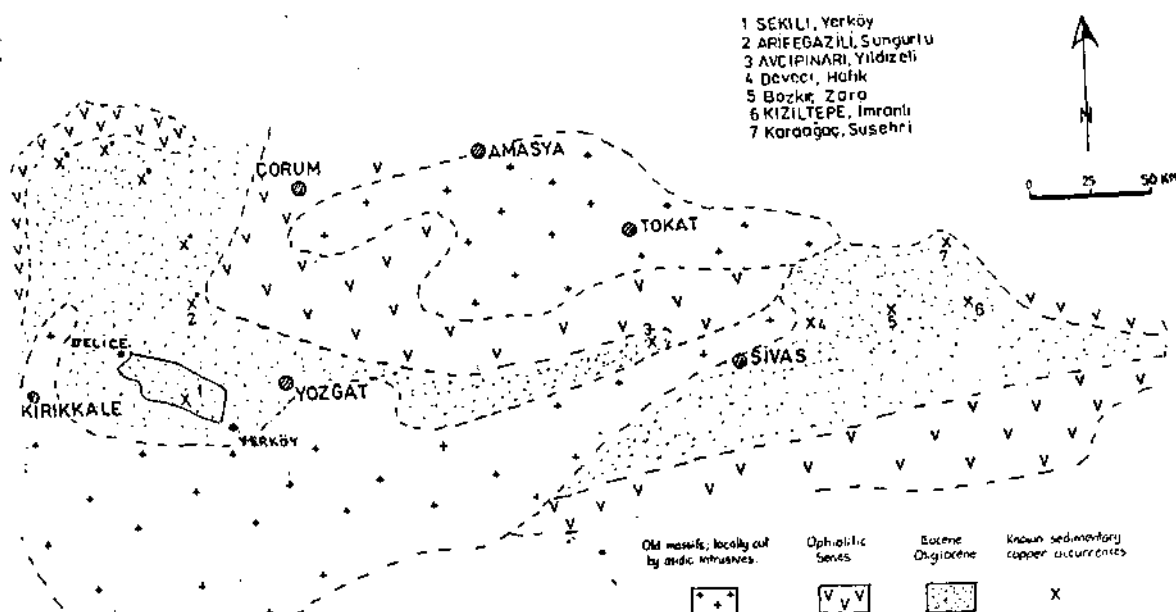


Fig.1— Geographic locations of sedimentary copper occurrences in Central Anatolia.

trated in the Çankırı-Çorum basin and in the vicinity of Sivas. These exposures (or prospects) which are known as red-bed type copper occurrences as they are found in red-colored fluvial deposits, show great lithologic, sedimentologic and some stratigraphic similarities to other red-bed type-occurrences in other parts of the world (for example, White Pine in Michigan (Hamilton, 1967), Nacimiento in New Mexico (Woodward et al., 1974) Corocoro in Bolivia (Ljungren and Meyer, 1964) and San Bartolo in Chile (Flint, 1986)).

The purpose of this article is to present information on the stratigraphic situation, sedimentologic characteristics and mechanisms of formation of the copper occurrences exposed between Delice and Yerköy (Fig.1, no.1). In this study, two 1: 25 000 scale geologic map sheets are prepared but as the mineralization is exposed over a large area, the geologic mapping is later expanded to cover a 350 km² area the boundaries of which are marked by Delice town in the west, Yerköy town in the southeast, Delice river in the south and Salmanlı village in the north. All the geologic information is compiled on a 1: 100 000 scale Kırşehir 1-32 sheet (Fig.2). During the field work numerous samples are taken to make petrographic, geochemical and paleontologic investigations.

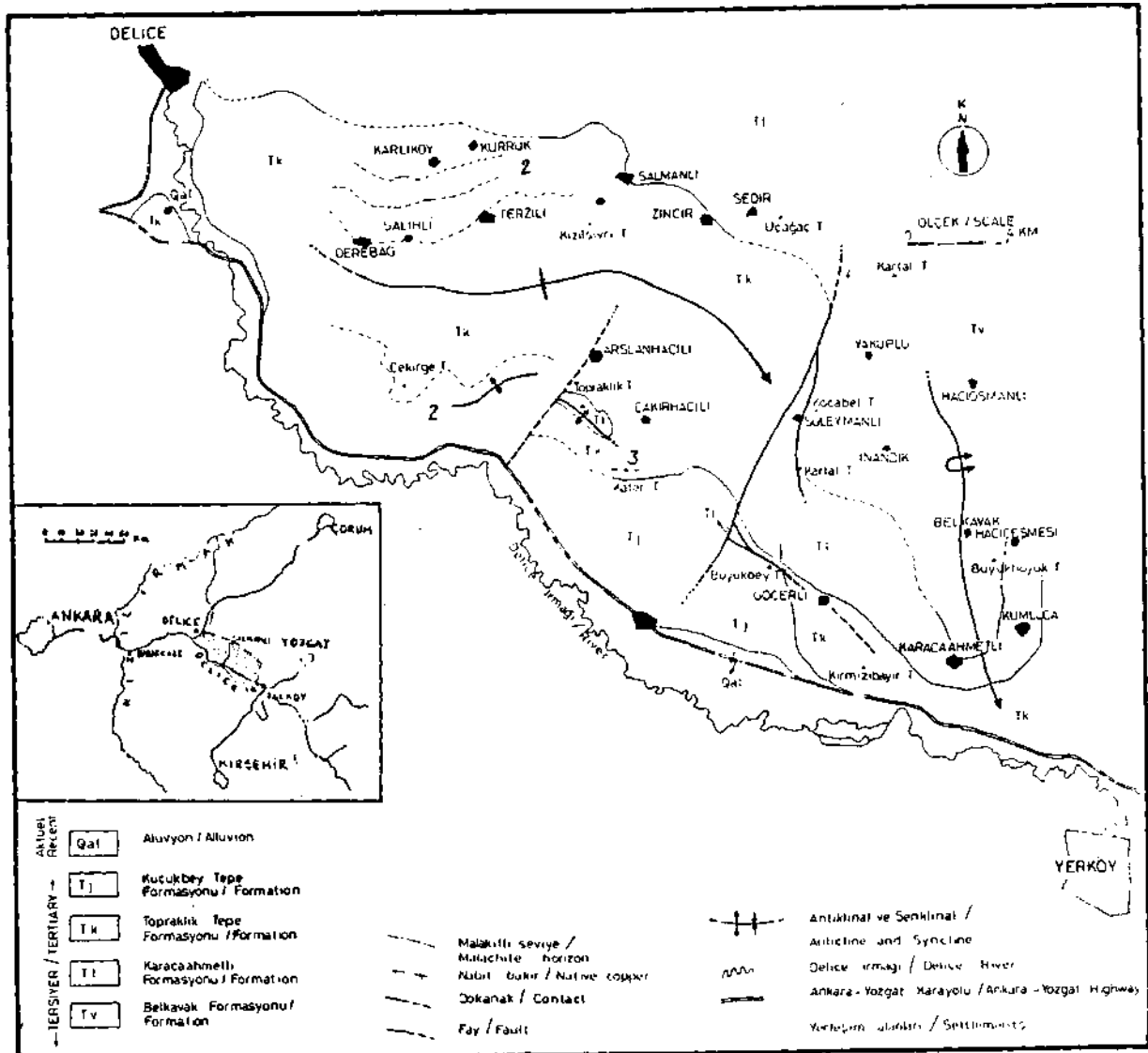


Fig.2— Geological map of the area between Delice and Yerköy (Kırşehir 1-32 sheet).

1— First ore type: Hacı Verim (Göçerli) occurrence; 2— Second ore type: Çekirge tepe and Terzili occurrences; 3— Third ore type: Çenik çayı occurrences.

RED-BED TYPE COPPER DEPOSITS

Red-bed type copper deposits are found in thick, red, purplish brown sandstones, siltstones, mudstones and sometimes in dolomitic rocks, generally located close to the evaporitic series and they are roughly concordant with their surrounding succession with a thickness varying from a few millimeters to a few meters, lateral extension reaching to several kilometers and occurring in the form of lenses and layers. The color of zones where the mineralization is found is mostly different than the underlying and overlying red deposits and is usually gray or greenish-gray. The mineralized zones almost always contain carbonized plant remains. The mineralized gray sandstones which do not contain carbonized material is generally associated with shales rich in organic matter.

The red arenitic, arkosic material and shale are derived from the surroundings. The red color of the sedimentary rocks is the result of the oxidation of ferrous iron to ferric iron leading to the formation of hematite as coatings around the grains or as a cement between them.

The most important minerals of the red-bed type deposits are copper sulfide and copper-iron sulfide minerals. The major primary minerals are chalcocite and pyrite. These deposits contain varying amounts of chalcopyrite, bornite, native copper, covellite, digenite, native silver and uraninite. Gangue minerals are quartz, feldspar, chlorite, illite, barite, gypsum, anhydrite and dolomite which are contributed mostly from the host rock.

Bastin (1933) gives Greta and Magnum (Oklahoma) and Nacimiento (New Mexico) as examples of such deposits. More recent investigations (Rose, 1976; Gustafson and Williams, 1981; Haynes, 1986 a) classified some of the famous deposits such as Kupferschiefer of Germany and Poland, Roan in Zambia and Zaire, Dzhezkazgan in the USSR and White Pine in the USA, as stratiform, red-bed type copper deposits. Haynes (1986 b) listed the various characteristics of the host rock which contain this type of deposit in a table (Haynes, 1986 b, Table 1) claimed that the depositional environment was one between shallow lacustrine and sabkha (Fig.3).

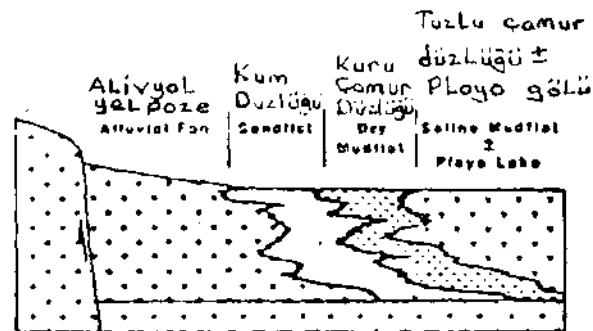


Fig.3— Section showing closed basin environment where sedimentary copper ores are deposited (taken from Haynes, 1986).

Flint (1986) suggested that the depositional environment was not only a low-energy environment but also the late orogenic molasse basins giving as examples the famous Coracora deposit in Bolivia, the Coloso deposit which is found in conglomerates in Northern Chile and the San Bartolo deposit in Chile. Among these, for example, the San Bartolo deposit is found in continental Tertiary sediments representing a deposition into a closed basin in an arid climate, an alluvial fan, playa environment and lacustrine facies conditions. The mineralization which is in the form of native copper, cuprite and atacamite is in sandstone and constitutes thin layers. It is deposited in a high-energy playa marginal sandflat environment (Flint, 1986). The ore minerals constitute the matrix of lithic

arkose and replaces the carbonate/sulfate cement of the rock. Native copper is found as sheets, filling the tectonic fractures as in Corocoro (Flint, 1986).

There are different opinions on the formation of red-bed type copper deposits. These opinions can be grouped in two major categories: epigenetic and syngenetic. Epigenetic opinion defends that mineralization forms following the completion of sedimentation as a result of diagenetic compaction. Some of the supporters of the epigenetic opinion claim that copper deposits are formed during bacterial sulfate reduction (Haynes, 1986 a) whereas some others propose a formation similar to the formation of "roll-type" uranium deposits (Shockey et al, 1974) and still some others suggest a mechanism where copper-rich solutions replace previously formed biogenic pyrite and anhydrite (Haynes, 1986 a). According to Rose (1976) a substantial amount of salty and chloride-rich connate water was mobilized from the sediments during the diagenetic compaction which dissolved the copper existing in the red-bed series and deposited them where the oxidation potential was low. The investigations of Haynes (1986 a) showed that chalcocite was deposited at the uppermost part (a zone of maximum 50 cm) of the depositional surface as a result of sulfate reduction by bacteria. The information on porosity and permeability behaviour of shales and sandstones under compression shows that the copper transporting solutions migrated along the stratification, not across it. The syngenetic opinion finds its support from the stratiform nature and concordant appearance of the ore with the walls of the host rock. In literature, the formation of syngenetic ore is explained by the influx of metal-rich fresh water into a chloride-rich lake or lagoon where the metals are deposited when they come into contact with a reducing environment (Dunham, 1964; Haranczyk, 1970; Garlick, 1974).

PREVIOUS WORK

There is no publication in the literature on the geology and formation of copper occurrences found in the study area. Some of these occurrences were pointed out to the author by Mr. Güner Aytuğ during a one day field trip in 1975 who worked for the Turkish Iron and Steel Works. Other than this unpublished investigation, the only other two unpublished reports are Teşrekli and Pehlivanoğlu's (1982) short notes on the occurrence of copper in the region and Ketin's (1954) report on the regional geology. A firm (the name of which is probably İZBAK Mining and Smelting Limited Corporation) operated some of the copper-carbonate zones in the early 1970's for a short time and constructed some leaching ponds on the Terzili road. The crushing and sieving machinery is dismantled and the leaching ponds are now left in ruin.

GEOLOGY-STRATIGRAPHY

The Middle Eocene Sekili-Göçerli group forms the base of the stratification (Fig.4) in the study area. This group consists of Belkavak and Karacaahmetli formations and is exposed in the northern and eastern parts. The Sekili-Göçerli group represents the northern flank of an approximately EW trending syncline between Delice-Salmanh-Sedir and underlies the red Topraklık tepe formation further south. The Belkavak formation consists of volcanic lavas (mainly andesite and to a lesser extent rhyolite and basalt), volcanic conglomerate and volcanic sandstone. This formation is interbedded with agglomerate, breccia and tuff layers further east between Yerköy and Yozgat. Various sandstones and limestones of fossil-rich marine Karacaahmetli formation overlies the Belkavak formation partly with an unconformity. The uppermost parts of the Karacaahmetli formation is characterized by beach sands with trace fossils and fossiliferous shallow sea limestones, and underlies the Topraklık tepe formation with a low-angle (15 degree) unconformity.

At the end of Middle Eocene the sea covering the study area completely retreated and to Late Oligocene (or Miocene) only the fluvial deposits of the Topraklık Tepe formation and lacustrine evaporites, limestones and

AGE	GROUP	FORMATION	THICK. (M)	LITHOLOGY	SEDIMENTARY STRUCTURE & FOSSILS	DEPOSITIONAL ENVIRONMENT	ORE TYPE
U. EOCENE - OLIGOCENE / MIOCENE	KÜÇÜKBEY T.	TOPRAKLIK TEPE	> 1200	Gypsum, anhydrite, mudstone, siltstone, little sandstone and lacustrine limestone.	Mudcracks, karst in limestones and porous structure.	Continental Sabhka	
			1960	UPPER and MIDDLE PARTS Red, brown, maroon volcanic arenite, volcanic conglomerate, mudstone / siltstone interbedded.	Cyclic series; graded bedding; planar and rarely trough cross bedding; mud pellets; remnants of codified plants; thin parallel laminar bedding. Teeth, trunk, vertebrae fossils (Ketin, 1954; Şenalp, 1978).	Deposits of flood plain, point bar and river beds.	Malachite native copper cuprite
				LOWER PART (Alcalis) Red and gray volcanic arenites, conglomerate, siltstone, locally some lacustrine Limestone tuff and gypsum.	Porous texture in Limestones. Locally nummulites at the bottom.		Malachite
EOCENE	SEKILI - GÖÇERLİ	KARACA AHMETLİ	1400	Gray, greenish gray volcanic arenites, siltstones, volcanic conglomerate; cream colored biosparite; locally gypsum fragments in upper parts.	Trace fossil marks graded bedding; low angle planar cross bedding. <i>Lucina, Ampullina, Seridium, various nummulites; some echinoids and brachiopods.</i>	Beach and shore environment	
			BELKAVAK	> 350	Volcanic lavas at the bottom; volcanic cong., sandstone, lithic tuff on top; local hydrothermal alteration.	Lava Flows	Continental

Fig.4— Stratigraphic column of the Delice-Yerköy area.

clastic sediments of Küçükbey Tepe formation were deposited. All these units were later folded, steepened (Fi-g.5), overturned on the southeastern flank (Fig.2) and faulted in the eastern part of the study area.

The copper deposits which this article deals with are all confined to the Topraklık tepe formation.



Fig.5— (a) Steepening and (b) overturning of the interbedding of the red and gray colored series located at the lower parts of the Topraklık tepe formation.

ORE TYPES

Three different ore types are recognized based on their stratigraphic location. These are:

1- The epigenetic native copper (f



Fig.6— Primary sheets of native copper and accompanied secondary cuprite and malachite mineralization, filling generally N50E/35-90° SE trending fault zones, characterized by slickensided fault planes, and cutting across red and gray sandstones and conglomerates.



Fig.7— The separate malachite horizons, the thickness of which hardly exceed a few centimeters. They are concordant with the bedding of the host rocks.

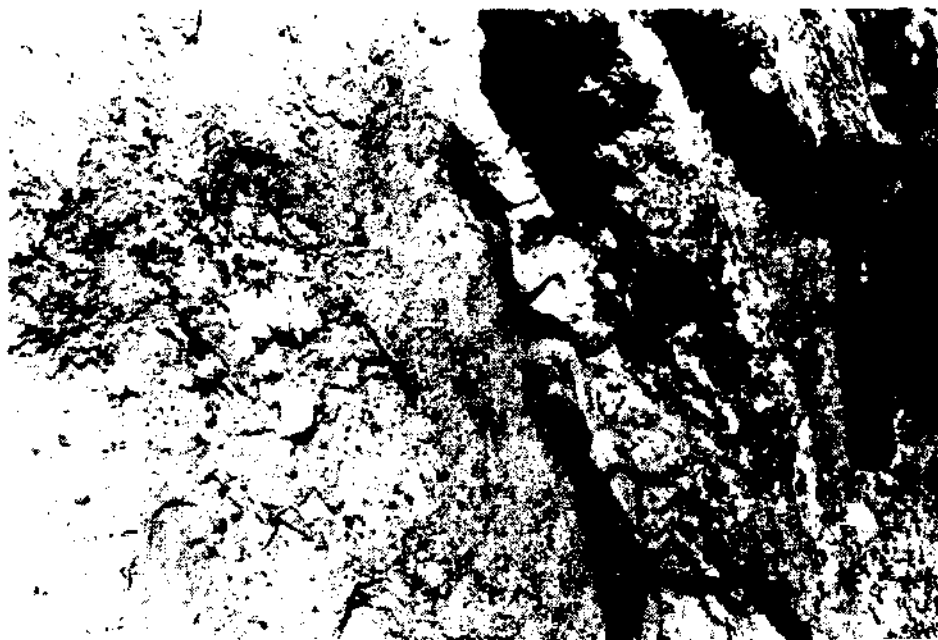


Fig.8— The appearance of malachite as cement and concretions in sandstones found at the base of red conglomerates (Göçerli occurrence).



Fig.9— Slickensided fault planes containing native copper mineralization and their close-up view.

Sandstones and conglomerates which host the first ore type show graded bedding (Fig. 10). They are overturned and dip nearly vertical (Fig.5). Sandstones at the bottom of this formation contain gypsum fragments up to 2 x 5 cm in size.

Native copper (Fig.11) is the most important primary mineral in this tectonically controlled ore type. Investigations under the microscope show the presence of small amounts of chalcocite inclusions in the native



Fig.10--Graded bedding in sandstones and conglomerates, host for the native copper mineralization.

copper. Cuprite and malachite which widely associate with native copper are formed secondarily as a result of oxidation at the surface. Some of the malachites which are locally found as concretions in sandstone are probably primary occurrences.

The presence of wedges and lenses of conglomerate in gray-colored sandstones, the cyclic and gradual transition from coarse to fine grain in the host rock, the presence of dark-colored heavy mineral lamination in sandstones, the occurrence of cross-bedding, absence of fossils and interbedding of fine grained red horizons with gray colored sandstones all indicate a fluvial depositional environment.

The second ore type is found in the gray-colored, fine-grained sandstones rich in plant residue. Earthy malachite and insignificant amounts of azurite are the major minerals. Mineralization is either in the form of cement binding the fine/medium sized grains of sandstones which contain a high percentage (up to 85 percent) of volcanic rock fragments or in the form of replacements around the carbonized plant residue (Fig. 12).

The second ore type is exposed west of the study area and constitutes three separate layers on the southern flank of the roughly E—W trending syncline (Fig.4), The thickness of the mineralized sandstone layers vary from 10 to 200 cm and extends intermittently several kilometers along the strike.

The presence of cyclic graded bedding, cross-bedding (sometimes trough-bedding) (Fig.13), mud pellets (Fig.14), thin parallel laminations (Fig.14 and 15), carbonized plant remains and the absence of marine fossils suggest that the mineralization is related with fluvial deposition and took place in point bar and flood plain environments.

The occurrence of mineralization in gray-colored sandstones enclosed in red series and the presence of organic remains only in the gray-colored horizons indicates the prevalence of temporary reducing conditions in .!



Fig.11— Sheets of native copper; their thickness varies from 1 to 10 mm.



Fig.12— Coalified plant remains which played an important role in the precipitation of second ore type. Mineralization replaces the plant residue from outside to inside and cements between the grains of enveloping sandstone.



Fig.13— Facies changes and sedimentary structures in mineralized host rock; bottom laminated fine-grained sandstones are overlain by sandstones with planar cross-bedding and top conglomerate layer.



Fig.14— Holes of mud pellets in cross bedded thin parallel laminated sandstones.



Fig.15— Fine grained sandstones characterized by heavy mineral (magnetite) laminations.

Continental oxidizing environment. The evidence gathered so far suggests that malachite has a primary origin, however, in the absence of bore hole samples it is still not impossible to claim that malachite is formed after the surficial alteration of other copper (oxide, sulfide or native) minerals.

The third ore type found where the Cenik stream cuts across the Çakırhacılı village road is exposed in roughly E—W trending, 70° S dipping, 6 m thick and 10-15 m long sandstones and conglomerates (Fig.8). Mineralization, the thickness of which is 75 cm, is in the form of malachite filling between the coarse grains of red sandstone. Under this horizon the fine-grained, laminated red sandstones contain sheets of native copper (Fig.16) along the fault planes trending parallel to the bedding. There are mine dumps and collapsed declines indicating that the native copper was previously mined.

Gypsum-anhydrite layers of the Küçükbey Tepe formation come over the mineralized zone eleven meters south. The spring water in the vicinity is not potable as it is bitter and salty. The Küçükbey tepe formation contains a rock salt deposit which is operated by the Monopoly Administration 2.5 km south of Sekili.

CHEMICAL ANALYSES

Several rock (grab) and stream sediment samples are taken and analysed for Cu, Ag, Au, Zn, Co, Ni and Mo and four of them for uranium. Only the results of Cu, Ag and U₃O₈ are given here and shown on geologic and stratigraphic sections in Figures 17, 18 and 19. The present data indicates the existence of a significant positive correlation among copper, silver and uranium.

Analytical results of stream sediment samples collected from the dry streams of the Hacı Verim (Göçerli) occurrence are shown in Figure 20. All the analyses except uranium were made by Perkin-Elmer's atomic absorption spectrophotometer in the Rock Chemistry Laboratory of the Geological Engineering Department of Hacettepe University. The detection limits of copper and silver are 5 and 1 ppm respectively. All the uranium analysis and some of the silver and gold analyses are done in the General Directorate of Mineral Research and Exploration (MTA).



Fig. 16—Sheets of native copper collected from fault planes cutting across red colored fine grained sandstones; outer parts of some of the native coppers are partly altered to cuprite and malachite.

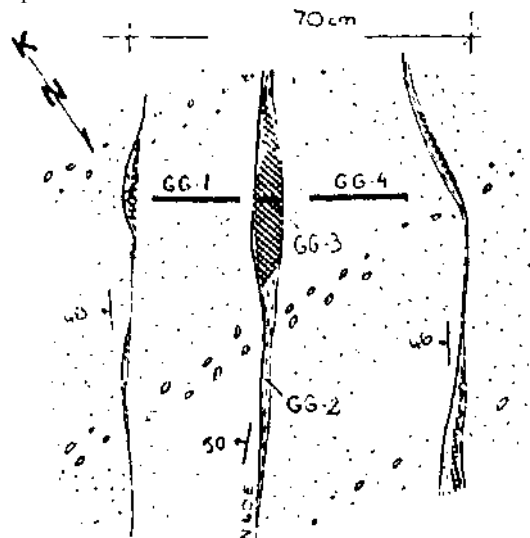


Fig. 17—Distribution of copper and silver (ppm) in channel samples collected from the traverses laid perpendicular to the mineralized veins in the Hacı Verim (Göçerli) occurrence.

GG-1: Cu 117, Ag 1; GG-2: Cu 8461, Ag not analysed; GG-3: 447000, Ag 23; GG-4: Cu 253, Ag1.

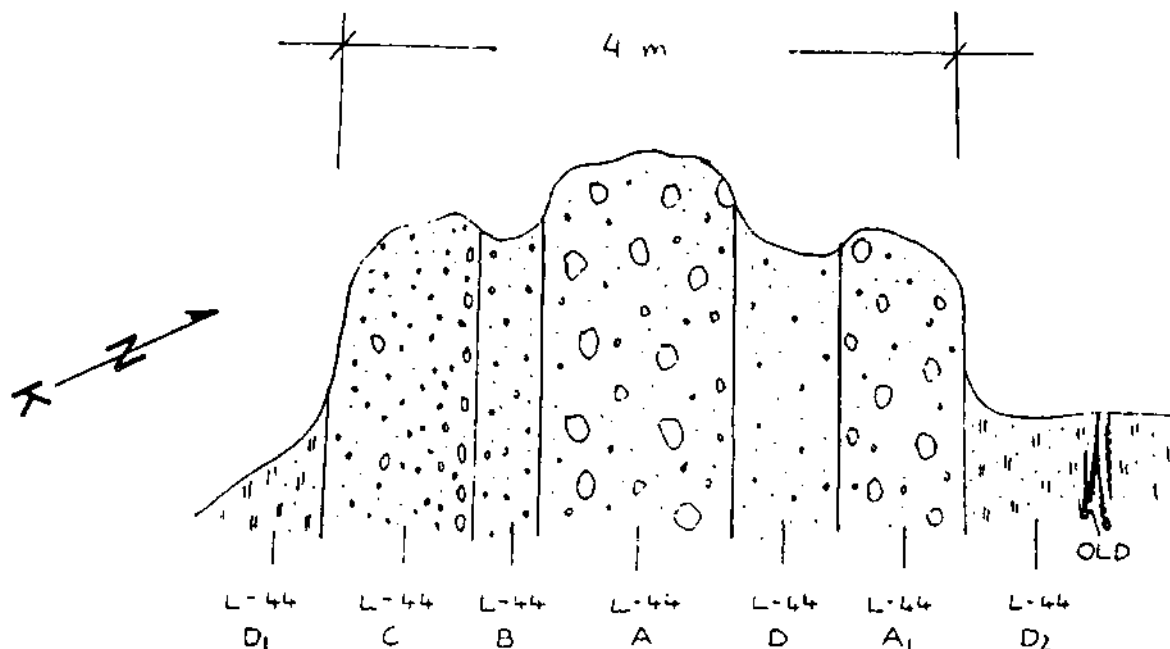


Fig.18—Distribution of copper, silver and uranium (ppm) in various sandstones and conglomerate layers in the Cenk çayı occurrence. L-44 A: Cu 972, Ag 3, U₃O₈ 13; L-44B: Cu not analysed, Ag 1; L-44 C: Cu 11000, Ag 1; L-44d₁: Cu 5, Ag 1; L-44d₂: Cu 45000, Ag 9; OLD: Cu 33000, Ag 10.

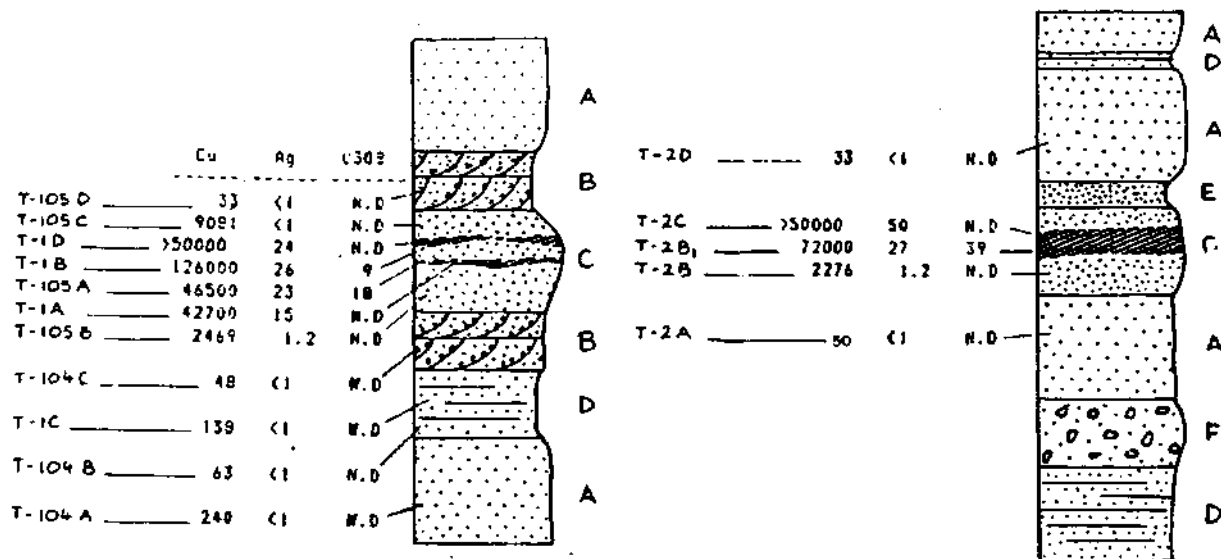
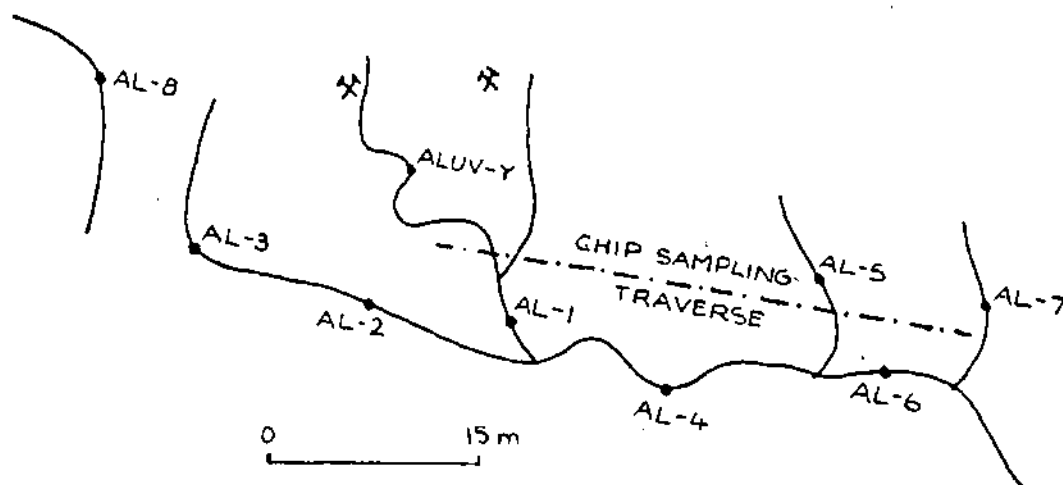


Fig. 19—Distribution of copper, silver and uranium (ppm) in samples collected from mineralized and barren horizons in Çekirge tepe and Terzili. N.D—not determined. A— red compact sandstone; B— cross bedded red sandstone with mud pellets; C— cream colored mineralized sandstone with carbonized plant residue; D— thin bedded, magnetite laminated sandstone; E— red sandstone with mud pellets; F— red conglomerate with clay pellets.

The results obtained for gold by the M.I.B.K. method at Hacettepe University are not verified by the cupulation method used by MTA Uranium analyses are done on second and third ore types and 22 gr/ton U₃O₈ (average of three samples) and 13 gr/ton U₃O₈ are found, respectively.



Example	Ag	Cu	Zn	Co	Ni
CHIP	-	681	56	12	22
ALUV-Y	5.5	% 9.1	35	10	23
AL-1	17	107	34	17	26
AL-2	-	42	36	17	26
AL-3	-	37	34	14	27
AL-4	-	91	27	14	27
AL-5	-	75	40	14	25
AL-6	-	81	37	14	25
AL-7	-	36	18	11	16
AL-8	-	33	31	10	20

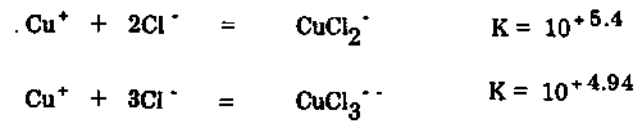
Fig.20—Distribution of Cu, Ag, Zn, Co and Ni in stream sediment samples (ppm) from the streams draining the Hacı Verim occurrence.

Analyses of samples collected from the mineralized host rock and its walls did not indicate any distinct anomalous values for Co, Au, Mo, Ni and Zn. The reason for this is probably the difference among the solubility, transportation and depositional parameters of these elements and those of copper, silver and uranium.

GENESIS

Copper is supplied by leaching from the Middle Eocene volcanics which now cover north and east of the study area. There is enough copper (and silver and uranium) in the volcanics to be the source for the mineralization in the field. For example, a rough estimate indicates that to have an ore deposit with a 2500 x 20 m area, 10 cm thickness, containing 1 % Cu and 25 ppm Ag, there must be a source rock with a 2500 x 100 m area, 10 m thickness containing 20 ppm Cu and 0.05 ppm Ag. The Middle Eocene volcanic rocks of the area contain sufficient amounts of these metals (e.g., 125 ppm Cu and 0.12 ppm Ag in andesites). Additionally, petrographic and sedimentological evidences are also in support of a volcanic source. The sandstone and conglomerate which host the mineralization contain up to 80 - 85 % volcanic rock fragments indicating that the source region was dominated by volcanic rocks.

The leaching process was accentuated by the hydrothermal activities which took place at the closing phase of the volcanism and such metal-rich solutions found their way to the streams following ephemeral rains. The



It is known that Cu^{++} also forms a complex with Cl^- (CuCl^+ , $K = 10^{+2.8}$), but this complex is not stable and decomposes quickly under surficial environmental conditions (Rose, 1976). Furthermore, at 1 atm. pressure and

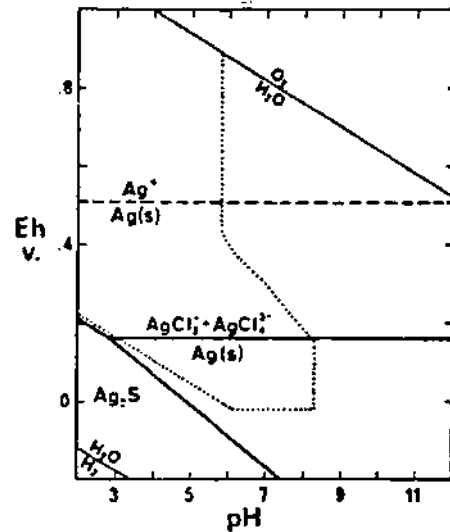


Fig.22—Eh—pH diagram of silver and comparison of its stability in the absence and presence of Cl^- . Dashed line shows the absence of Cl^- , heavy lines show 0.5 m Cl^- and 10 m Ag , dotted line indicates the 10 m Cu area (taken from Rose, 1976).

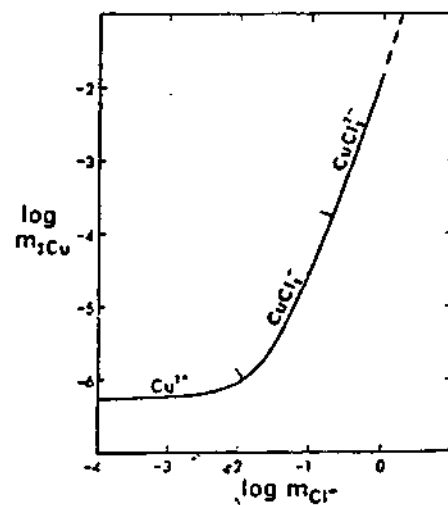


Fig.23—Maximum solubility of Cu in relation to Cl^- content at pH 7 in the Cu-O-H-Cl system (taken from Rose, 1976).

strong argillization of the feldspars in the volcanic rock fragments is in support of the prevalence of such a hydrothermal phase. Further evidence for hydrothermal activities are the argillization of the volcanics (Fig.21) along the road between Yerköy and Yozgat, and the presence of widespread crystal quartz, amethyst and opal veins distributed irregularly in the volcanics in the vicinity of Belkavak village.

From the geochemical point of view, however, it is not possible to mobilize substantial amounts of copper with surface waters (Rose, 1976). Such a mobilization is possible only at moderate oxidation conditions with chloride-rich waters, as such waters would combine with copper and silver to form chloro-metal complexes (Rose, 1976).



Fig.21– Hydrothermal veins characterized by argillization, hematitization, limonitization and zeolitization cutting the volcanic rocks of Belkavak formation with a steep angle. Sample from an argillic zone containing 438 ppm copper.

Silver is a by-product commonly seen in red-bed type copper deposits. For example, the Creta ore (Oklahoma) contains 2 % Cu, 30 gr/ton Ag; the White Pine (Michigan) ore contains 1 % Cu, 30 gr/ton Ag; the high-grade Corocoro ore (Bolivia) contains 40 gr/ton Ag, and Nacimiento (New Mexico) 175-250 gr/ton Ag (Rose, 1976). The association of silver with copper is explained by the ease of silver ions to form complexes with Cl^- as Cu^+ ions. While native silver quickly precipitates under mildly reducing (-1-0.5 v) conditions in a Ag-O-H system, its solubility increases rapidly in a 0.5 m NaCl solution and the area showing the solubility of silver in this system shows close similarity to the area of the CuCl_2^- - CuClg^- in the Cu-O-H system (Fig.22). The formation of copper complexes in relation to the Cl^- concentration and the increase in the solubility of copper at pH:7 are shown in the Cu-O-H- Cl^- system (Fig.23).

According to Rose (1976), water that contains 350 ppm Cl^- easily transports copper at a moderate oxidation potential in 25°C. In general, it is difficult to find surface or underground waters containing 350 ppm Cl^- . Such high Cl^- concentration can be obtained when seasonal surface and underground waters wash the sand flats having a continental or marine origin. The following complexes are formed (Rose, 1976) when Cl^- is combined with Cu^+ at the surface at 25°C

25°C, relatively mobile copper carbonate ions such as $\text{Cu}(\text{CO}_3)_2^-$ and $\text{CuCO}_3(\text{OH})_2^-$ are formed under $P_{\text{CO}_2} > 10^{-3.5}$ and $P_{\text{CO}_2} < 10^{-5}$, respectively (Garrels and Christ, 1965) (Fig.24).

It is not clearly established yet whether the second type stratiform malachite deposits are an epigenetic or a syngenetic type; while the occurrence of the mineralization in sandstones and conglomerates as a cement and

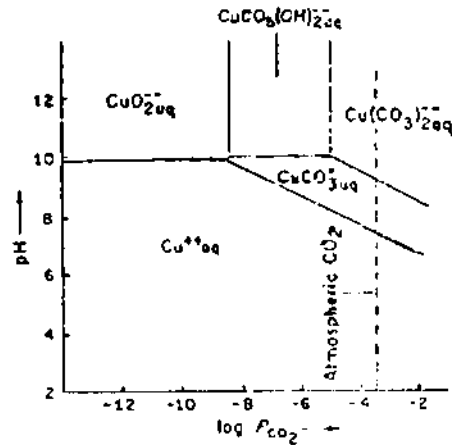


Fig.24—Distribution of dissolved copper ions as a function of pH and P_{CO_2} (atmospheric) at 25°C and 1 atm. total pressure (taken from Garrels and Christ, 1965).

concretions suggest a syngenetic origin, the replacement of carbonized plant residue by the mineralization and the occurrence of the mineralization in the fault zones support an epigenetic origin.

The present evidence indicate that a dry climate prevailed in the study area from time to time developing salt flats and promoting an increase in the concentrations of Cl^- , SO_4^- and carbonate ions in the environment. The rain which follows a dry season quickly ascends the water table and leads to the formation of complex metal ions as copper and silver combine with chloride and sulfate ions. Repetition of this process over a few seasons or the circulation of the rain water through some subsurface evaporitic layers increases the salinity and the metal-salt concentration. The other possible mechanisms of ore formation are a) salty (brine) and metal rich waters that were trapped in a closed basin and formed a syngenetic deposit there as the water is lost by evaporation, b) such waters were transported as underground waters and formed epigenetic ore deposits when they met a reducing environment created by decaying plant residue, c) the flush of oxygen-rich rain water after a dry season into such closed basins may have caused the precipitation of copper and other associated metals, and d) waters rich in copper, other metals, chloride, sulfates and carbonates precipitate their metal load in the low-energy environments such as point bars and flood plains where such waters come in contact with decaying plants and decomposing organic matter. One or more than one of these mechanisms were probably effective in the Delice-Yerköy area.

Copper complexes precipitate in alkaline environments ($\text{pH} > 7$) as a result of the increase in the levels of P_{CO_2} and $f_{\text{H}_2\text{S}}$. According to the theoretical modelling of Haynes and Bloom (1987 a,b), native silver, native copper and copper sulfide minerals such as chalcocite, bornite and covellite precipitate in an orderly manner in response to the increase in the H_2S fugacity. Native silver saturates from waters saturated with calcite, quartz, gypsum

hematite containing 3 molal Cl^- , 0.11 molal HCO_3^- , 800 ppm Cu and 1 ppm Ag at a $\text{pH}=7.6$ and $f_{\text{H}_2\text{S}} = 10^{-5.2}$ bars. Native silver precipitation is complete prior to native copper saturation at $f_{\text{H}_2\text{S}} = 10^{-2.8}$. The deposit contains only native copper and native silver as long as the H_2S fugacity does not exceed 10^{-2} bars and under such circumstances 96 % of copper and all the silver precipitate. If the water contains Pb, Zn, Co, Fe ions and the H_2S fugacity reaches to 10^{-2} bars level, based on the conditions of transportation, varying amounts of sulfides of Zn, Co, Pb, Fe and Cu are precipitated. The presence of chalcocite in native copper only in minor amounts may suggest that in the study area the H_2S fugacity hardly reached $10^{-1.8}$ bars.

The stability of some copper species are shown on a Eh-pH diagram (after Garrels and Christ, 1976) for the Cu- O_2 -S- CO_2 system at 25°C , 1 atm. total pressure, CO_2 partial pressure of $10^{-3.5}$, and total dissolved sulphur content of 0.1 (Fig.25). This diagram indicates that under surface conditions malachite crystallizes at a pH range

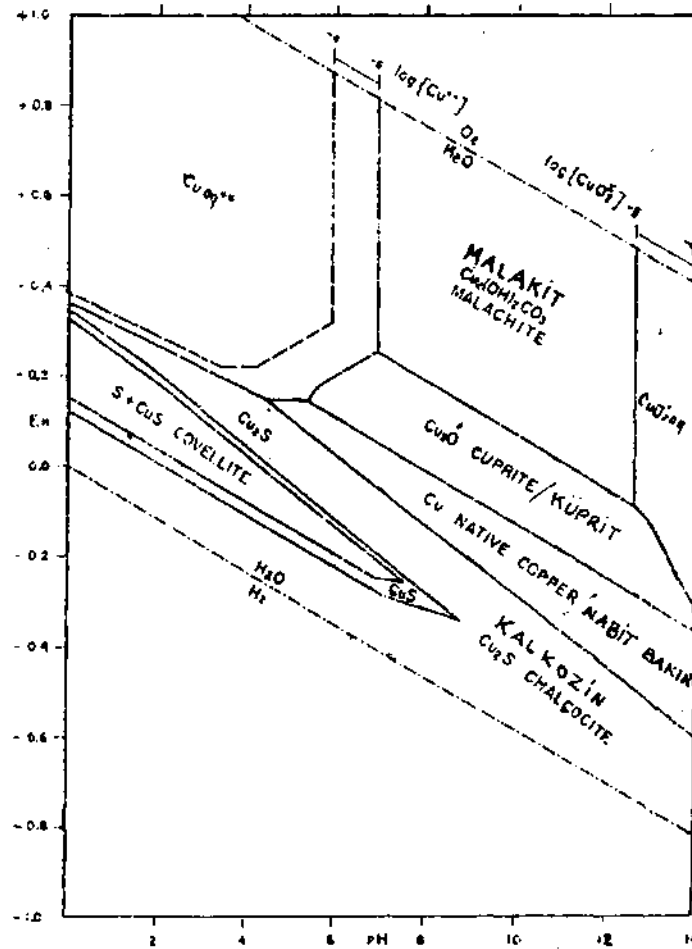


Fig.25—Stability relations among some copper compounds under 1 atm. total pressure, $\text{P}_{\text{CO}_2} 10^{-3.5}$, total dissolved sulfur 10^{-2} conditions in Cu- H_2 - O_2 -S- CO_2 system (taken from Garrels and Christ, 1965).

of 7 to 12. According to Garrels and Christ (1965), as the CO_2 partial pressure is increased the stability field of malachite expands into the field of cuprite. In dry climatic conditions malachite is more stable than azurite as not enough moisture is available in the air for the stability of azurite. It is also seen from this diagram that the field of the native copper remains unaffected at atmospheric and higher PCO_2 conditions. Under the given conditions a reducing environment is required for the precipitation of sulfides. The general absence of sulfides in the study

area indicates either the geochemical conditions for the formation of such minerals have never been attained or previously formed sulfides were altered to malachite under a bicarbonate rich environment. Microscopic investigations to answer this problem are still in progress.

The native copper seen in the fault zones is most probably a product of remobilization. In other words, copper was leached from previously deposited cupriferous layers and filled the tensional fractures. The areal closeness of mineralized zones to the evaporitic series dictated that the metals could have been transported as chloride complexes. The high permeability of the host sandstones prevented the reduction of sulfates to sulfide by bacterial action (Haynes and Bloom, 1987 *b*) so that the environmental condition of low H₂S fugacity is created for the precipitation of native copper. The compressional phase following the general tensional movements caused small displacements along the mineralized fractures and led to the formation of native copper sheets filling irregularly the slickensided fault zones. The presence of pressure twinings in native copper seen under the ore microscope also support this.

RESULT

As a result, the depositional basin where red-bed type thick sediments (Topraklık Tepe formation) are deposited is a stream system flowing in a plain surrounded by steep mountains. This plain is cut by a few meandering rivers. Fine and sometimes coarse grained sediments brought by floods fill between these rivers and the low plains. Some plant and wood trash are deposited as a result of the loss in the stream energy in places like point bars and flood plains. The decay and coalification of this material created the environment suitable for the precipitation of copper (silver and uranium).

The constitution of the fluvial sediments in large (80-85 %) by volcanic rock fragments shows that the basin was fed by the surrounding volcanic mountains. The volcanic rocks evidently contain sufficient amounts of copper, silver and uranium.

The salinity of the basin is increased in response to seasonal aridness and metals formed complexes with Cl⁻, sulfate and carbonate anions. Metals of such solutions are then either deposited as independent layers where decaying organic matter is found or as material cementing between grains of sandstone and conglomerate. This type of stratiform malachite occurrences are seen in the middle parts of the Topraklık tepe formation.

Underground waters which circulate through the evaporitic series partly remobilized the stratiform ores and copper dissolved in this way is deposited as native copper in local fault zones in the lower and upper parts of the Topraklık tepe formation. The ages of the faults and the mineralization are not known definitely. Low H₂S fugacity needed for the deposition of native copper instead of sulfide minerals is provided by the high permeability of the host sandstones and high chloride activity by the evaporates in the close vicinity.

The probable metallic copper and silver reserves of the study area are 2500 tons and 3.5 tons, respectively. The contribution of the these occurrences to the country's economy will be about 11-12 billion TL at 1989 prices. The possible potential (geologic potential) is about ten times these figures.

ACKNOWLEDGEMENTS

This project study (Project no. 88-01-010-01) is financed by the Research Fund of Hacettepe University. The Research Fund's contribution is gratefully acknowledged.

I am thankful to Baki Varol from Ankara University for his stimulating discussions on stratigraphic and sedimentologic subjects both in the field and in the laboratory, to Sönmez Sayılı for providing access to the

analyses of gold, silver, and uranium in the laboratories of the General Directorate of MTA and to Alaattin Erkal and Gönül Karayığit for the chemical analyses in Hacettepe University.

Manuscript received December 15, 1988

REFERENCES

- Bastin, E.S., 1933, The chalcocite and native copper types of ore deposits: *Econ.Geol.*, 28, 407-446.
- Dunham, K.C., 1964, Neptunist concepts in ore genesis: *Econ.Geol.*, 59, 1-21.
- Flint, S., 1986, Sedimentary and diagenetic controls on red-bed ore genesis: *Econ.Geol.*, 81, 761-778.
- Garlick, W.G., 1974, Depositional and diagenetic environments related to sulfide mineralization. Mufulira, Zambia- a discussion: *Econ.Geol.*, 69, 1344-1351.
- Garrels, R.M. and Christ, C.L., 1965, *Solutions, minerals and equilibria*: New York, Harper and Row, 450 p.
- Gustafson, L.B. and Williams, N., 1981, Sediment-hosted stratiform deposits of copper, lead and zinc: *Econ.Geol.*, 75th Anniv. vol., 139-178.
- Hamilton, S.K., 1967, Copper mineralization in the upper part of the Copper Harbor Conglomerate at White Pine, Michigan: *Econ.Geol.*, 62, 885-904.
- Hararczyk, C., 1970, Zechstein lead-bearing shales in the Fore-Sudetic monocline in Poland: *Econ.Geol.*, 65, 481-495.
- Haynes, D.W., 1986 a, Stratiform copper deposits hosted by low-energy sediments. I. Timing of sulfide precipitation- An hypothesis: *Econ.Geol.*, 81, 250-265.
- 1986 b, Stratiform copper deposits hosted by low-energy sediments. II. Nature of source rocks and composition of metal transporting water: *Econ.Geol.*, 81, 266-280.
- and Bloom, M.S., 1987 a, Stratiform copper deposits hosted by low-energy sediments: III. Aspects of metal transport. *Econ.Geol.*, 82, 635-648.
- and —, 1987 b, Stratiform copper deposits hosted by low-energy sediments: IV. Aspects of sulfide precipitation. *Econ. Geol.*, 82, 875-893.
- Ketin, İ., 1954, Yozgat bölgesinin jeolojik lövesi hakkında memuar: MTA Rep., 2141, 50 p., Ankara, Turkey.
- Ljunggren, D.A. and Meyer, H.C., 1964, The copper mineralization in the Corocoro Basin: *Econ.Geol.*, 59, 110-125.
- Rose, A.W., 1976, The effect of cuprous chloride complexes in the origin of red-bed copper and related deposits: *Econ.Geol.*, 71, 1036-1048.
- Shockey, P.N.; Renfro, A.R., and Peterson, R.J., 1974, Copper-sulfide solution fronts at Paoli, Oklahoma: *Econ.Geol.*, 69, 266-268.
- Teşrekli, M. and Pehlivanoğlu, H., 1982, Yozgat ili Sekili köyü civarı bakır zuhurları incelemesi hakkında rapor: MTA, Maden Etüt Arşiv no. ME-1812, 6 p., Ankara, Turkey.
- Woodward, L.A.; Kaufman, W.H.; Schumacher, O.L. and Talbott, L.W., 1974, Strata-bound copper deposits in Triassic sandstones of Sierra Nacimiento, New Mexico: *Econ.Geol.*, 69, 108-120.

FORMATION OF TÜRKMENTOKAT-KARATEPE (ESKİŞEHİR) MAGNESITE ORE BEDS

Kadir SARIİZ**

ABSTRACT.— Magnesite ore has a tendency to settle in the F. W directed cracks and fissures developed strictly under structural control of serpentines and comprises vein and lensoid beddings; in addition, it is observed that it shows transitions to irregular and stockwork beddings. Two different mineral associations were found after analyzing the samples taken from the veins and the lenses. The first one is the primary association, magnesite and quartz and the other is the secondary association, calcite and dolomite. The mineral content of the samples have been figured out from their basic element analysis and seemed that magnesite shows 91.74%, quartz 0.74 %, dolomite 2.42 %, calcite 1.17 % and serpentine shows 1.72 % average values. Because the magnesite ore with having concentric and colloform structure reflects a rhythmic deposition in a gel like colloidal media, the physicochemical environmental behavior of solutions containing water with CO_2 (Mg^{2+} , dissolved from serpentines, is included) have been investigated, the experimental studies on the $\text{MgO}-\text{SiO}_2-\text{CO}_2-\text{H}_2\text{O}$ and the $\text{MgO}-\text{CO}_2-\text{H}_2\text{O}$ systems have been performed. According to this, the observed primary mineral association of the ore bed seems to be the product of the $\text{MgO}-\text{SiO}_2-\text{CO}_2-\text{H}_2\text{O}$ system, it is determined that the magnesite ore has formed under 150 °C thermal and 2000 bar liquid pressured conditions with various mole fractions of CO_2 . When the magnesite ore, bedded as batroidal and concretionary masses on the surface (around Sığıryatağı hill and other small occurrences) and in the shallow depths (near 12 meter), in the $\text{MgO}-\text{CO}_2-\text{H}_2\text{O}$ system is taken into consideration and evaluated, it is presumed that the magnesite ore might have formed from the mineral deposits containing $\text{Mg}(\text{OH})_2$ or $3\text{Mg}(\text{OH})_2 \cdot 3\text{H}_2\text{O}$ in their compositions. According to the data given above, the formation of the local magnesites reveals two different facts. The first is having a hydrothermal origin, the second is being an infiltration type gel magnesite deposition which its process is still continuing and will continue.

MINERAL PHASES IN THE EDİGE OPHIOLITE BODY

Ayla TANKUT* and Naci M.SAYIN*

ABSTRACT.— Ediğ e ophiolite body contains upper mantle and a part of crustal sequences, as a remnant of an oceanic lithosphere slice. The upper mantle sequence is composed of the primary assemblages of: olivin+ orthopyroxene + clinopyroxene + chromium spinel, in the tectonite ultramafics; and olivine + clinopyroxene + orthopyroxene in the cumulate ultramafics. The crustal sequence is characterized by the phases of: Plagioclase + clinopyroxene + olivin + orthopyroxene. Amphibole + serpentine + chlorite + prehnite + pumpellyite + sphene are the common secondary phases. The pyroxenes of the cumulate rocks are characterized by high Mg and very low contents of Na, K and Al. The plagioclase composition in the lower level gabbros range from An₄₀ to An₉₀. The amount of amphibole development and albitization increase with stratigraphic height that, in the upper level gabbros the pyroxenes are almost completely replaced by amphibole and all the plagioclases are albite. Chromites of the tectonites are of podiform type. All the evidences suggest that the mineral assemblages in various rock types of the Ediğ e ophiolite body are similar to the corresponding rocks of the oceanic lithosphere. Minerals of the cumulates suggest direct crystallization from spreading ridge magma. They have undergone metamorphic reconstitution correlated with ocean floor metamorphism.

INTRODUCTION

Ophiolite bodies provide important geological and geochemical evidences for understanding of formation of oceanic lithosphere at the mid ocean or back arc spreading environments. The mineralogy gives supporting data to the findings of petrography and chemistry. It gives information about the subsolidus transformations and phase changes caused by the events which take place in the oceanic realm or/and orogenic zones where the ophiolitic material has been tectonically transported.

Minerals investigated in this study belong to an incomplete ophiolite body previously called Ediğ e ultramafic body (Tankut and Sayın, 1989) in the Ankara melange. Although general geology of the body and geochemistry of its rocks have been described by Tankut and Sayın (1989) and Tankut and Gorton (in press), respectively, little information on the detailed mineralogy and phase chemistry is available.

This paper presents the results of electron microprobe, X-ray diffraction and electron microscope studies of silicate minerals from the cumulate sequences, and chromites from the tectonite sequences in the ophiolite body, described above. Main objective of this investigation is to determine the compositions of the primary and secondary minerals, and to interpret the subsolidus changes in the mineral phases.

PREVIOUS WORK

A brief review of the general geological and geochemical features of the Ediğ e ophiolite body, previously described by Tankut and Sayın (in press) and Tankut and Gorton (1988), is presented here.

The body (Fig.1) has an incomplete ophiolite stratigraphy (Penrose conference, 1972). It contains tectonite and cumulate ultramafic rocks and cumulate gabbros that, it is regarded to represent mantle and a part of the crustal sequences (Tankut and Gorton, in press) of the Tethyan oceanic lithosphere (Fig.2). Stratigraphically upper layers of a classic ophiolite, as sheeted dykes pillow basalts and sedimentary cover are lacking. The boundary between the mantle and crustal sequences are not well defined due to the intense deformation and serpentinization.

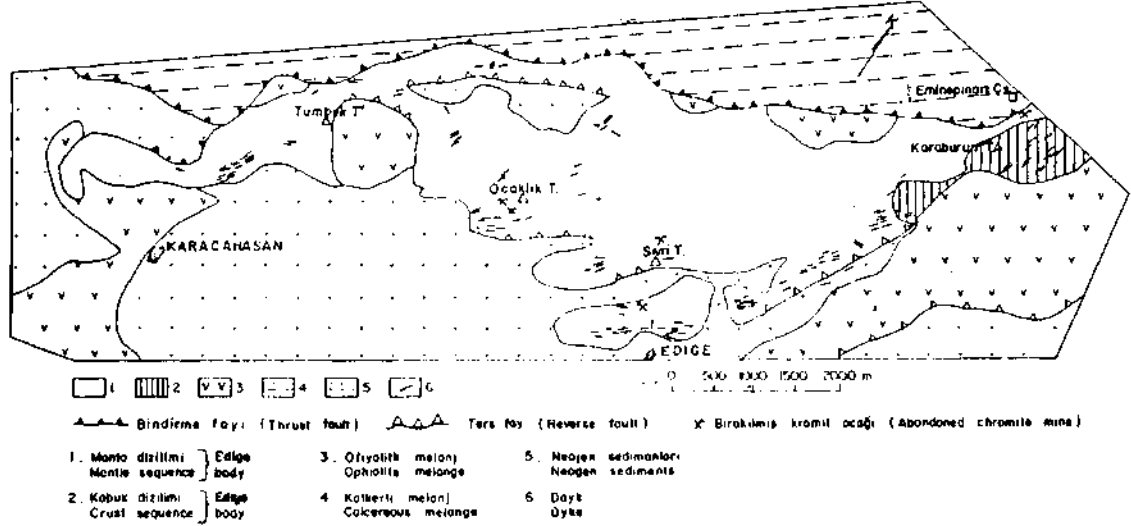


Fig.1— Geologic map of Edige ophiolite body. Simplified after Tankut and Sayin (1989).

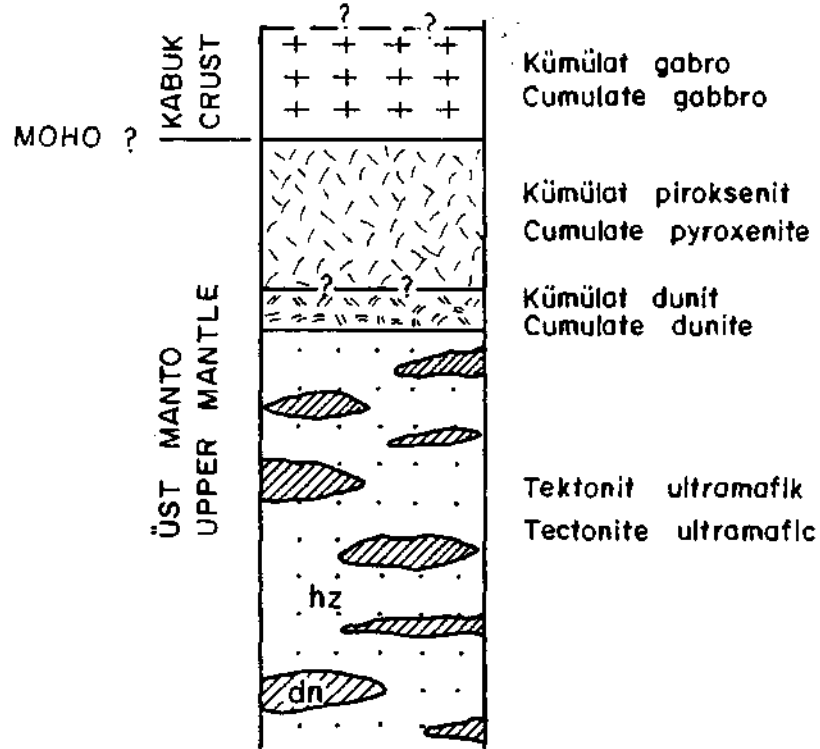


Fig.2— Generalized columnar section of the Edige ophiolite body.

The tectonite sequence is composed predominantly of harzburgite and lesser dunite. The latter is in the form of irregular lenses and interlayers. There are also abundant orthopyroxenite and websterite layers. Chromite is concentrated to form the pod shaped ore bodies or occurs as thin layers within the dunite.

The cumulate sequence is thin and incomplete in the exposed outcrops. The rock types range from ultramafic cumulates to felsic differentiates. Ultramafic cumulates occur at the base of the sequence, indicating with the order of crystallization, and include serpentinized dunite, clinopyroxenite and websterite. Gabbroic members

are only layered gabbros. Small lenses or dykelike bodies of only felsic material occur as being sandwiched between the gabbro layers.

DISTRIBUTION OF MINERALS

Rocks were sampled from both tectonite and cumulate sequences. Since the body does not show its original

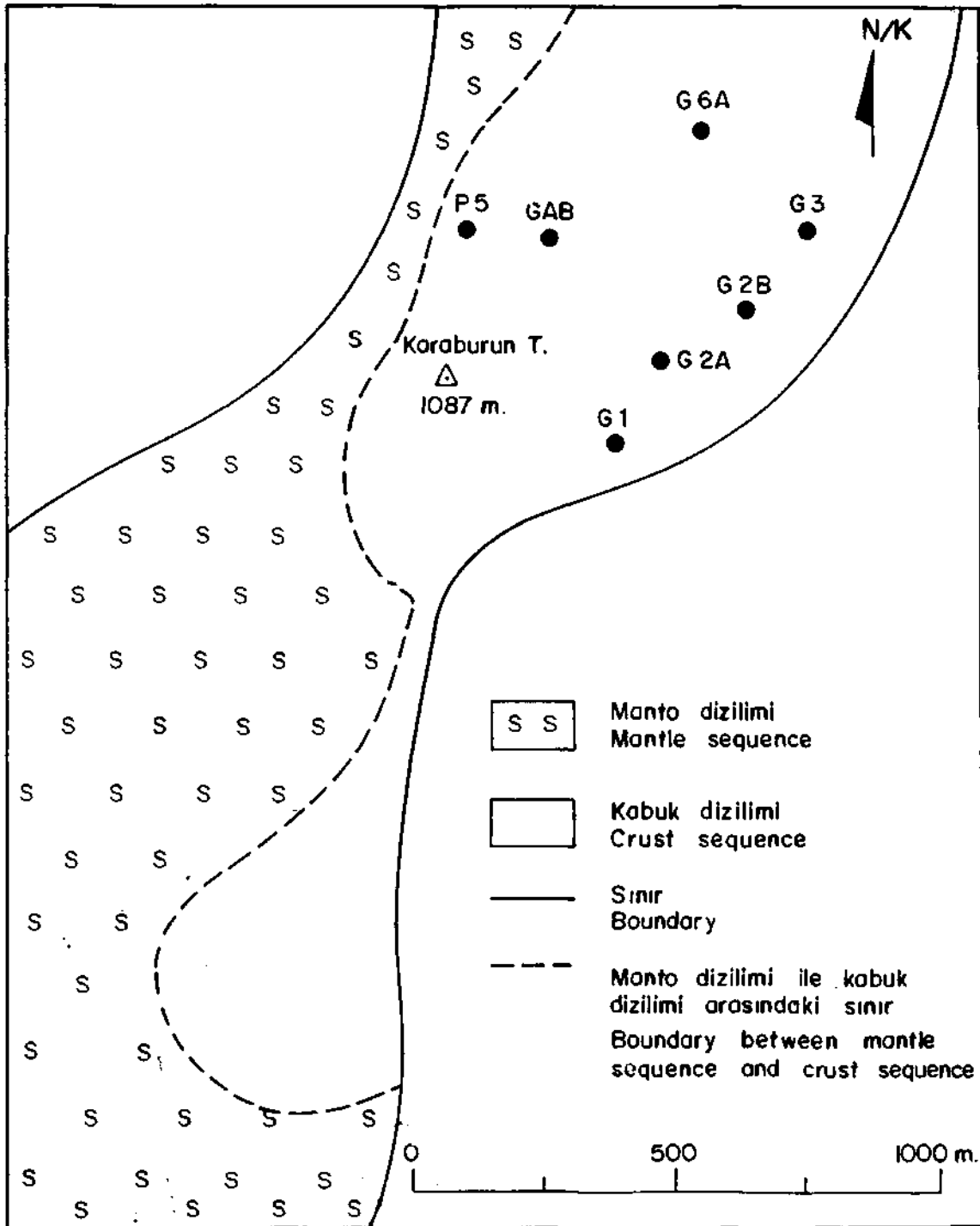


Fig.3- Location map of Edge body.

position, stratigraphical relations of the rocks were inferred by brief field observations (Fig.3).

Tectonite sequence

Primary textures and mineral associations of the rocks are generally obliterated because of the intense serpentinization. Relict minerals preserved in some of the rocks have given information about the original features. In this respect, in order to discriminate harzburgite from dunite the original modal pyroxene proportions were determined from the bastites, pseudomorph of pyroxenes, since they have well preserved crystal outlines of previous pyroxenes. The best preserved mineral is chromium-spinel. It is associated with olivine and constitutes the chromitites. It also occurs as a disseminated accessory in the harzburgite as anhedral picotite and chromite, and in the dunite as euhedral chromite. Serpentine, talc, occasionally actinolite, tremolite, chlorite, magnesite and silica minerals are the common alteration products.

Cumulate sequence

The lowest unit of the cumulate sequence is dunite. It constitutes a severely serpentinized zone between tectonite and cumulate sequences. Serpentinization obliterate the original textures and mineralogy. Pyroxenites occupy stratigraphically higher levels below the gabbros. They are clinopyroxenite and websterite and contain minerals ranging in size from medium to pegmatite. Cumulate texture is well presented by the interlocked sub-hedral grains of pyroxene and interstitial small grains of pyroxene and olivine between the coarser pyroxenes.

In the gabbro sequence alternation of mafic mineral rich and felsic mineral rich bands construct the layering. The rocks display well preserved cumulate texture, and deformational textures are rare. Cumulus olivine, pseudomorphosed by serpentine, plagioclase, clinopyroxene and subordinate orthopyroxene are the primary mineral phases throughout the layered gabbro sequence. Olivine is confined to the lowermost gabbro layers. Orthopyroxene poikilitically encloses the clinopyroxene and occurs as an intercumulus phase. Plagioclase, occurring in a minor amount, also appears as an intercumulus phase in the rocks of the lower levels. It is in cumulus status and occurs in a large amount in the rocks of the higher levels. The extremely low contents of REE indicate the cumulate origin of the layered rocks (Tankut and Gorton, in press). Green amphibole is a secondary mineral and the degree of its development increases with stratigraphic height. In the rocks from higher levels, almost all the pyroxenes are replaced by amphibole. Small relict pyroxene patches and abundant magnetite dots on the grains indicate the previous existence of pyroxene. Plagioclases display albitization which increases towards the upper layers. Commonly prehnite and rarely pumpellyite are present as the other secondary phases. The rocks of the felsic dykelike bodies have color index less than 5. They are composed predominantly of albite. Amphibole pseudomorph of clinopyroxene, prehnite, rarely pumpellyite and sphene are the common constituents. Their bulk rock composition displays desilicification (SiO₂, down to 46.50 %) and calcium enrichment (CaO, up to 24.93 %) relative to gabbros (Tankut and Gorton, in press). Such a bulk rock composition can well be attributed to the presence of prehnite and pumpellyite. The composition is similar to those of rodingites but the absence of hydrogarnet, characteristic mineral of rodingites, excludes this possibility.

MINERAL CHEMISTRY

Data of mineral chemistry, presented here, belong to the minerals of websterite and gabbro members of the cumulate sequence and to the chromites which are the most stable phases of the tectonite sequence.

Mineral analyses of silicates (except serpentine) were made on a computer controlled energy dispersive electron microprobe in the University of Toronto. Natural minerals were used as standards. Several plagioclases were also determined by simple optical methods and a few grains, in two rocks, by Universal stage.

EDIGE OPHIOLITE

were analysed in MTA laboratories by X-ray fluorescent technique.

Relevant rock samples were collected from various layers. Position of the samples, in the order of increasing height, from the contact between tectonite and cumulate is, P5, G4B, G6A, G2A, G2B (Fig.3). P5 is websterite and the others are layered gabbros. G1 and G3 come from the felsic dyke like bodies.

Orthopyroxene

Orthopyroxene in both websterite and layered gabbro is enstatite (Fig.4). The grains show homogeneity within the samples (Table 1). The En content ranges from 85 in the websterite to 75 in the layered gabbro.

Table 1— Orthopyroxene composition in the cumulate rocks of Edige body

	<i>P5</i>		<i>G6A</i>	
	<i>Grain 1</i>	<i>Grain 2</i>	<i>Grain 1</i>	<i>Grain 2</i>
SiO ₂	54.12	53.64	54.03	54.57
Al ₂ O ₃	1.29	1.86	1.90	1.62
FeO _T	6.96	7.47	15.10	14.66
MnO	n.d.	0.18	n.d.	n.d.
MgO	33.29	33.48	27.96	27.10
CaO	2.81	2.23	1.23	1.45
Na ₂ O	1.69	1.79	n.d.	n.d.
Total	100.16	100.65	100.22	99.40

Structural formulae on the basis of 6(O)

Si	1.95	1.92	1.92	1.93
Al	0.05	0.08	0.08	0.07
Fe	0.19	0.20	0.45	0.45
Mn	n.d.	0.005	n.d.	n.d.
Mg	1.61	1.61	1.50	1.49
Ca	0.098	0.08	0.05	0.06
Na	0.11	0.11	n.d.	n.d.
En	84.89	85.02	74.92	74.51
Fs	9.96	10.65	22.71	22.62
Wo	5.15	4.07	2.37	2.87
Mg [#]	89.50	88.63	76.74	76.71

FeO_T = Total FeO

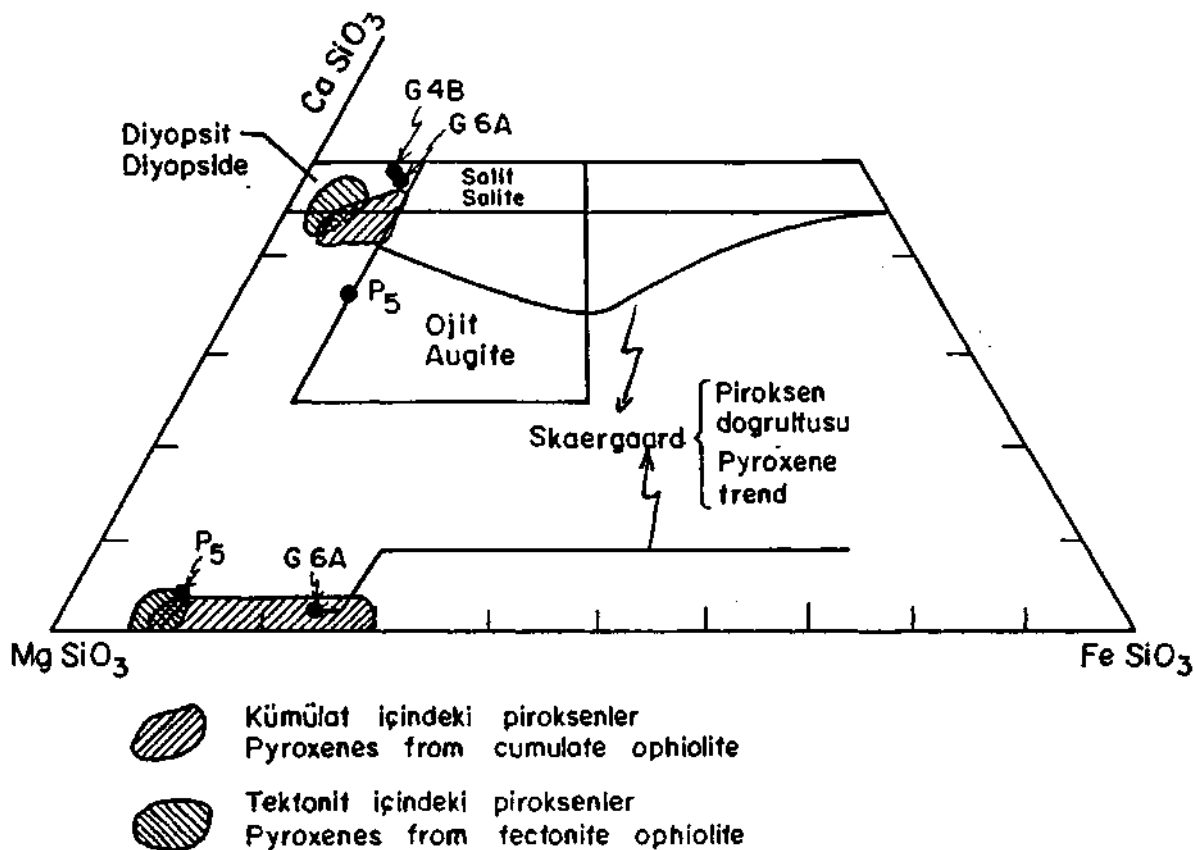


Fig.4— Pyroxene compositions from the cumulate rock of Edge body (Poldervaart and Hess, 1951).
Discrimination after Coleman (1977).

The orthopyroxene of the gabbros contain more Fs (= 23) and less Wo (=2.50) relative to the websterite (Fs = 10, Wo — 4.50). That means, there is positive correlation between Ca^{2+} and Mg^{2+} negative correlation between Ca^{2+} and Fe^{2+} . Al_2O_3 content is low and less than 2%.

Mg number ($Mg \# = \frac{Mg^{2+}}{Mg^{2+} + Fe^{2+}}$) of the orthopyroxene decreases from nearly 89 in the websterite to nearly 77 in the gabbro. The coexisting clinopyroxene in the gabbro has higher Mg #: (82-84).

Clinopyroxene

Clinopyroxene of the gabbros show fairly homogeneous composition within the grains and within the samples (Table 2). In the pyroxene composition diagram (Poldervaart and Hess, 1951), the clinopyroxenes of the gabbros fall in the diopside field (Fig.4). However, the "grain 2" in the sample G4B has Fs as much as 9.77 and so the clinopyroxene approaches the salite composition. Clinopyroxene of the websterite (P5) is augite. Due to the single spot analysis on one grain, information about the compositional variation within the grain and within the sample could not be obtained. The Mg of the clinopyroxenes are almost similar in the websterite (= 82) and gabbro (81.82-84.17).

Amphibole

Amphibole, as a secondary mineral occurs more commonly in the gabbros. The pyroxenes in the websterites show slight uralitization. Complete amphibole replacement with relict pyroxenes (mainly clinopyroxenes), exists

Table 2—Clinopyroxene composition in the cumulate rocks of Edige body

	<i>P5</i>	<i>G6A</i>			<i>G4B</i>				
	<i>Grain 1</i>	<i>Grain 1</i>		<i>Grain 2</i>	<i>Grain 1</i>			<i>Grain 2</i>	<i>Grain 3</i>
		<i>Spot 1</i>	<i>Spot 2</i>		<i>Spot 1</i>	<i>Spot 2</i>	<i>Spot 3</i>		
SiO ₂	52.65	52.22	52.17	52.55	52.32	52.36	51.90	51.83	52.04
Al ₂ O ₃	2.41	2.15	1.51	0.90	1.12	0.95	1.16	1.92	2.25
TiO ₂	n.d.	n.d.	n.d.	n.d.	n.d.	n.d.	n.d.	0.18	0.24
FeO _T	6.98	6.18	5.97	5.71	5.92	5.3	5.82	6.17	6.18
MnO	0.45	n.d.	n.d.	n.d.	0.17	n.d.	n.d.	n.d.	n.d.
MgO	19.09	15.96	15.54	15.69	15.39	15.81	16.11	15.82	15.83
CaO	17.86	24.17	25.03	25.93	24.58	25.75	26.83	23.51	24.10
Na ₂ O	1.09	n.d.	n.d.	n.d.	n.d.	n.d.	n.d.	n.d.	n.d.
Total	100.53	100.68	100.22	100.78	99.50	100.17	101.82	99.43	100.64

Structural formulae on the basis of 6(O)

Si	1.90	1.91	1.93	1.96	1.95	1.96	1.95	1.93	1.90
Al	0.10	0.09	0.07	0.004	0.05	0.04	0.05	0.08	0.09
Ti	—	—	—	—	—	—	—	0.005	0.007
Fe	0.21	0.19	0.18	0.17	0.18	0.16	0.17	0.19	0.19
Mn	0.01	n.d.	—	—	0.005	—	—	—	—
Mg	1.02	0.87	0.84	0.84	0.84	0.85	0.83	0.88	0.86
Ca	0.69	0.94	0.98	0.99	0.97	0.99	0.99	0.94	0.94
Na	0.07	—	—	—	—	—	—	—	—
En	52.88	43.36	42.13	41.80	42.19	42.39	41.66	43.42	43.22
Fs	10.85	9.42	9.08	8.54	9.11	7.97	8.45	9.97	9.47
Wo	35.57	47.21	48.79	49.66	48.44	49.64	49.89	46.61	47.31
Mg#	82.06	82.15	82.26	83.04	81.82	84.17	83.14	82.04	82.03

in the gabbros (G2A, G2B), which are assumed to come from higher levels and rocks of dykelike felsic bodies. Beside a few remnant pyroxene patches on the grains, the lower Mg (Mg # = 68-75) content of the amphiboles than that of the pyroxenes (Mg # > 81, those of lower layer gabbros have been considered) which were supposed to be replaced, and the CaO content which is half of that in pyroxenes (Tables 2 and 3) confirm the secondary origin of the amphiboles (Stakes et al., 1985). Based on the analyses at two spots of a selected grain in the sample G2A, the composition within a grain seems to be quite homogeneous. It also does not change much between the different grains (Table 3). However, compositional difference is displayed between the amphiboles of the gabbros

Table 3— Amphibole composition in the upper stratigraphical level gabbros.

	Amphibole				
	G1		G2A		G2B
	Grain 1	Grain 2	Grain 1		Grain 1
			Spot 1	Spot 2	
SiO ₂	50.59	51.40	53.63	53.21	54.23
Al ₂ O ₃	6.03	4.73	4.74	5.67	2.19
TiO ₂	0.27	0.20	0.43	0.38	0.26
FeO	11.70	12.14	9.87	10.23	10.45
MnO	0.18	0.32	—	—	n.d.
MgO	15.45	15.19	16.52	16.36	17.29
CaO	11.59	10.96	12.35	12.14	12.66
Na ₂ O	2.26	1.55	1.29	1.93	n.d.
K ₂ O	n.d.	n.d.	n.d.	0.11	n.d.
Total	98.07	96.49	98.83	100.03	97.08
Structural formulae on the basis of 24 (O,OH,F,Cl)					
Si	7.28	7.49	7.54	7.42	7.76
Al	1.02	0.81	0.79	0.93	0.37
Ti	0.03	0.02	0.05	0.04	0.03
Fe	1.41	1.48	1.16	1.19	1.25
Mn	0.02	0.04	—	—	—
Mg	3.32	3.30	3.46	3.40	3.69
Ca	1.79	1.71	1.86	1.81	1.94
Na	0.59	0.44	0.35	0.52	—
K	0.03	—	—	0.02	—
Mg #	69.85	68.47	74.89	74.02	74.67

(G2A, G2B) and those of the felsic bodies (G1). The latter is rich in Fe and Al. The Mg of the amphibole in the felsic dykelike rocks is as low as = 69 whereas that of the gabbros varies between 74 and 75 (Table 3). All the amphiboles are comparable in composition to actinolite (Fig.5).

Plagioclase

Microscopically plagioclases in all the rocks are unzoned. Optical determination suggest that plagioclase range from An₄₀ to An₉₀ in the lower level gabbros. The An content below 60 is most probably due to the sub-

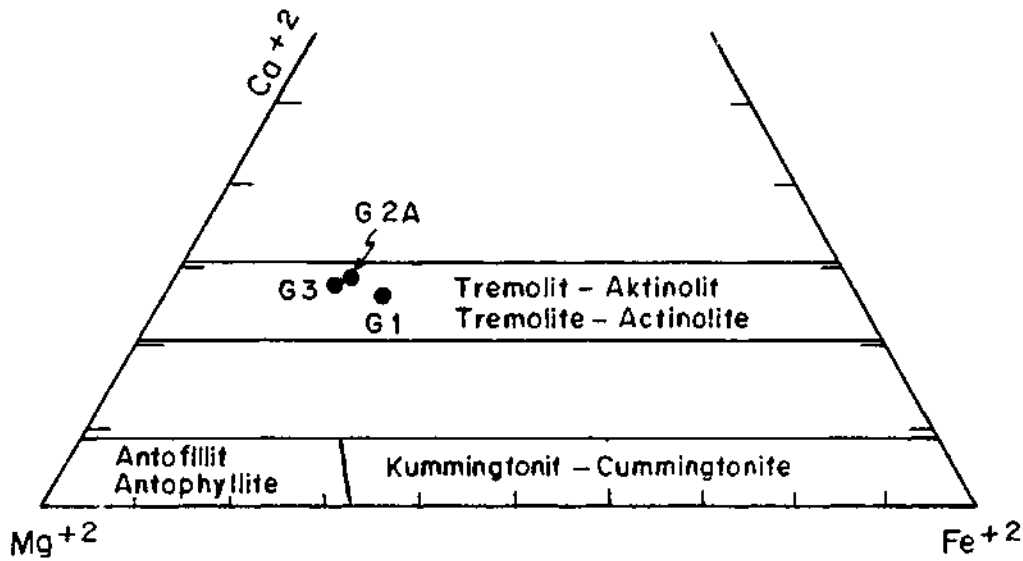


Fig.5- Amphibole compositions from the gabbros of upper layer, Edige body (Deer et al.,1963).

Table 4- Plagioclase, prehnite, pumpellyite composition in the gabbros and felsic dyklike bodies of Edige body

	Plagioclase		Prehnite				Pump.***	
	G4B	G2A	G1		G3		G2B	
	Grain 1	Grain 1	Grain 1		Grain 1		Grain 1	
			Spot 1	Spot 2	Spot 1	Spot 2		
SiO ₂	45.85	69.35	43.33	43.29	42.54	43.02	42.03	36.95
Al ₂ O ₃	34.15	20.05	24.61	24.95	24.47	24.30	24.49	28.73
FeO	0.21	n.d.	1.94	0.90	n.d.	n.d.	0.50	4.36
MgO	n.d.	n.d.	n.d.	n.d.	n.d.	n.d.	n.d.	n.d.
CaO	18.25	n.d.	27.02	26.89	28.08	28.01	25.06	24.01
Na ₂ O	1.09	11.57	n.d.	n.d.	n.d.	n.d.	n.d.	n.d.
Total	99.55	100.97	96.90	96.03	95.09	95.33	92.08	94.05
Structural formulae O(32)			Structural formulae 24* (O,OH) ; 28** (O,OH,H ₂ O)					
Si	8.55	11.87	6.00	6.00	6.00	6.00	6.00	5.94
Al	7.43	4.13	3.81	3.97	3.86	3.88	4.10	5.36
Fe	0.02	-	0.24	0.08	-	-	0.06	0.57
Mg	-	-	-	-	-	-	-	-
Ca	3.57	-	3.93	3.95	4.14	4.12	3.85	4.12
Na	0.43	4.00						
Or	0	0						
Ab	10.75	100						
An	89.25	0						

solidus equilibration. EMP analysis of one plagioclase crystal from the specimen G4B gives An₈₉ (Table 3) and universal stage measurement of another one from G6A was found to be An₄₀. All the plagioclases in the upper level gabbros represented by G2A and G2B show refractive index less than that of the Canada balsam. EMP analysis of a crystal in the sample G2A gives almost pure albite, Ab₁₀₀ (Table 3). The universal stage measurements on G2A and G2B also gave An₄ and X-ray diffraction patterns of the samples G2A and G2B (from the felsic dykelike rocks) indicate the presence of albite (Fig.6).

Prehnite and pumpellyite

Prehnite exists in the high level gabbros (G2A, G2B) and dyke like rocks (G1, G3). It exhibits its characteristic rosette form, made by the aggregation of small radiating crystals (Deer et al., 1965) X-ray diffraction records of G2A and G1 also verify the presence of prehnite (Fig.6). The results of analyses, by EMP, given in Table 4, shows that it displays its constant composition throughout the grains.

Table 5— Chromite compositions in the chromitites of tectonite sequence of Edige body

	A1	B3	C1	F1
Cr ₂ O ₃	60.02	61.76	60.20	58.76
Al ₂ O ₃	8.34	8.69	10.70	12.19
MgO	10.76	10.34	12.63	13.03
FeO _T	15.86	15.73	15.79	14.91
SiO ₂	0.57	1.46	0.22	n.d.
CaO	0.40	0.59	n.d.	0.18
Total	95.95	98.57	99.54	99.07
Fe ⁺² O*	15.58	17.09	14.36	13.89
Fe ⁺³ O ₃ *	1.16	0.89	1.71	1.32
Structural formulae on the basis of 32 (O)				
CRAT	0.82	0.84	0.77	0.75
ARAT	0.17	0.18	0.21	0.23
FRAT	0.01	0.01	0.02	0.02
F/FM	0.43	0.47	0.39	0.37
M/FM*	0.57	0.53	0.61	0.63
F/M	0.75	0.89	0.64	0.59

FeO_T=Total FeO

* Calculated according to the stoichiometry of chromite.

A1— Tümbek tepesi; B3— Çaklı tepesi; C1— Edige köyü; F1— Emine pınar çeşmesi.

$$F/FM = \frac{Fe^{+2}}{Fe^{+2} + Mg^{+2}}, \quad M/FM = \frac{Mg^{+2}}{Fe^{+2} + Mg^{+2}}$$

$$CRAT = \frac{Cr^{+3}}{Al^{+3} + Cr^{+3} + Fe^{+3}}, \quad FRAT = \frac{Fe^{+3}}{Al^{+3} + Cr^{+3} + Fe^{+3}}, \quad ARAT = \frac{Al^{+3}}{Al^{+3} + Cr^{+3} + Fe^{+3}}$$

Pumpellyite has been detected by microprobe analysis. One grain in the sample G4B has a composition which corresponds to that of pumpellyite (Deer et al., 1963).

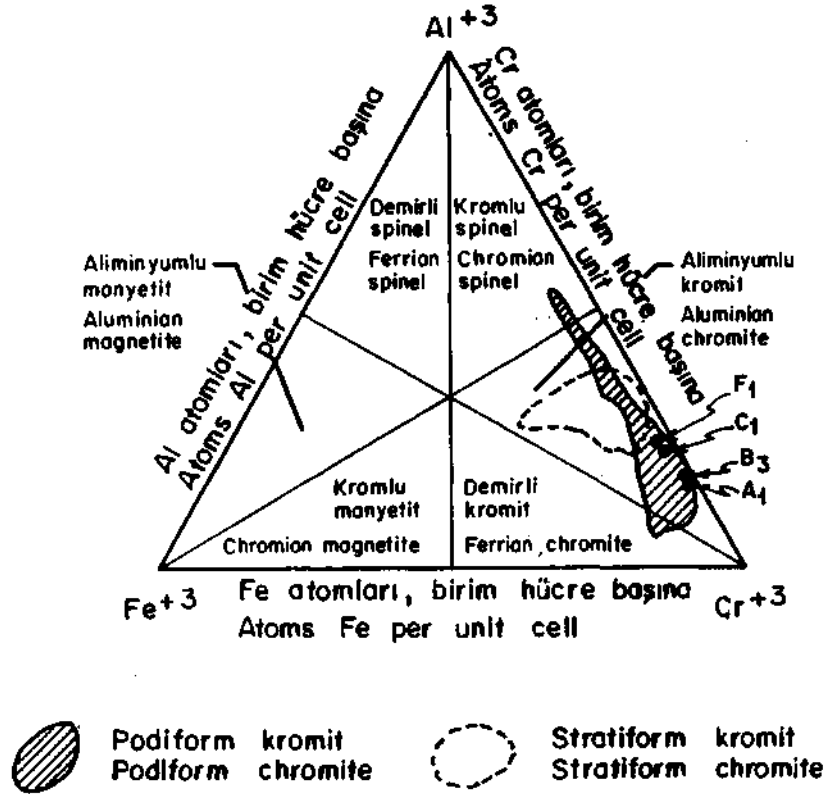


Fig.7– Compositions of chromites from the chromitites in tectonite sequence, Edige body (diagram after Stevens, 1944). Classification after Dickey (1975).

Chromite samples have been collected, from the chromitites of the ore seams of various localities in the tectonite sequence, for analysis. Compositions have been determined on clean chromite powders by XRF technique. However, some silicate impurity, remained in the analyzed powder is reflected as SiO_2 , which is up to 1.5% (Table 5).

The chromites are characterized by high Cr_2O_3 (58.76 % - 61.76 %) and low Al_2O_3 (8.34 % - 12.19 %). The total FeO is almost constant around (15 %). The chromites fall in the aluminian chromite field (Fig.7) in the composition diagram (Stevens, 1944).

RESULTS AND DISCUSSION

The primary phase assemblages of "olivine + orthopyroxene + clinopyroxene + chromium spinel" in the tectonite ultramafic rocks, and "olivine + clinopyroxene + orthopyroxene" in the cumulate ultramafic rocks characterize the mantle sequence of the Edige ophiolite body. The gabbroic rocks of the crustal sequence display the primary assemblage of "plagioclase + clinopyroxene + olivine + orthopyroxene", the first three being the main cumulus phases in the rocks. Amphibole + serpentine + chlorite + prehnite pumpellyite + sphene are the secondary minerals. The amount of amphibole development increases with stratigraphic height that, in the upper level gabbros the pyroxenes are almost completely replaced by amphibole.

Mg-Fe relationship, represented by "Mg number" (Mg#) is one of the best indices which reflect the primary magma composition of rocks, since, Mg-Fe cation proportion changes very little during the subsolidus equilibration (Elthon and Scarfe, 1983; Elthon et al., 1985). In the crustal sequence of Edige body, similarity of the Mg numbers of clinopyroxenes in websterite (82) and gabbro (83). Suggests the same magma source for these rocks. On the other hand considerable amount of decrease of Mg # of the orthopyroxene from the websterite to gabbro can be attributed to the fractional crystallization process. Intercumulus nature of the orthopyroxene and the higher Mg # of the coexisting clinopyroxene may also imply the same process and can be explained by late crystallization of orthopyroxene. All the findings described above, support the cumulate nature of the crustal material in the Edige body.

Compositional range for orthopyroxene and clinopyroxene of the cumulate rocks (Fig.4) is comparable to those of the oceanic crust (Coleman, 1977). Both phases are rich in magnesium (Tables 1 and 2). Although the orthopyroxene of the gabbro is relatively iron rich with ferrosilite value of 23 mole %, the classic trend shown by the pyroxenes of tholeiitic magma (as Skaergaard) is not followed by the Edige pyroxenes (Fig.4). Their low Na₂O and K₂O (Tables 1 and 2) content indicate the depleted nature of the magma which occurs in spreading ridge

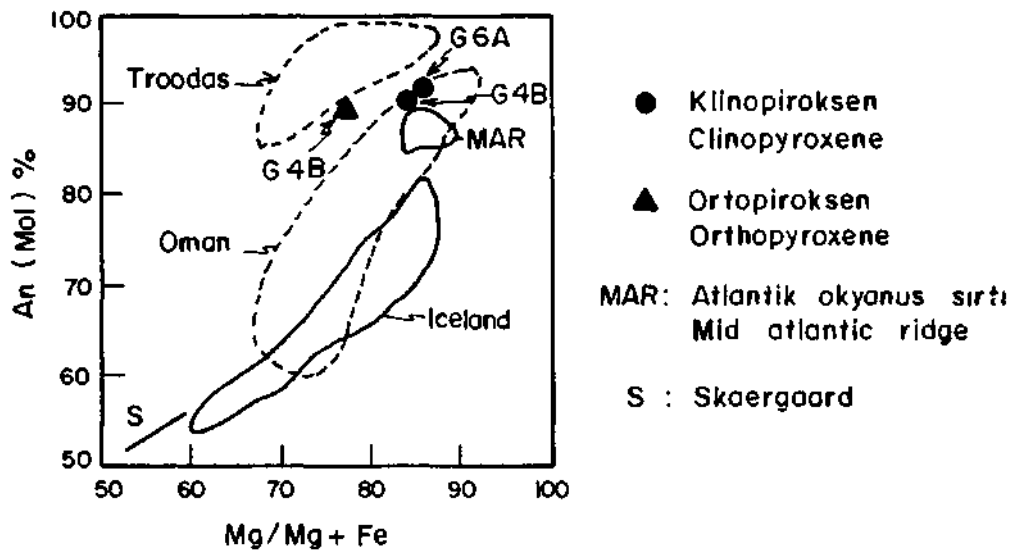


Fig.8- Compositions of coexisting pyroxene plagioclase, from the banded gabbros of Edige body (other data from Thy, 1987). Iceland data from microcrystals of alkalic glasses. The plagioclase of the G6A was determined by optical method as An₉₀.

environment (Malpas and Langdon, 1985). This feature therefore supports the suggestion, made by Tankut and Gorton (in press), about the depleted nature of the upper mantle as a source of the rocks in the Edige body, based on bulk rock REE contents. The low Al₂O₃ contents (Tables 1 and 2) of the pyroxenes are correlated with those crystallized at shallow depths like in oceanic crust. Plagioclase composition in the lower level gabbros range from An₄₀ to An₉₀. The composition between An₆₀ and An₉₀ are commonly reported from the gabbros of ocean floor (Prinz et al., 1976; Burns, 1985). The similarity of coexisting pyroxene and plagioclase compositions to those of ocean floor is illustrated in Figure 8. The "chromites of Edige body display properties (Fig.7) typical of podiform types (Dickey, 1975). In the structural formula, the bivalent oxide site (RO %) is occupied by 55 % - 63 % MgO (except sample B3), and this is comparable to those of podiform chromites (55% - 75%) described by Thayer (1964).

In the lower level gabbros, development of secondary amphibole after pyroxene, serpentine after olivine and low anorthite (An₄₀) content of plagioclases, suggest sea floor metamorphism at temperatures (450°-550°C) in amphibolite facies (Coleman, 1977; Stakes et al., 1985). The higher level gabbros (G2A, G2B) are characterized by albite, complete replacement of pyroxene by actinolite and appearance of new phases as prehnite, pumpellyite, chlorite and sphene. This paragenesis indicate greenschist facies conditions. Greenschist facies metamorphism has been reported from mid ocean ridges to appear within the upper parts of the ophiolite, including the upper parts of the gabbros (Coleman, 1977).

The rocks of the felsic dyklike bodies (G1, G3) also display the same paragenesis as the high level gabbros in the Edige body. These rocks were interpreted by Tankut and Gorton (in press) to have a cogenetic relationship with the cumulate gabbros and to be probably the late differentiates of a common magma, depending on their incompatible (REE included) element contents. The lower Mg (= 69) of their amphiboles than those of the gabbros (= 75) support this view (Table 3). Similar bodies have been reported from other oceanic lithosphere environments (Coleman, 1977) being interpreted as the silicic differentiates (Stakes et al., 1985; Hopson et al., 1981). However, the bulk rock composition of the felsic rocks in the Edige body, show desilicification and Ca, Al enrichment (Tankut and Gorton, in press). In the light of the features described above, these rocks might have been produced from the magma as late differentiates after the crystallization of the gabbros and reconstituted by metasomatism at the sea floor.

Finally, all the evidences discussed above lead to the conclusion that the mineral assemblages in various rock types of the Edige ophiolite body are similar to the corresponding rocks of the oceanic lithosphere. The minerals of the cumulates suggest direct crystallization from the spreading ridge magma. They have undergone metamorphic reconstitution correlated with ocean floor metamorphism.

ACKNOWLEDGEMENT

Microprobe analyses were carried out at the Geology Department, University of Toronto. All the laboratory staff are acknowledged with thanks. Thanks are due to Mr. Taml Akyüz for the XRF analyses of chromites in MTA, to Mr. Akın Geven for the universal stage measurements and to Mr. Mümtaz Kibar for the XRD records.

A. Tankut is grateful to Drs.C.Cermignani and M.P.Gorton for their kind help in the EMP laboratory. Above all A.Tankut is indebted to Prof.M.Üzümeri for his kind help and concern during her one year stay in Toronto.

Manuscript received March 20, 1989

REFERENCES

- Burns, L.E., 1985, The border Ranges ultramafic and mafic complex, southcentral Alaska : cumulate fractionates of island-arc volcanics: *Can. J. Earth Sci.*, 22, 1020-1038.
- Coleman, R.G., 1977, *Ophiolites : ancient oceanic lithosphere?* : Springer-Verlag, 229, New York, Ny.
- Deer, W.A.; Hovie, R.A. and Zussman, J., 1963, *Rock forming minerals* : Longmans Press, 5 vol., London.
- Dickey, J. S.Jr., 1975, A hypothesis of origin for podiform chromite deposits : *Geochim. Cosmochim. Acta*, 39, 1061-1074.
- Elton, D. and Scarfe, C.M., 1983, Highpressure phase equilibria of a high-magnesia basalt and the genesis of primary oceanic basalts : *Am.Mineral.*
- ; Casey, D.F. and Komor, S., 1984, Cryptic mineral-chemistry variations in a detailed traverse through the cumulate ultramafic rocks of the North Arm Mountain massif of the Bay of Islands ophiolite, Newfoundland : *Gass, I.G., Lippard,*

- S.J. and Shelton, A.W., eds., Ophiolites and oceanic lithosphere, 83-97, London.
- Hopson, C.A.; Coleman, R.G.; Gregory, R.T., Pallister, J.S. and Bailey, E.H., 1981, Geologic section through the Semail ophiolite and associated rocks along a Muscat-ibra transect, southeastern Oman Mountains: *J. Geophys. Res.* 86, 2527-2544.
- Malpas, J. and Langdon, G., 1984, Petrology of the Upper Pillow Lava suite, Troodos ophiolite, Cyprus : Gass, I.G., Lippard, S.J. and Shelton, A.W., eds., Ophiolites and oceanic lithosphere, 155-167, London.
- Poldervaart, A. and Hess, H.H., 1951, Pyroxenes in the crystallization of basaltic magma: *Jour. Geol.*, 59, 472-489.
- Prinz, M.; Keil, K.; Green, J.A.; Bonatti, E. and Honnorez, J., 1976, Ultramafic and mafic dredge samples from the equatorial mid-Atlantic ridge and fracture zones : *Journal of Geophysical Research*, 81, 4087-4103.
- Stakes, D.S.; Taylor, H.P., Jr and Fisher, R.L., 1985, Oxygenisotope and geochemical characterization of hydrothermal alteration in ophiolite complexes and modern oceanic crust : Gass, I.G., Lippard, S.J. and Shelton, A.W., eds., Ophiolites and oceanic lithosphere, 199-213, London.
- Stevens, R.E., 1944, Composition of some chromites of the western Hemisphere : *Am.Miner.*, 29, 1-34.
- Tankut, A.T. and Gorton, M.P., (in press), Geochemistry of a mafic-ultramafic body in the Ankara melange, Anatolia, Turkey : Evidences for a fragment of oceanic lithosphere Moores, E., ed., *Proc.Symposium, Troodos 87, Ophiolites and oceanic lithosphere*,
- and Saym, M.N., 1989, Edige ultramafik kütlesi: *Turkish Journal of Engineering and Environmental Sciences*; 13/2, 229-244.
- Thayer, T.P., 1964, Principal Features and origin of podiform chromite deposits and some observations on the Guleman-Soridag District, Turkey : *Econ.Geol.*, 59-8, 1497-1524.
- Thy, P., 1987, Petrogenic implications of mineral crystallization trends of Troodos cumulates, Cyprus: *Geol.Mag.*, 124 (1), 1-11.

GEOLOGY OF THE BALIKESİR-BANDIRMA REGION (NORTHWEST ANATOLIA), PETROLOGY OF THE TERTIARY VOLCANISM AND ITS REGIONAL DISTRIBUTION

Tuncay ERCAN*; Erdem ERGÜL*; Ferit AKÇÖREN*; Ahmet ÇETİN**; Salahi GRANİT*** and Jerf ASUTAY*

ABSTRACT.— In the studied area, the basement is formed by the Late Palaeozoic aged metamorphic Fazlıdağ formation which contains locally lenses and bands of marble and serpentinite. These rocks are cut by a granitic and granodioritic intrusion called Kapıdağı granite which is Late Palaeozoic in age. It is unconformably overlain by the Early Triassic aged Karakaya formation consisting of a wide range of detritic rocks and some limestone blocks. This formation is underlain by the Middle to Late Triassic aged Çaltepe formation consisting of conglomerate, sandstone, sandy limestone and limestone and Late Jurassic to Early Cretaceous aged Akçakoyun formation respectively. The latter one mainly consists of limestones and unconformably overlies the Çaltepe formation. Towards the top of this sequence there is the Late Cretaceous aged Yayla melange which is composed of sedimentary, metamorphic and ophiolitic association and has a tectonic contact within each other. The Tertiary in the region is characterized by Paleogene aged Çataldağ and Ilıca-Şamlı granodiorites and granites, some terrestrial sedimentary rocks which one of Mio-Pliocene age and Miocene to Pliocene aged are also exposed. The Quaternary is cropped out at some thin deposits. In this study petrochemical analyses of the volcanic rocks have been carried out and it has been understood that they are in calc-alkaline character and also have some crustal features. In the light of these data the volcanic rocks have been compared with other volcanics of the region and their distribution has also been given.

PROGRESSIVE BRITTLE-DUCTILE DEFORMATION OF THE DEMİRKÖY PLUTON OF THE STRANDJHA MASSIVE OF THRACE - TURKEY

M.Atilla ÇAĞLAYAN*; Metin ŞENGÜN* and Ayhan YURTSEVER**

ABSTRACT.— Demirköy pluton, a Lower Cretaceous granitic body of the Strandjha massive of Thrace-Turkey, vary compositionally from a syeno-granite to quartz-diorite. The periphery of the granite has been converted to mortar gneiss and mylonite gneiss/schist. The host rocks, where they are of a pelitic origin, have been transformed into foliated contact schists comprising cordierite and andalusite. The intensity of shear shows a progressive diminution away from the periphery. The brittle-ductile deformation is ascribed to the emplacement of the granite causing multistage developments of multidirectional cleavage, kink type folding and shear pods that are observable in macroscopic and microscopic dimensions. The deformation is not attributed to large displacements, but is rather interpreted as the cumulative result of an echelon shearing.

INTRODUCTION

This article aims at presenting details of peripheral macro and microstructures of the Demirköy pluton of the Strandjha massive (Fig.1).

The cataclastic deformation was interpreted as a product of thermo-dynamic metamorphism by Üşümezsoy and Öztunalı (1981). This approach is fairly different from that of Aykol (1979) who defended an auto-cataclastic process resulting from rapid uprising of the pluton.

In Turkey, investigations on granite tectogenesis and related cataclastic processes have started in the last decade and may be considered fairly new in comparison to world-wide research on the subject since the beginning of the 19th century.

We have observed in the field that the structural elements of the pluton and those of the country rock are parallel. However, the detailed investigation of the microstructures suggests an outward push.

There has been a mechanical process during the emplacement, presumably through forceful injection, which has caused realization of shear zones leading to destruction and recrystallization of the granite as well as the country rock.

The area was mapped (Fig.2) to understand cause-effect relationship of the microscopically observed cataclastic deformation of the granite periphery and the country rock of the Demirköy pluton. We have tried to understand the deformational episodes; and relationship between deformation and crystallization by field mapping, (Fig.3) collecting oriented samples and textural interpretation of these oriented samples.

MAIN CHARACTERISTICS OF THE DEMİRKÖY PLUTON

Demirköy pluton lies in the eastern segment of the Strandjha massive. It has a slightly elongated shape, parallel to the general NW trend of the massive.

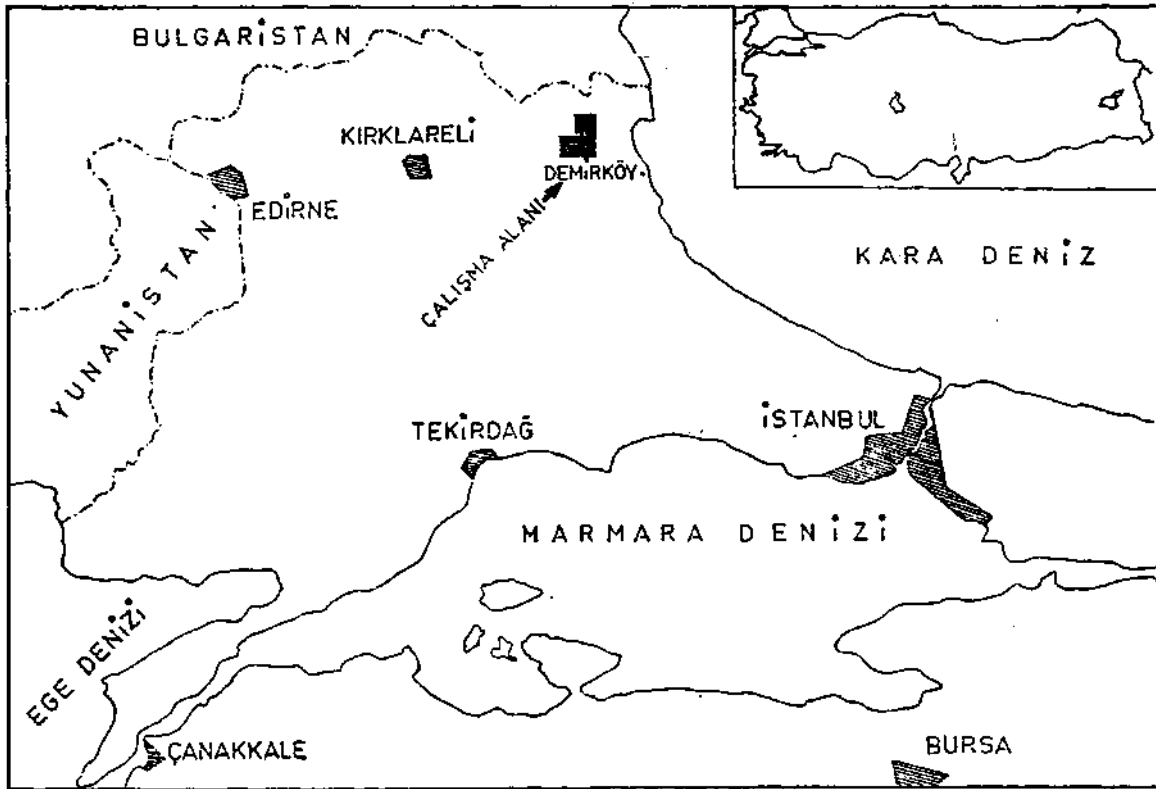


Fig.1— Location map.

The plutonic body was nomenclated as dioritic intrusions (Ksiazkiewicz, 1930), Demirköy magnetiferous granite lacolith (Pamir and Baykal, 1947), granite (Akartuna, 1959), granitic intrusions (Bürküt, 1966), Dereköy magmatic series (Aykol, 1979) and Demirköy pluton (Üşümezsoy, 1982; Aydın, 1982).

The pluton comprises a magmatic series varying compositionally from syeno-granite to quartz-diorite. It has intruded into basement rocks of the Strandjha massive that has generally suffered a metamorphism in amphibolite facies with local migmatitic areas (Bürküt, 1966; Yurtsever et al., 1986). It intrudes the Dolapdere formation of Jurassic age (Kapaklı formation of Aydın, 1974, 1982; Strandjha group of Üşümezsoy, 1982). It is covered by a sedimentary wedge starting with conglomerates and sandstones and minor volcanic intercalations.

K/Ar dating of the pluton (Aydın, 1982) gave an age of 83.1 ± 2.0 and 83.5 ± 2.5 ma from samples taken from the Dereköy pluton which Aydın (1982) considered a part of the Demirköy pluton. He suggested that the Coniacian age, thus found, is rejuvenated due to younger volcanic events. Tokel and Aykol (1987) claim a Santonian-Campanian age for the Demirköy granodiorite which, they suggest, is a part of the Srednogorie-Strandjha-Pontides chain.

Sharp contacts between the pluton and the country rock, a fairly wide aphanitic margin and granophyric textures are suggestive for an epizonal emplacement (Buddington, 1959).

Formation of augens in the contact aureole, penetrative character of the lineations and foliations, formation of a conformable fold envelope through formation of strain-slip cleavage and marginal thrusting are structural

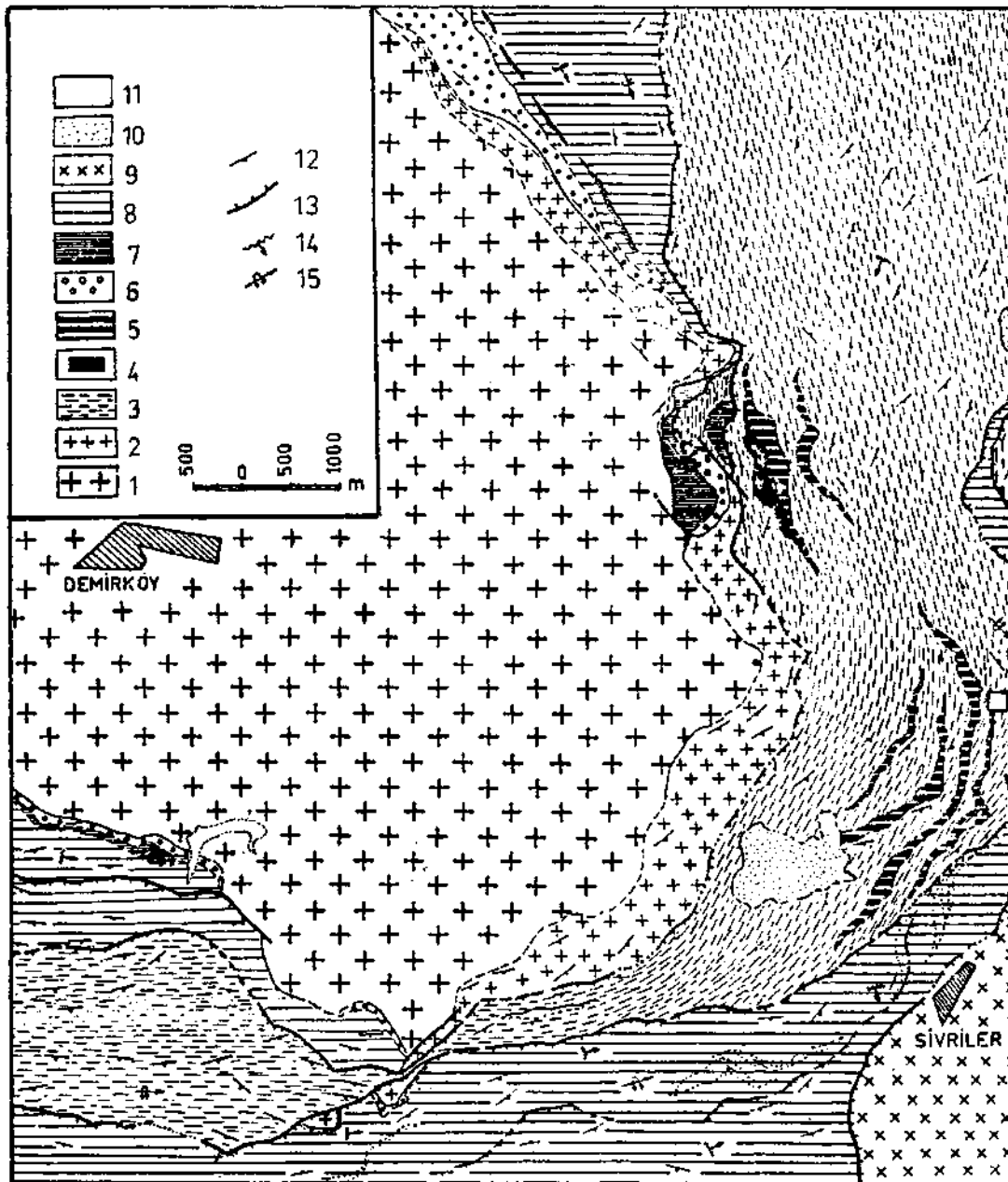


Fig.2— Geological map of the eastern and southeastern segments of the Demirköy plutone.

1-Demirköy pluton- 2- Microgranite, foliated granite; 3- Cataclastic granite; 4- Mylonite gneiss; 5- Mylonite schists; 6- Contact schists comprising cordierite and andalusite; 7 Marble+ Skarn; 8- Phyllite, chlorite schist and quartzite; 9- Sivri-ler granite; 10-Plio-Quaternary sediments; 11-Alluvium; 12-Foliation; 13-Thrust fault; 14-Microfold; 15-Fold axis.

elements seen peripherally. These structural features of the Demirköy pluton resemble those of the Colville batholith as described by Higgins (1971).

MICROSTRUCTURES OF THE CONTACT AEROLE

Symmetric and asymmetric axial planes of the contact schists are parallel to the contact plane throughout the

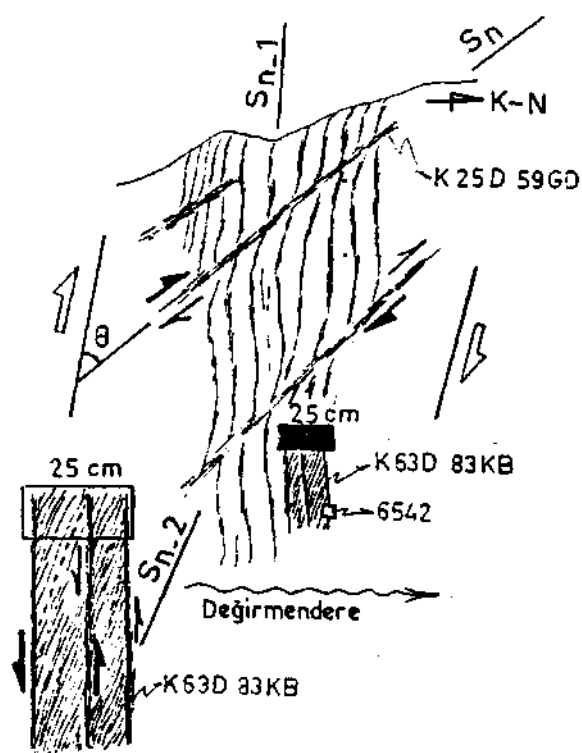


Fig.9— Mesoscopic structures. Early and late foliation, cross banding.

periphery. The observed microstructures consist of those produced by rotation of mineral grains such as garnet, pyrite, cordierite and andalusite, and, asymmetric pressure shadow areas.

Rotation of garnets and asymmetric pressure shadow areas

As it is seen in Plate I, fig.1, there is a marked difference between behaviour of the matrix and the grains of foliated rocks of the sheared zones, presumably due to different elastic behaviour. The matrix is fine grained so that it can flow around the grains while the clasts may have been broken up several times prior to and/or during shearing and consequent rotations. The fold axes of the mica flakes surrounding the garnet grains, as exemplified by the garnet in the lower part of Plate I, fig.1, defines the sense of rotation. Two asymmetric pockets, made up by a crushed quartz and feldspar mosaic, are seen in the upper-left and lower-right corners of the garnet grains. These are often seen as wings of durable feldspar porphyroclasts as a result of strain accumulation and thus brecciation of the grains. These asymmetric shadow areas are also known as "pressure tail" (Simpson and Schmid, 1983) and "pressure shadow wings" (Schoneveld, 1977). Pressure shadow areas can be used as a reliable indicator of the sense of rotation (Takagi, 1986)

Rotation in garnets as well as pressure shadow areas indicate a right-handed shear for the specimen.

Rotated crystals of andalusite and cordierite

Traces of rotation are very pronounced in the pinnitized cordierite porphyroblasts of the andalusite-cordierite schists (Plate I fig.2). The incipient foliation of these rocks are defined by orientation of the mica flakes. Andalusite is in the form of idiomorphic porphyroblasts and is occasionally seen to have been rotated. S shaped

wave of the cordierite (Helisitic structure) is at an angle to the early foliation planes. Waving is due to rotation and is indicative of a multi-phase deformation. The spindle and flattened shape of the grains point to growth during blastesis.

The examples given above are microstructural features showing shearing during the emplacement of the granite. These examples certify a couple between the granite and the country rock. Deformation is progressive and directionally defined.

MICROSTRUCTURES IN GRANITIC ROCKS

The symmetric and asymmetric structures caused by shearing are "oblique incremental quartz elongation", "displaced broken grains", and "mica fish".

Oblique incremental quartz elongation

Deformational characteristics of quartzo-feldspathic veins or the geometry of the recrystallized quartz mosaic that fill up the fractures within a rock or a mineral can be used for interpretation of the sense of shear. A quartz vein extending inclined to the foliation plane in a fine grained quartzo-feldspathic rock in Plate I, fig.3; Fig.4. The grains have been recrystallized in an orientation roughly perpendicular to the apparent foliation plane. This example of oblique incremental elongation points to a right-handed shear.

Schmid et al. (1981), have pointed out that the c axes of calcite crystals are oriented perpendicular to the dynamically generated foliation planes. Brunei (1980) and Simpson (1980) have observed similar phenomena in grains between aggregates of mylonite or mylonitic gneisses and suggested that the preferred orientation of grains were achieved by a progressive shear in late stages of the deformational episode.

Displaced broken grains

Feldspar porphyroclasts are seen in Plate II, fig.1 in a quartzo feldspathic, finely powdered matrix with

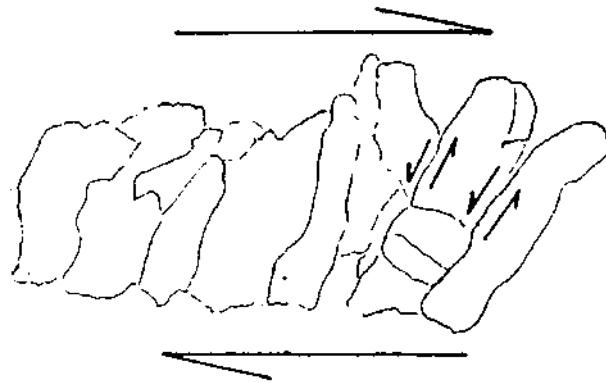


Fig.4 Sketch showing sense of movements that is opposite to that of the main shear in quartzo-feldspathic vein.

cohesion. The elongation and geometry of the grains, the simultaneous extinction, relative setting of crystal edges, or simply crystals being in the same optic orientation, show that all of the three pieces belong to the same

clast. The interstitial area is filled by a recrystallized quartz matrix. This is often seen in mylonitic rocks, a rotational movement along micro-fractures that are oblique to the-foliation planes (Fig.5). The grain setting seen in this figure, point to a right-handed shear. The quartz mosaic filling up the fracture zones, has been re-fractured and crushed in the peripheric zones (Plate II, fig.1; fig.5).

Recrystallized quartz mosaic following brecciation and formation of mortar gneiss in a typical sequence of events for progressive brecciation. Takagi (1986) points out that durable grains such as feldspar and pyroxene porphyroclasts in foliated mylonitic rocks are often observed to have extension fractures and broken grains with concurrent rotations.

Spindle-shaped micas (mica fish)

Foliated rocks of granitic origin and phyllonites often comprise spindle-shaped porphyroclasts (Plate II, fig.2), possibly of micro-pull apart origin (Hanmer, 1986). The spindle-shaped mica aggregates or "pockets" are

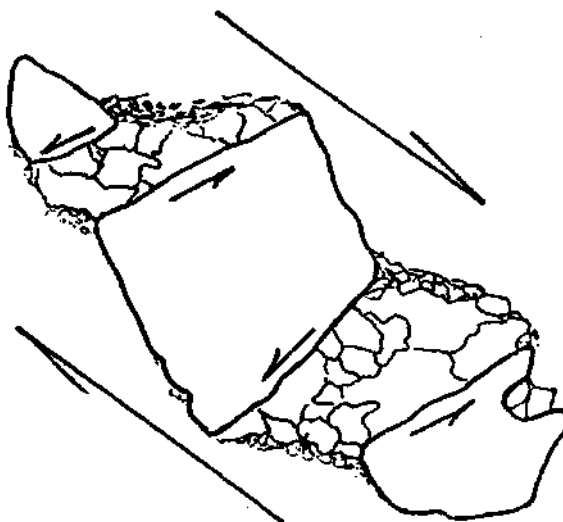


Fig.5– Sketch showing sense and direction of movements of rotated clasts.

often referred to as "mica fish" (Plate II, fig.3) and is used for determination of the sense of shear (Lister and Snoke, 1984). A large mica clast in a fine-grained quartzo-feldspathic matrix in Plate II, fig.3. The mica clast is oriented oblique to the incipient foliation defined by the elongation of fine grained crystals. The mica cleavage plane (001) makes an angle of 28° with the foliation plane. The direction pointed out by this acute angle, defines the direction of movement. A sinistral movement is suggested by the mica fish of Plate II, fig.3.

TEXTURAL ANALYSIS OF MACRO AND MICROSTRUCTURES

We have, so far, concentrated on microstructures formed by shearing of the granite and the host rock. We will, now, have a look on the macrostructures and dependent microstructures which are, again, consequences of shearing processes.

There will always be medium or large grains in the course of crushing and powdering of the granitic rocks in shear *zones* of the periphery, in addition to the clay-silt size, equigranular powder. This feature plays a role for

PLUTON OF THE DEMİRKÖY

confusion of a mylonitic granite with a sandstone. These rocks often display micro shear planes that resemble sedimentary structures such as lamination and cross-bedding.

The crystals are elastic within a given interval in the ideal case. However, beyond these limits, a stationary deformation is encountered. The grain is broken when the stress exceeds the amount required (Turner, 1968). The larger clasts are broken into small granules which tend to get dislocated in the slip planes that are apt to get parallel to the larger shear zones. There is a variety of distribution of trends of these zones and the broken grains in these crushed zones (Zeck, 1974).

The appearance of the rock specimen depends on the number and intensity of deformational episodes (Marker, 1950). As it is known, a mineral growth, formation of a cleavage plane or formation of a fold is defined as "late" for the proceeding and "early" for the following deformational episode (Spry, 1969). Three progressive deformational episodes were recognised through mesoscopic observation (Fig.3). On the other hand, five episodes was established from studies of thin sections.

Banded structure : definition and origin

The main mesoscopic and microscopic features (Plate III, fig.1) on the granite periphery are banded structures. These may be as wide as tens of meters and are in the form of narrow strips, they are continuous and have the appearance of an alternating sedimentary sequence. The medial sections of the bands preserve, generally, the primary characteristics of the rock. As the shear zones are approached, the grain size diminishes considerably and an incipient foliation is observed. The crushed grains of sheeted minerals are concentrated in the lamination of the cataclastic matrix. Fining up of grains and compositional changes have formed colour bands. Recrystallized micas are formed synkinematically. The mechanical wrenching that was formed by slip along grain borders, have contributed to formation of foliation planes (Fig.3). The schistosity planes are thin in the slip planes and gets thicker away from these zones.

This type of banding or foliation was defined as "flow structures" by Lapworth (1885) and Waters and Campbel (1935). These planes can be distinguished as continuous or discontinuous (Burg and Laurent, 1978) and are ascribed to segregation of material of different physical characteristics in different layers (Higgins, 1971). The mechanism of formation starts with generation of lenticular pods, and with progressing cataclasis, formation of subparallel shear planes are followed by laminar flow structures (Fig.3 : Higgins, 1971). This process was considered in four steps by Ramsay (1980): approach, curving tips, intersection and merging.

Cross-banding

Shear bands, defined by fine grained and mica-rich shear planes, joins obliquely to another foliation plane (Plate III, fig.1 and Fig.6). These colour bands or compositional banding resemble cross-bedding, and join obliquely the foliation plane by drawing a sigmoidal path (Fig.6). Passchier (1986) has shown that there is an angle of 45° between cross-banding centre and late stage foliations.

The cross-banding referred as 'transfer zone" by Boyer (1981), is defined by colour contrast and tectonic fabric and bears typical characteristics of a brittle-ductile deformation in the early period of formation of cleavage.

Relation of shear to folding

Folds, different in dimension and geometry, are observed to form along shear cleavage due to different behaviour of material in the microlithons. Ductile faults (Ramsay and Graham, 1970), shear pods and button structures (Roper, 1972) are encountered along the shear cleavage and microlithons.

Isoclinal folds have been formed in overpowdered mylonite gneiss/schists (Fig.8) while assymetric and/or overturned conjugate folds (Fig.7) have been generated in the shsar bands of granitic rocks of quartzo-feldspathic composition. In bands rich in phyllosilicates, crenulations have developed in folds formed by flow. These struc-

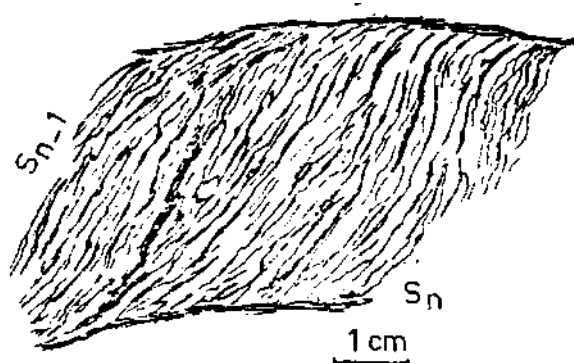


Fig.6— Early and late foliation in mesoscopic structures. Note that the foliation planes run at an angle of 45° .

tures are probably synchronous. The axial planes of these folds and attitude of shear planes are conformable embracing the pluton peripherically.

Thrusting will be realized due to relative movement of one band with respect to another if the stresses parallel the foliation planes. The relative movement of flow structures will fold the material in microlithons so that conjugate folds (Fig.7) and microfolds with flow cleavage will be formed (Fig.8). Differential movements between the walls of shear cleavages have resulted in offset of ductile fractures (Plate III, fig. 2). The prograde character of the movement will result in refolding or rupture in the wings of these ductile faults. There will be folds, formed perpendicular to those formed earlier (Fig.7), in addition to breakup and movement along fault planes, with consequent formation of microthrusts.

The axial planes of folds of the late stage cross-cut the foliation planes formed during the earlier phase of deformation. The material in the flanks elongates and thins with prograde deformation while thickening occurs in the apex (Fig.8). As the angle between the flanks is minimized, there will be flow to the apex and the boundaries get sharper. The apex is finally detached as the flanks thin out. Thus, the earlier foliation (S_{n-1}) is eradicated.

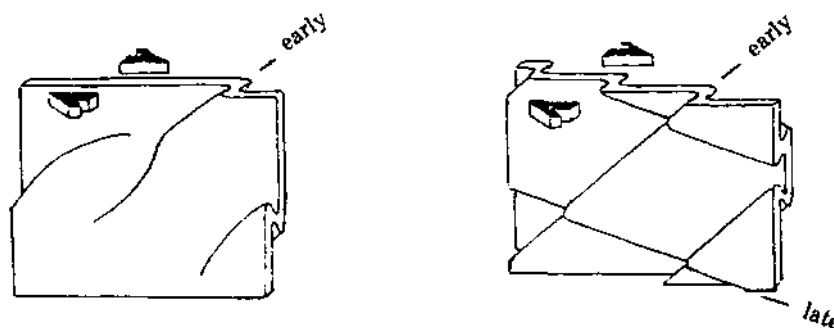


Fig.7— Schematised diagramme (after Berthé and Brun, 1980) showing formation of the conjugate folds in microlithons.

The new foliation planes (S_n) starts to conform with attitude of the earlier foliation planes. The relict structures from the early foliation are shear pods (Plate III, fig. 3). and mica buttons of the apex (Fig.8) (Roper, 1972) and trend generally at an angle to the banding.

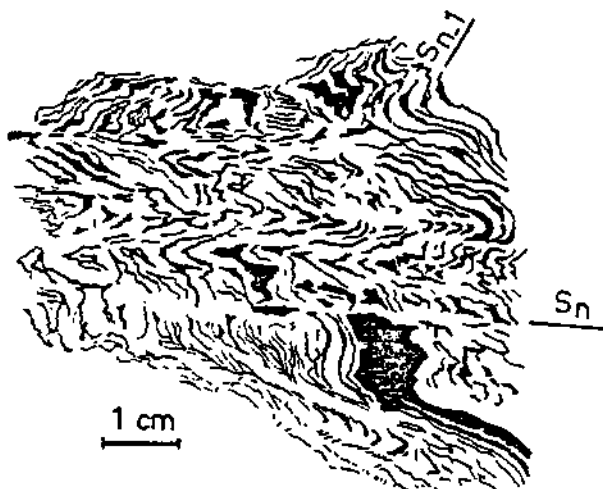


Fig.8— Tight and recumbent isoclinal folds. Button structure at crests of folds formed by the new foliation.

The translation along these flow structures have caused formation of thrust slices. These movements, which are the cumulative result of a prograde deformation, are responsible for enhancement of the movements of micro-lithons or shear bands.

DISCUSSION AND CONCLUSION

The structural forms and events are consequences of deformation and rupture of granitic and host rocks during the emplacement.

The total displacement of the thrust slices is the cumulative result or vectorial addition of dextral and sinistral movements.

- 1— Contact metamorphism of hornblend-hornfels facies is encountered in the country rocks.
- 2— The cataclastic zone, characterized by a brittle-ductile deformation, embraces the pluton with a peripheral attitude.
- 3— Andalusite-cordierite bearing contact schists encircle and embrace the granite periphery which is converted into a zone of mortar gneiss.
- 4— Rupture and displacement in quartz, feldspar and micas of the granite and the country rocks; rotation and pressure shadow area in cordierite and garnet, oblique incremental elongation in quartz, displacement of broken grains leading to oblique rearrangement of grains and mica fish are frequently observed microstructural features.
- 5— The micro-and-macrostructures seen along the granite boundary are conformable.

6— Multi dimensional banded structures-cross banded structures, plus folds and thrusts of various dimension and character are encountered.

7— Rupture and folding followed each other and ended up with conversion of shear slices into en echelon micro-thrusts.

8— The deformational process in mylonitic rocks, starting with undulatory extinction and ending up with micro-thrusts, is a direct consequence of multistage and progressive simple shear.

9— The cause of simple shear is emplacement of the granite. The steepness of the structural elements around the granite periphery have been realized in the latest stage of emplacement

10— The total movement observed along the granite periphery is the cumulative result of the described progressive deformation.

REFERENCES

- Akartuna, M., 1959, Çatalca-Karacaköy bölgesinin jeolojisi : İÜFF Monografileri, 13 p.
- Aydın, Y., 1974, Etude Petrographique Et Geochimique De La Partie Centrale Du Massif D'Istranca (Turquie): These. L'Universite de Nancy (unpublished).
- 1982, Yıldızdağları (Istranca) Masifinin Jeolojisi : Doçentlik tezi, ITU Maden Fakültesi, 107 p.(unpublished).
- Aykol, A., 1979, Kırklareli-Demirköy Sokulumunun Petrolojisi ve Jeokimyasi: Doçentlik tezi, ITU Maden Fakültesi, 204 p (unpublished).
- Berthe, D. and Brun, J.P., 1980, Evolution of folds during progressive shear in the south Armorican shear zone. France : Journal of Struc.GeoL, 2, 1-2, 127-133.
- Boyer, S.E., 1984, Origin and significance of compositional layering in late Precambrian Sediments Blue Ridge province, North Carolina USA: Journal of Struc.GeoL, 6, 1-2, 121-133.
- Brunei, M., 1980, Quartz fabrics in shear-zone mylonites evidence for a major imprint due to late strain increments: Tectonophysics, 64, T33-T44.
- Buddington, A.F., 1959, Granite emplacement with special reference to North America: Geol.Soc.Am.Bull., 70, 671-747.
- Burg, J.P. and Laurent, Ph., 1978, Strain analysis of a shear zone in a granodiorite: Tectonophysics, 47, 15-42.
- Bürküt, Y., 1966, Istranca kristalen masifinin petrojenezi: Madencilik VIII, 4, 165-180.
- Hanmer, S., 1986, Asymmetrical pull-aparts and foliation fish as kinematic indicators : Journal of Struc.GeoL 8,2, 111-122.
- Harker, A., 1950, Metamorphism. A study of the transformations of rock masses: Methern and Co. Ltd.London, 362 p.
- Higgins, M.W., 1971, Cataclastic rocks : Geological Survey Professional paper. 687, 79 p., Washington.
- Ksiazkiewicz, M., 1930, Sur la geologic de L'Istranca" et das Territoires voisins : Cracovie.

- Lapworth, C., 1885, The highland controversy in British geology : Nature, 32, 558-559.
- Lister, G.S. and Snoke, A.W., 1984, S-C Mylonites : Jour. of Struc.Geol., 6, 617-638.
- Pamir, H.N. and Baykal, F., 1947, Istranca masifinin jeolojik etüdü : MTA Rep., 2257 (unpublished).
- Passchier, C.W., 1986, Flow in natural shear-zones the consequences of spinning flow regimes : Earth and Planetary Sci. Letters. 77,70-80.
- Ramsay, J.G., 1980, Shear zone geometry: a review: Journal of Struc.Geol., 2, 1-2, 83-99.
- and Graham, R.H., 1970, Strain variation in shear belts : Canadian Journ. of Earth Sci., 7, 786-813.
- Roper, P.J., 1972, Structural significance of "Button" or "fish" "scale" texture in phyllonitic schist of the Brevard zone North-western, South Carolina: Geol.Soc. of Am.Bull., 83, 853-860.
- Schoneveld, C., 1977, A study of some typical inclusion patterns in strongly paracrystalline-rotated garnets : Tectonophysics, 39, 453-471.
- Schmid, S.M.; Casey, M. and Starkey, J., 1981, The microfabric of calcite tectonites from Helvetic nappes (Swiss Alps) : Thrust and nappe tectonics: Geol. Society of London Special Publication, 9, 151-158.
- Simpson, C., 1980, Oblique girdle orientation patterns of quartz C axes from a shear zone in the basement core of the Moggia Nappe, Ticin Switzerland: Journal of Struc. Geol., 2, 243-246.
- and Schmid, S.M., 1983, An evolution of criteria to deduce the sense of movement in sheared rocks: Geol.Soc. of Am. Bull., 94, 1281-1288.
- Spry, A., 1969, Metamorphic textures : Pergamon press, 350 p., Oxford.
- Takagi, H., 1986, Implication of mylonitic microstructures for the geotectonic evolution of the Median Tectonic Lane, Central Japan : Journal of Struc. Geol., 8,1, 3-14.
- Tokel, S. and Aykol, A., 1987, Kırklareli-Demirköy granitoidinin jeokimyasi : Kuzey Tethis ada yayı sisteminde Srednogorie-Istranca bölümünün evrimi : Türkiye Jeoloji Kurultayı Bildiri Özetleri, p. 17.
- Turner, F.J., 1968, Metamorphic petrology: McGraw Hill Book Co., 403 p., New York.
- Üşümezsoy, Ş., 1982, Istranca Masifinin Petrojenetik evrimi: Doktora tezi, İÜ Müh.Fak., İstanbul, 94 p. (unpublished).
- and Öztunalı, Ö., 1981, Istranca ve Eybek masiflerinde kataklastik dokunun evrimi : Istanbul Yerbilimleri, 2,3-4, 129-137.
- Waters, A.C. and Campbel, C.D., 1935, Mylonites from the San Andreas fault zone: Am.Journal of Science., 29, 473-503.
- Yurtsever, A.; Çağlayan, M.A.; Şengün, M.; İmik, M.; Önder, V.; Özcan, İ; Bozkurt, H. and Arda. A., 1986, Yıldızdağları (Istranca masifi) Kırklareli metagraniti üzerine: Türkiye Jeoloji Kurultayı Bildiri Özetleri, p.25.
- Zeck, H.P., 1974, Cataclastites, hemiclastites, holoclastites, blastoditto and myloblastites-cataclastites rocks : Am.Jour.Sci., 274, 1064-1073.

PLATES

PLATE-I

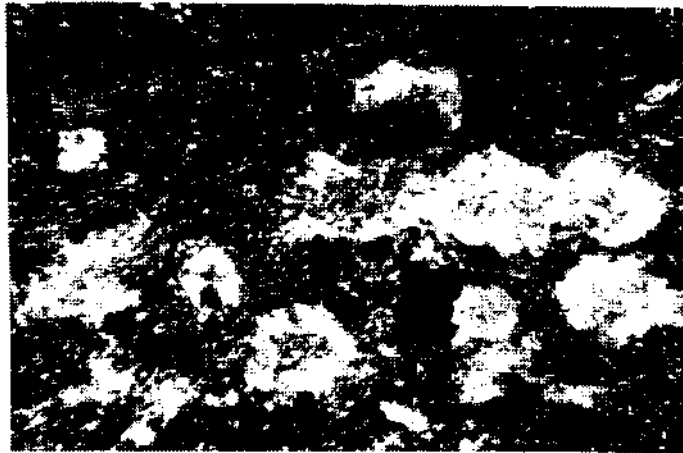
Fig.1- Rotation in garnets. Note the microfolds defined by mica flakes and the asymmetric pressure shadow areas. Crossed nicols.

Fig.2- Pinitized ksenomorphic cordierite and idiomorphic andalusite in a contact schist. Crossed nicols.

Fig.3- Photomicrograph of grains with throw with respect to one another in a quartzo-feldspathic vein.



1



2



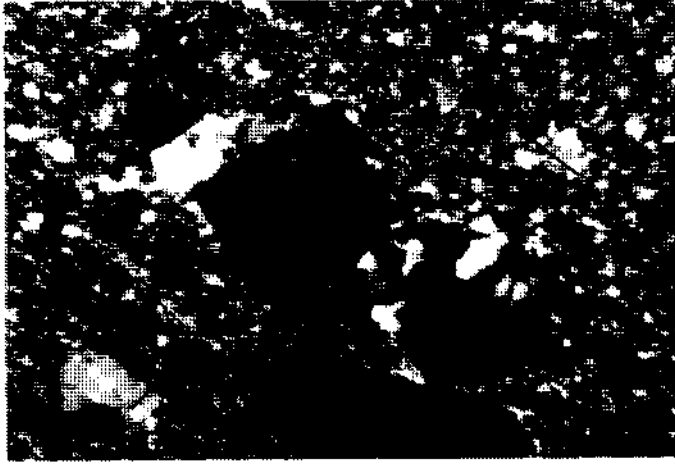
3

PLATE-II

Fig.1— Feldspar clasts of the same orientation. Note the throw is oblique to the direction of main shear.

Fig.2— Spindle shape quartz porphyroclasts produced by shear.

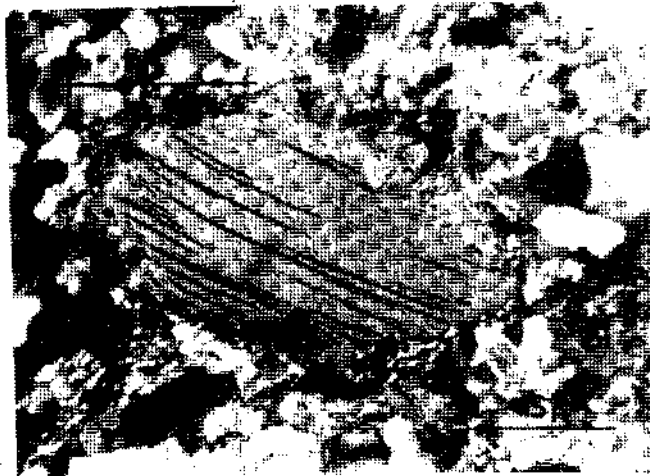
Fig.3— Mica-fish, oblique (28°) to the foliation, indicating a left-lateral shear. Crossed nicols.



1



2



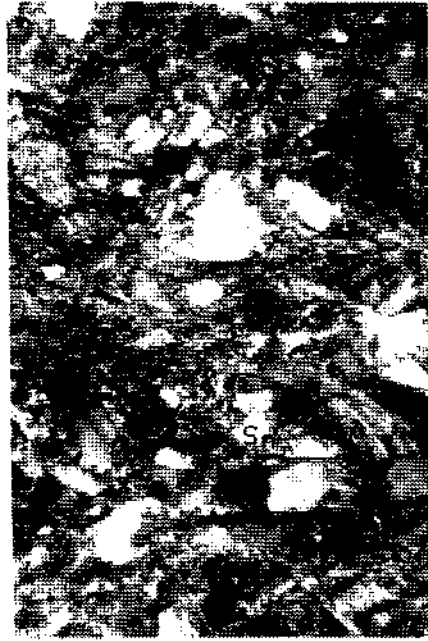
3

PLATE-III

Fig.1— Shear cleavage. Note the orientation of mica flakes that is oblique to the cleavage.

Fig.2— A ductile fault formed in a mica rich shear pod. Crossed nicols.

Fig.3— Mica pods denuded by the early and late foliation. Note that the foliation planes are at right angles. The section passes through the crest.



1



2



3

INTERPRETATION OF NEW GEOCHEMICAL, RADIOMETRIC AND ISOTOPIC DATA ON EASTERN AND SOUTHEASTERN ANATOLIA

Tuncay ERCAN*; Tatsuya FUJITANI****Jun-İchi MATSUDA****; Kenji NOTSU*****; Selçuk JOKEL***** and Tadahide Uj*****

ABSTRACT.— Collision zone volcanism that had started at Middle Miocene in Eastern and Southeastern Anatolia was examined. Major, trace and rare earth element analyses, measurements of the strontium isotope ($^{87}\text{Sr}/^{86}\text{Sr}$) and radiometric dating by K/Ar method of the samples from various regions were carried out. Diagrams that were plotted according to major element contents of the volcanic rocks show calcalkalic, alkaline and partly tholeiitic features. Volcanic rocks were named according to petrography and the results of the chemical analysis. Trace element contents of the volcanics generally fit the mean values of the upper continental crust, partly the mean values of lower crust and rarely the mean values of the mantle. Sr isotope ratios of the samples range between 0.70350-0.70640. These results indicate that the crustal slab related to the subducting Arabian plate contaminated the magma which formed the volcanics. According to K/Ar datings the oldest age of 11.4 ± 0.9 my is from Eleşkirt Kösedâğ dacites and the youngest age of 30,000 years are from obsidians of Nemrut Mountains and trachyandesitic lavas of Tendiirek Mountains. The distribution of the volcanics of the Eastern and Southeastern Anatolia and their volcanologic, geochemical, petrographic, radiometric, isotopic features are discussed.

THE OSTRACODA BIOSTRATIGRAPHY AND ENVIRONMENTAL INTERPRETATION OF THE MONTIAN-CUISIAN SEQUENCE IN THE SOUTH OF POLATLI (SW ANKARA)

Mehmet DURU* and Nuran GÖKÇEN**

ABSTRACT.— In the present study, the ostracoda fauna of the sedimentary rocks of Lower Paleogene situated in south of the Polath Town have been stratigraphically examined, its biozones have been distinguished and the findings are interpreted from the chronostratigraphic and environmental point of view. By evaluating the stratigraphic distribution of 44 ostracoda species, the existence of 4 biozones in Montian—Cuisian have been proposed. It is interpreted that the Tertiary sequence of the region was first deposited in a continental and then in a marine environment.

STRATIGRAPHY AND MICROPALAEONTOLOGY OF THE MUT-ERMENEK TERTIARY SEQUENCE

Ümit TANAR*** and Nuran GÖKÇEN**

ABSTRACT.— Mut Tertiary basin, situated in the Mediterranean Region of Anatolia, covers mainly the upper district of Göksu river. The study area is bounded by the villages of Karaman, Mut, Ermenek, Gülnar and Sarıkavak. The study Tertiary sequences transgressively overlie the Paleozoic and Mesozoic aged basement. The oldest unit of the Tertiary sequence (Yenimahalle formation) is the Post-Eocene detritics exposing in the west and indicate limnic and/or brackish environment. Fakırca formation which rest upon these detritics, is primarily of the Upper Oligocene and Lower Miocene age. The ostracod and the foraminifer contents of the formation indicate the environmental change between limnic and brackish conditions. This formation is conformably overlain by Derinçay formation including bentonic-planktonic foraminifers and ostracod fauna and indicate shallow marine environment of Burdigalian. The Tertiary sequence is succeeded by Köşelerli formation and microfauna contents designate shallow marine sedimentation at the end of Burdigalian and beginning of Langhian. According to the fossil contents and field observations, Mut formation which generally placed at the top and exhibited lateral and vertical extinction to Derinçay and Köşelerli formations, indicates Langhian-Serravalian timespan.

A NEW CARBONIFEROUS AND PERMIAN FINDING IN THE KARAKAYA NAPPE

Erdin BOZKURT****

ABSTRACT.— In the study area, two rock units crop out. The first of them is the Karakaya nappe, which is a tectonic unit. The second unit is the Pliocene cover rocks, which unconformably overlie the Karakaya nappe. In the investigated area, the Karakaya nappe is composed of different blocks floating in a litarenitic sandstone matrix. As a result of detailed litho- and bio-facies studies, one of these blocks is dated to be Visian-Serpukovian, the other to be Asselian-Sakmarian. Well-bedded and 150 meters thick succession observed in of these blocks is informally named as the Beytepe formation.